Bainite in Steel: A Century of Microstructural Discovery, Mechanistic Debate, and Dynamic Transformation

May 2025

C. Garcia-Mateo (cgm@cenim.csic.es)

National Center for Metallurgical Research (CENIM-CSIC) Madrid, Spain

European Commission

This research is funded by the European Union under the RFCS project WarP – Grant Nº 101112425.

Silesian University of Technology

First and foremost………

First and foremost.........

Happy Birthday, Silesian University! 🎉

Eighty years of academic excellence, innovation, and community—a remarkable milestone. It's an honour to be part of this celebration and to contribute to the legacy of such a distinguished institution.

First and foremost………

I would also like to express my gratitude to Professor Adam Grajcar—for the kind invitation to speak today, and for many years of fruitful scientific collaboration and personal friendship. It is an honour to work alongside you.

INDEX

INDEX

- **Bainite historical context**
  - Discovery and Early Characterization
  - Emerge of competing Theories
  - Characterization through time
  - Evolution of theories through time

Steel Early Characterization (Pre-1930s)

Fe-C Phase Diagram
Sir William Chandler Roberts-Austen (1897) published the first complete Fe-C diagram, synthesizing earlier 19th-century studies on carbon's role in steel.

Ferrite and Cementite
•These were long-established constituents of steel, forming the basis of microstructures like pearlite. Ferrite (α-iron) body-centered cubic phase, while cementite (θ-Fe_3C) is an iron carbide.

Pearlite
•Identified as a lamellar mixture of ferrite and cementite, formed during slow cooling of austenite. By the 1920s, **finer pearlite** variants (later termed "**troostite**") were recognized.

Martensite
•A hard, needle-like phase formed by rapid quenching of austenite. Its transformation mechanism was studied extensively in the early 20th century.

Discovery and Early Characterization (1920s-1940s)

In the 1930s, E.S. Davenport and Edgar Bain discovered a new steel microstructure that:

- Occupied a transformation temperature range between **pearlite and martensite**. Initially, they provisionally called it "**martensite-troostite**" as it appeared intermediate between the then-known martensite phase and what was called **troostite** (later identified as fine-pearlite).

- This microstructure was **subsequently named "bainite"** by Bain's colleagues at the United States Steel Corporation, though **scientific acceptance of the term was slow**, with metallurgical textbooks as late as **1947** failing to mention bainite by name.

Edgar C. Bain

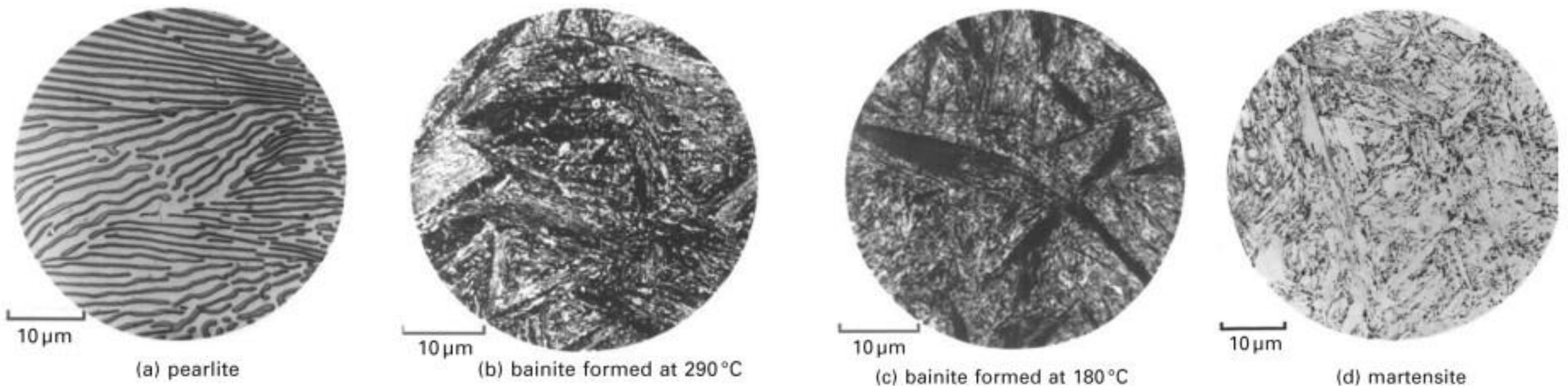

Microstructures in a eutectoid steel:
(a) Pearlite formed at 720 °C
(b) bainite formed at 290 °C
(c) bainite formed at 180 °C
(d) martensite.

Discovery and Early Characterization (1920s-1940s)

Optical microscopy (OM) was the <u>primary characterization tool</u> available to metallurgists.
Bain and Davenport made several fundamental observations after isothermal holding experiments, where austenitized steel specimens were rapidly quenched to specific intermediate temperatures (250–550°C) and held to allow transformation :

- C-curve kinetic behavior in time-temperature-transformation **(TTT) diagrams**. They established the **<u>temperature range</u>** for bainite formation: approximately 125-550°C, depending on alloy content.
- They **<u>identified two distinct morphologies/ranges</u>**: 'upper-range' bainite forming at higher temperatures and 'lower-range' bainite forming near the martensite start temperature.

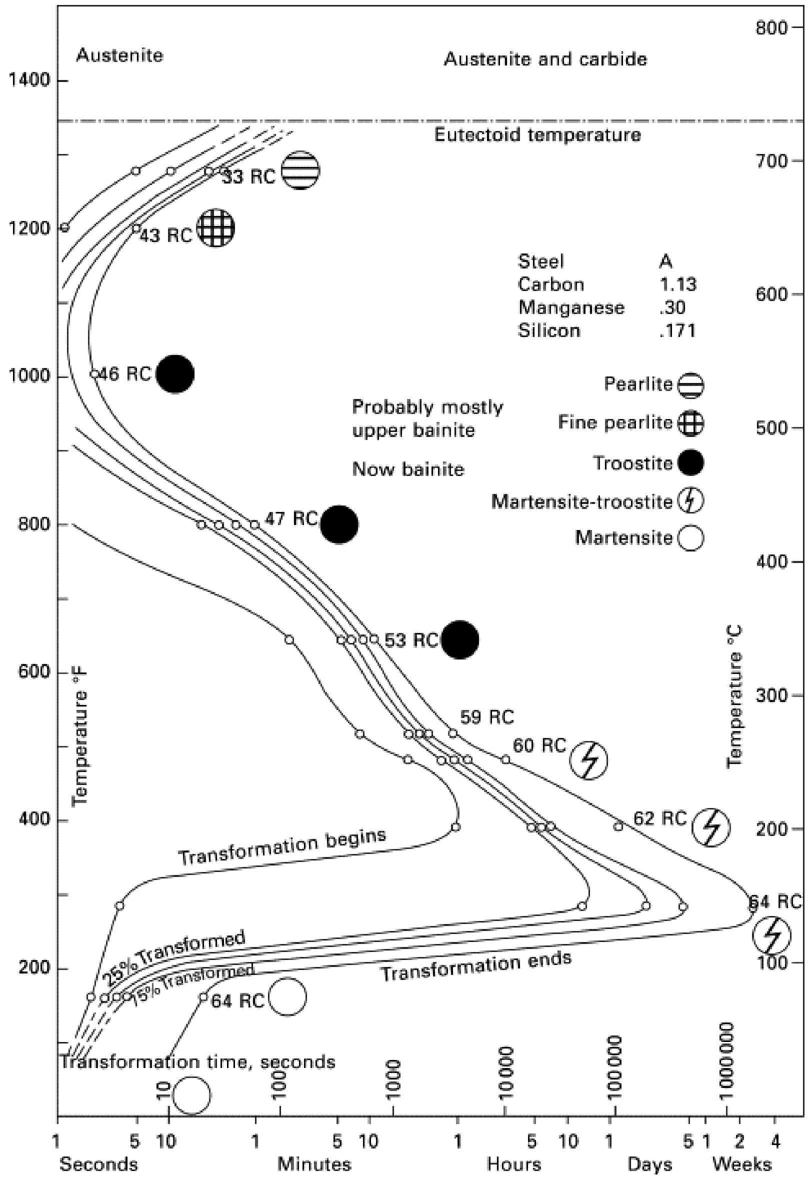

Bain, E.C. (1939). Functions of the Alloying Elements in Steel. American Society for Metals.
Davenport, E.S., & Bain, E.C. (1930). Transactions of the Metallurgical Society of AIME, 90, 117-154.

Discovery and Early Characterization (1920s-1940s)

Fundamental observations

- They noted **bainite appears darker than untempered martensite** under a light microscope due to its more complex substructure.
- Bainite's **hardness exceeded tempered martensite** at equivalent strength levels, suggesting unique dislocation substructures.
- The microstructure comprised **non-lamellar ferrite plates with intervening carbides or carbon-enriched austenite**, differing fundamentally from pearlite's alternating layers.
- **Transformation arrested before completion**, leaving retained austenite, a phenomenon later termed the "**incomplete reaction**”.
- **Early speculations**: Initial hypotheses suggest a hybrid mechanism combining aspects of **diffusion-controlled and shear transformations**

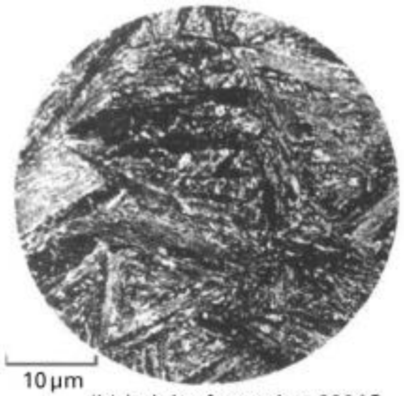

(b) bainite formed at 290 °C

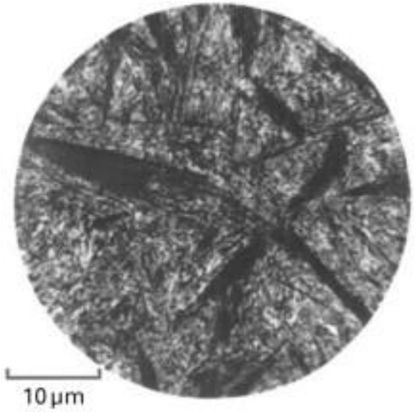

(c) bainite formed at 180 °C

Development of Transformation Theories (1950s-1960s)

Hot-stage OM shows **surface relief** ➢ transformation is accompanied by a **shear** (as martensite).

T. **Ko and S. A. Cottrell** : J. Iron & Steel Inst., 172 (1952),307.

K. **Tsuya** : J. Mech. Lab., Japan, 2 (1956), 20.

The introduction of **transmission electron microscopy (TEM)** to metallurgical research in the **1950s** represented a quantum leap in the ability to study bainite.

Development of Transformation Theories (1950s-1960s)

With TEM, for the first time, researchers could visualize **microstructural details at a much finer scale than optical microscopy** allowed.

Lower bainite

Upper bainite

Tempered martensite

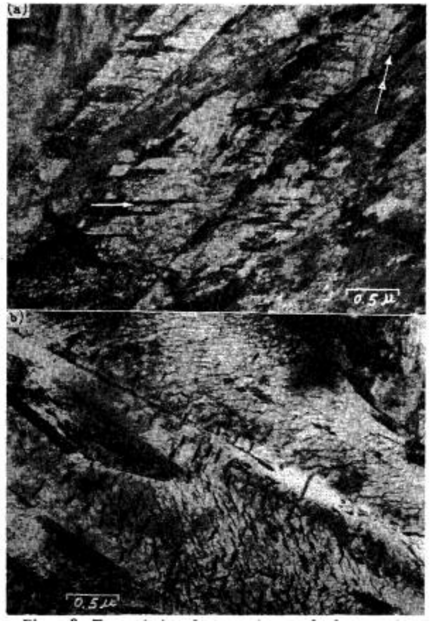

- Differences in morphology and formation conditions, leading to the **classification** of **upper and lower bainite**.

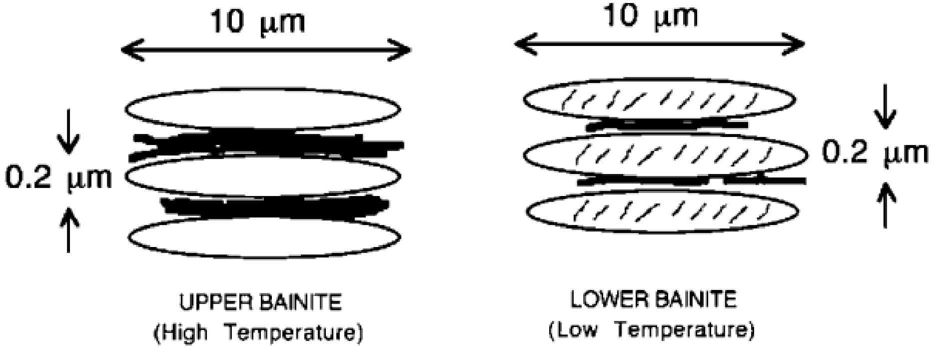

Shimizu, K.; Ko, T.; Nishiyama, Z. Transmission Electron Microscope Observation of the Bainite of Carbon Steel. *Trans. Japan Inst. Met.* **1964**, *5*, 225–230, doi:10.2320/matertrans1960.5.225.

Development of Transformation Theories (1950s-1960s)

Sub-structures and lattice imperfections. A. J. **Baker**, P. M. Kelly, J. Nutting : Electron Microscopy and Strength of Materials, (1963), Chapter 20.

Lower bainite

Upper bainite

Tempered martensite

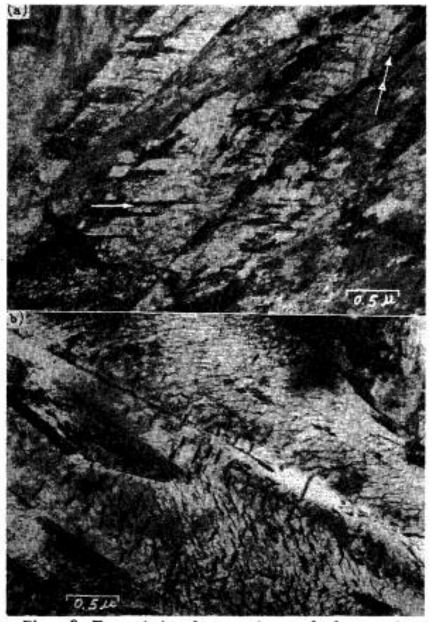

Shimizu, K.; Ko, T.; Nishiyama, Z. Transmission Electron Microscope Observation of the Bainite of Carbon Steel. *Trans. Japan Inst. Met.* **1964**, *5*, 225–230, doi:10.2320/matertrans1960.5.225.

Development of Transformation Theories (1950s-1960s)

This period saw the **emergence of competing theories about bainite's transformation mechanism**:

1. The **displacive theory** proposed that bainite forms by a shear transformation, similar to martensite, with a disciplined motion of atoms rather than chaotic transfer associated with diffusion.

2. The **diffusional theory** (implied in the references but not explicitly detailed) suggested transformation was controlled primarily by carbon diffusion.

TEM evidence began supporting aspects of the **displacive** theory by revealing:

- The plate-like morphology of bainite and dislocation density, consistent with minimization of strain energy from shape deformation during transformation.

- Evidence of displacements occurring during bainite growth, suggesting a combination of deformation and crystal structure change similar to martensite. **Invariant-plane strain shape deformation proposed.**

Advanced Microstructural Characterization (1970s-1990s)

The 1970s and 1980s saw the widespread adoption of **scanning electron microscopy (SEM)** in metallurgical studies, providing complementary information to TEM investigations.
The **higher depth of field and larger viewable areas of SEM** allowed researchers to better understand the three-dimensional aspects of bainitic structures.

During this period, researchers more clearly established the differences between upper and lower bainite:

1. **Upper bainite** (400-550°C): Forms in sheaves containing several laths of ferrite approximately parallel to each other. Carbon is rejected from ferrite, leading to carbon-rich austenite between laths and cementite formation.

2. **Lower bainite** (250-400°C): Exhibits a more plate-like form with fewer low-angle boundaries between laths. Cementite nucleates at the interface between ferrite and austenite.

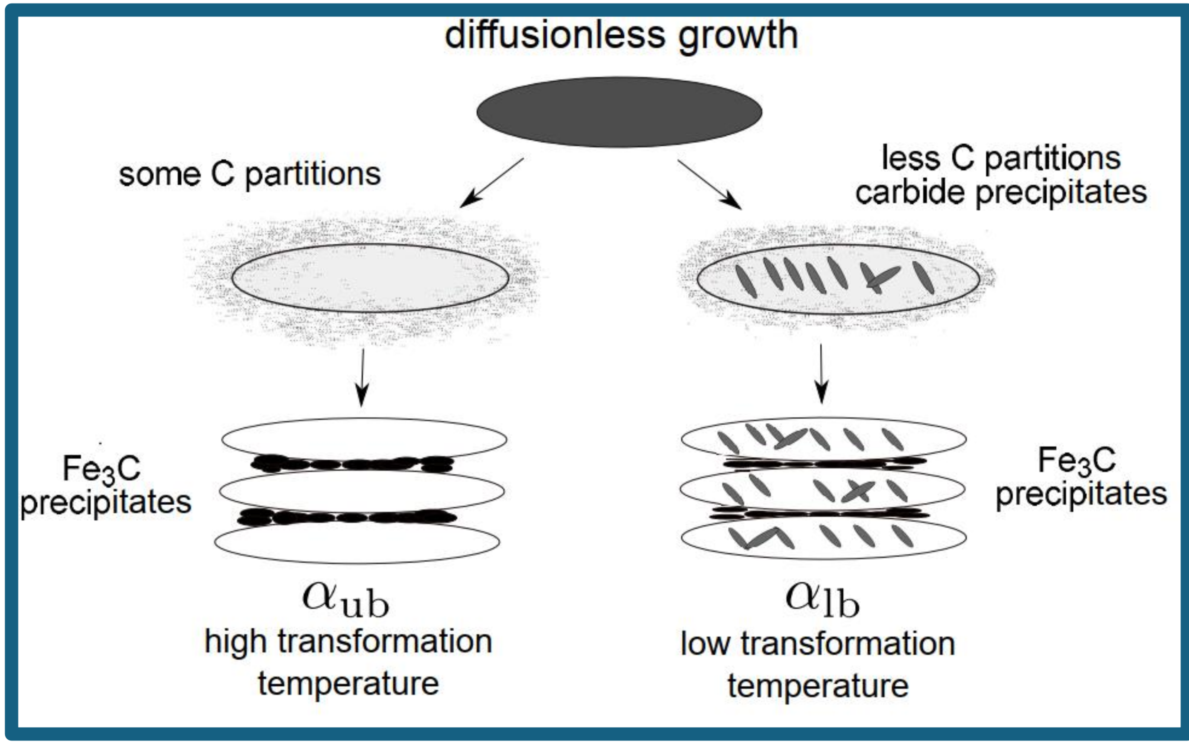

The introduction of **more sophisticated TEM techniques, including dark-field imaging** and **selected area diffraction**, helped researchers observe **crystallographic aspects (**Kurdjumov-Sachs relationship to the surrounding austenite**) that further supported the displacive** transformation theory.

Crystallographic Understanding and Nanostructured Bainite (2000s-2010s)

Electron backscatter diffraction (EBSD) coupled with SEM in the **late 1990s and early 2000s** revolutionized our understanding of bainite's crystallographic nature.

- Though EBSD allowed researchers to **map crystallographic orientations across larger areas**, providing statistical data on orientation relationships between phases.

- A **significant discovery** during this period was the **confirmation that bainitic ferrite can have a tetragonal crystal structure (BCT)** rather than the cubic (BCC) structure traditionally associated with ferrite. **This tetragonality results from carbon supersaturation in bainitic ferrite and supports the displacive transformation theory.**

- The early **2000s** also saw the development of **nanostructured bainitic steels**, characterized by:
  - Extremely fine bainitic ferrite plates (tens of nanometers thick).
  - Retained austenite with two distinguishable morphologies: thin films between ferrite plates and larger blocks.
  - High dislocation densities ($\sim 5.1 \pm 2.7 \times 10^{14}$ m^{-2}), similar to martensitic structures.
  - Excellent combinations of strength, toughness, and ductility.

Modern Analytical Techniques (2010s-Present)

The most recent decade has seen the application of **atom probe tomography (APT)** to bainitic steels, allowing three-dimensional mapping of elements at the atomic scale.

This has provided unprecedented **insights into carbon distribution** within bainitic structures, clarifying the nature of carbon supersaturation in **bainitic ferrite** and carbon enrichment in **retained austenite.**

In-situ Xray and Neutron Difraction can **track lattice parameter** changes in both ferrite and austenite, providing direct evidence of **carbon partitioning** and its effect on **stabilizing retained austenite.**

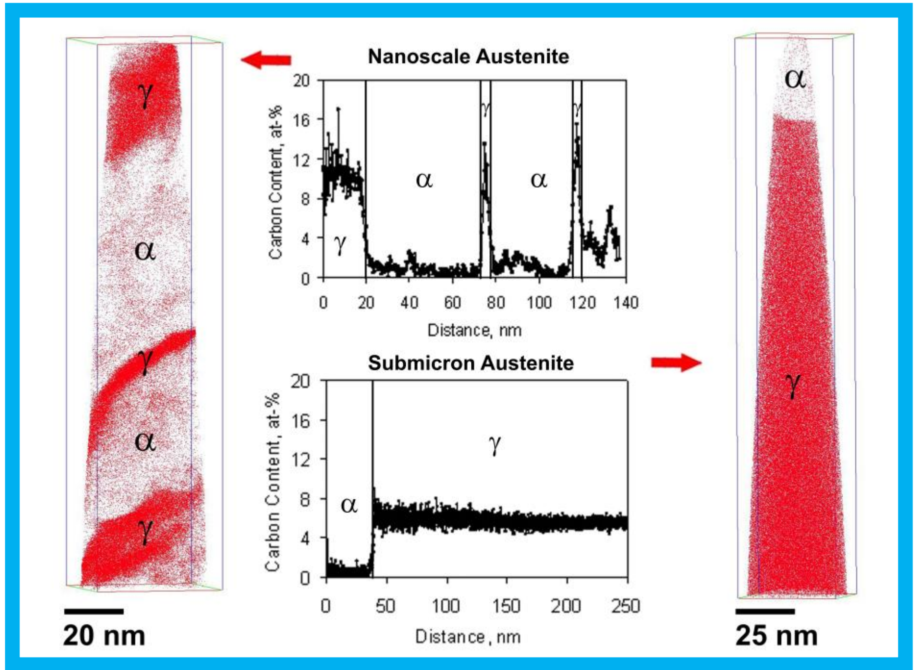

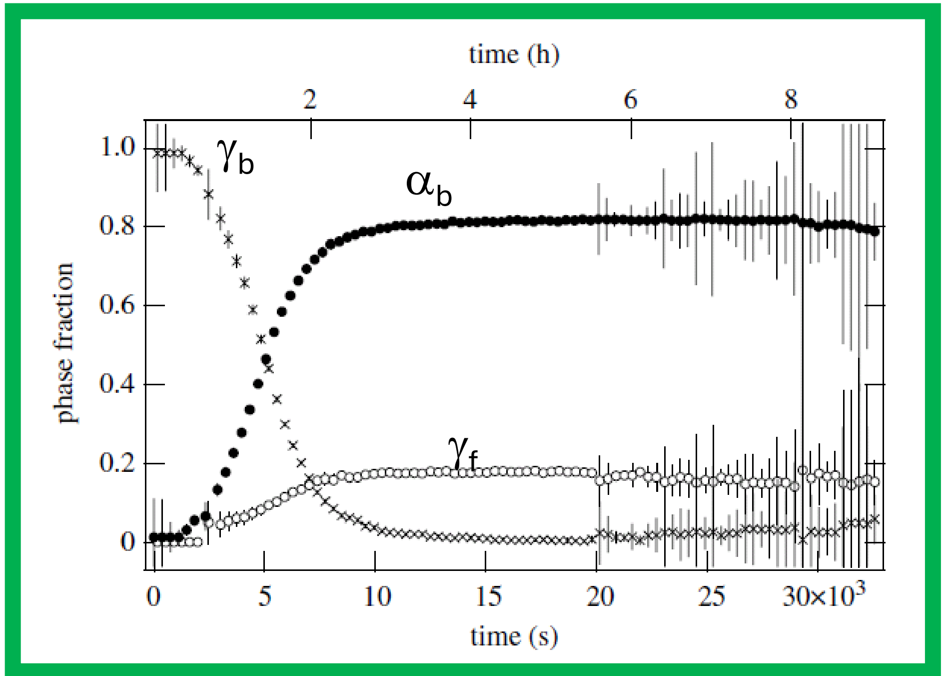

Two theories about bainite transformation mechanisms. Evolution through time.

1920s-1930s: Initial Observations

Early speculations: Initial hypotheses suggest a **hybrid mechanism** combining aspects of diffusion-controlled and shear transformations

1950s-1960s: Emergence of Competing Theories

Displacive Theory Foundations

- TEM observations reveal plate morphology and dislocation structures resembling martensite
- Concept of invariant-plane strain shape deformation proposed
- Theory formalized: Bainite grows via shear mechanism without carbon diffusion during transformation

Diffusive Theory Development

- Alternative hypothesis suggests carbon diffusion controls growth rate
- Proposes similarity to Widmanstätten ferrite formation
- Argues surface relief effects don't preclude diffusion control

Two theories about bainite transformation mechanisms. Evolution through time.

1970s-1980s: Experimental Differentiation
Key advances through TEM/SEM.

Displacive evidence:

- Discovery of carbon supersaturation in bainitic ferrite
- Observation of incomplete reaction phenomenon (transformation stops at T_0 curve)
- Mechanical stabilization effects unique to displacive transformations

Diffusive counterpoints:

- Cementite precipitation patterns suggest carbon migration
- Temperature-dependent transformation rates cited as diffusion evidence

1990s: Quantitative Modelling
Bhadeshia's kinetic model (1982-1992) successfully predicts:

- Autocatalytic nucleation behavior
- Temperature dependence of plate thickness
- Incomplete transformation phenomenon

Model strongly supports displacive mechanism with subsequent carbon partitioning

Two theories about bainite transformation mechanisms. Evolution through time.

2000s: Crystallographic Validation

- Tetragonal distortion in bainitic ferrite ($\delta \approx 1.0008$)
- Kurdjumov-Sachs orientation relationships with austenite

Both ***features match martensitic (displacive)*** transformation signatures

2010s: Atomic-Scale Confirmation

Atom probe tomography (APT) shows:

- Carbon supersaturation (0.1-0.3 wt%) in fresh bainitic ferrite
- Delayed carbide precipitation (seconds-minutes after transformation)
- Carbon gradients at α/γ interfaces *consistent with post-transformation partitioning*

Two theories about bainite transformation mechanisms. Evolution through time.

2020s: Current Status
Displacive mechanism dominates for ferrite formation

•**Displacive Theory**: Fundamentally relies on a displacive mechanism, similar to martensite. This means a shear-like transformation with coordinated atom movements and little or no diffusion during the *initial* growth step. Carbon diffusion occurs *after* the initial ferrite formation.

•**Diffusional Theory**: **Initially**, it considered a ledge propagation growth mechanism. However, the **newer** considerations accept a **mixed mechanism that is reconstructive and displacive growth** of the bainitic ferrite

Key Points:
•The core difference lies in whether atom movement is primarily *coordinated* (displacive) or *diffusion-controlled* during the initial growth of the ferrite.

•Both theories acknowledge the role of carbon diffusion in the overall bainite transformation process, particularly concerning carbide precipitation and the incomplete reaction.

Fielding, L.C.D. **The Bainite Controversy**. *Mater. Sci. Technol. (United Kingdom)* **2013**, *29*, 383–399, doi:10.1179/1743284712Y.0000000157.

INDEX

- **Explaining Bainitic transformation**
  - Transformation Mechanisms
  - Displacive & Diffusionless transformation.
  - Evolution of the transformation
  - Morphologies
  - Thermodynamics. To-Line
  - Understanding the C journey in bainite

Explaining Bainite (Personal point of view and experience)

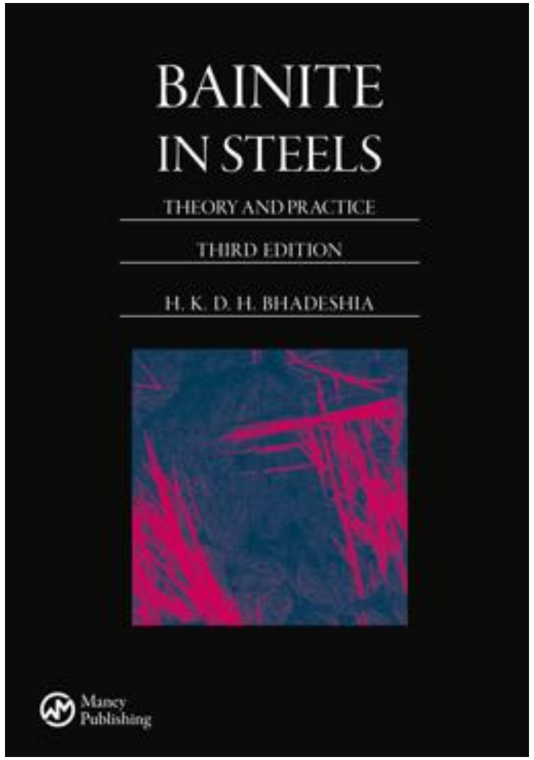

H.K.D.H Bhadeshia. Bainite in Steels. The Institute of Materials (2001) London. 3d Edition

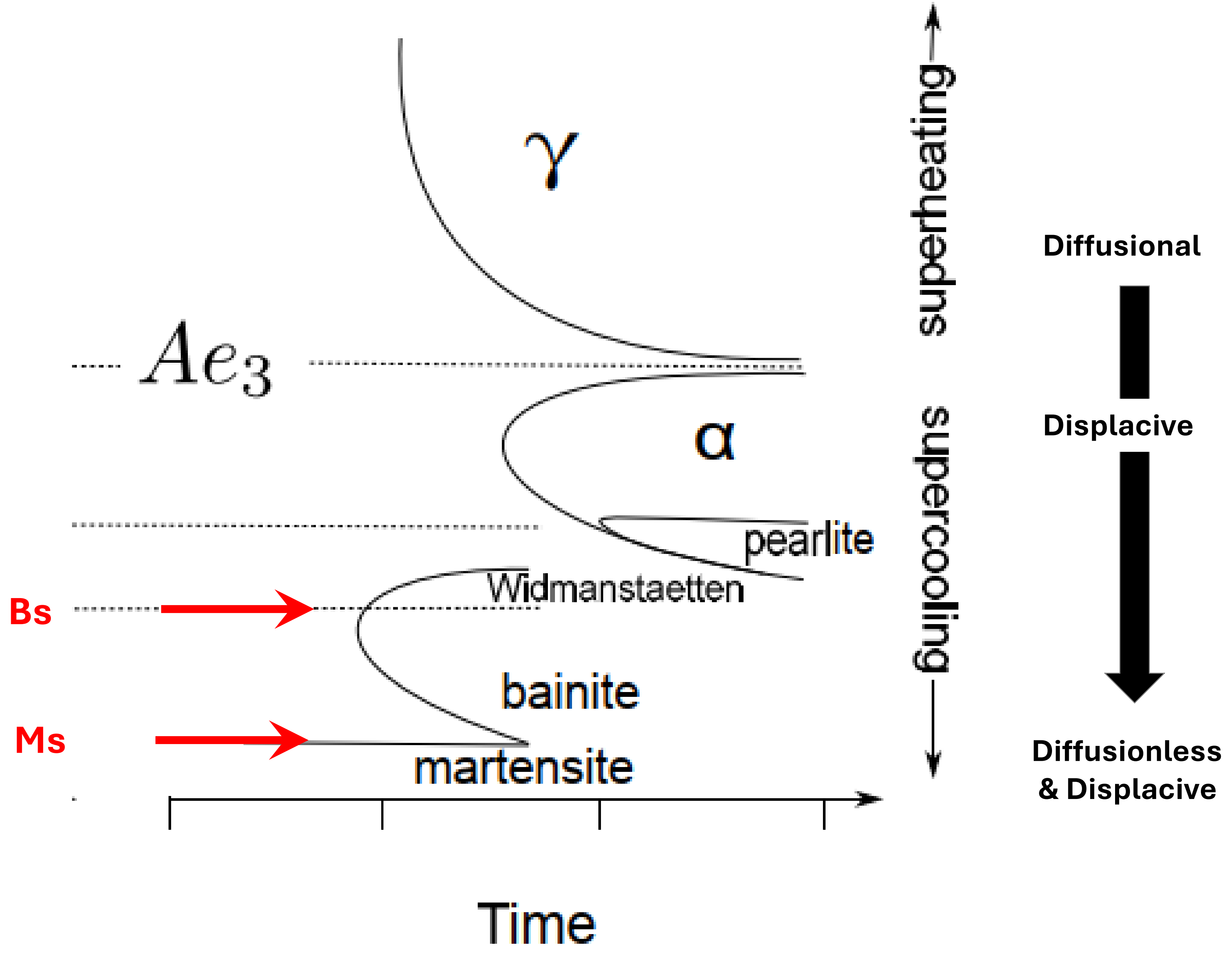

Bainite. No-Equilibrium . Atomic Mechanisms of Transformation

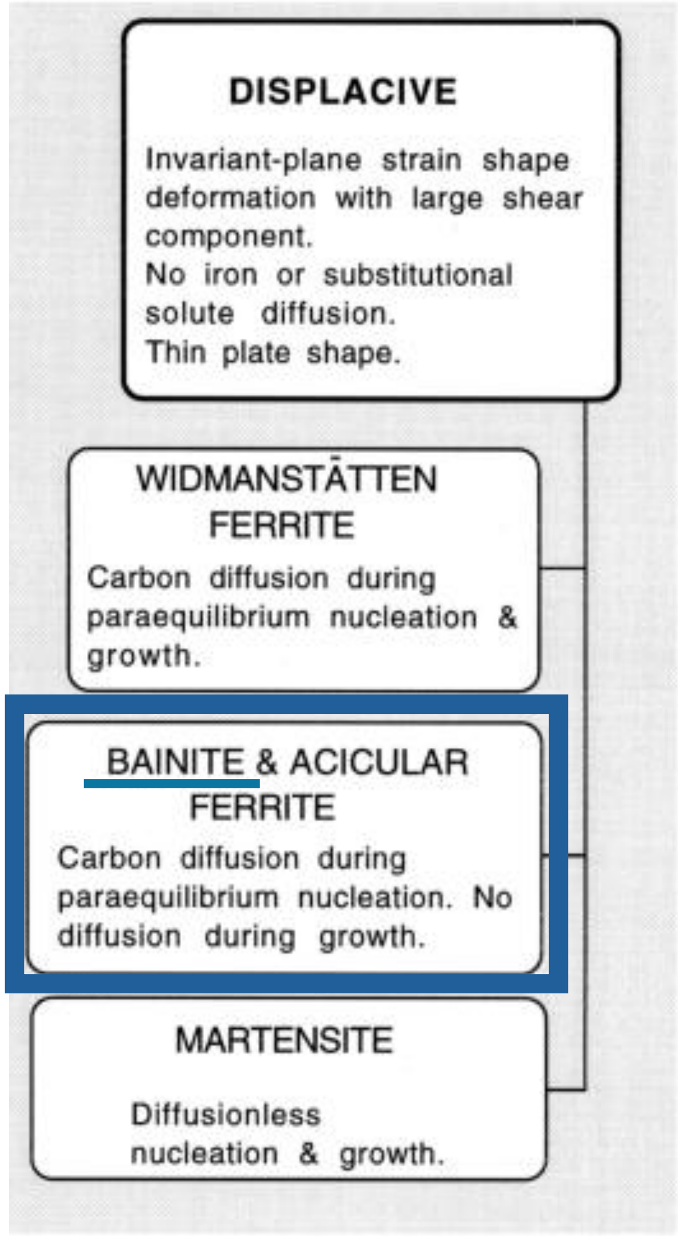

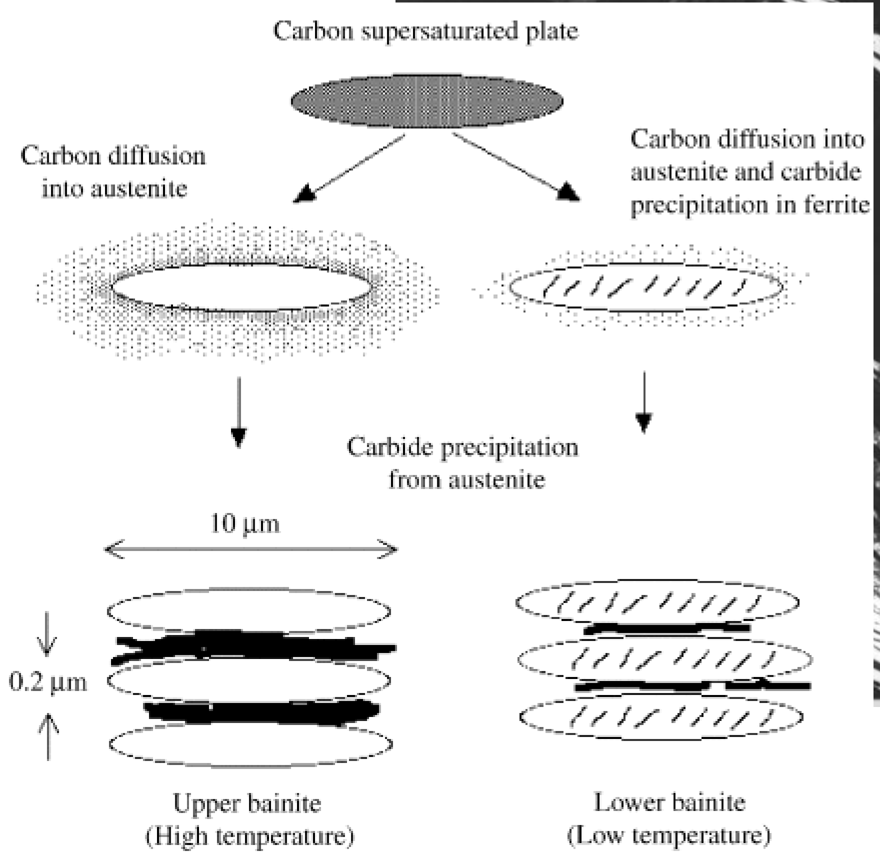

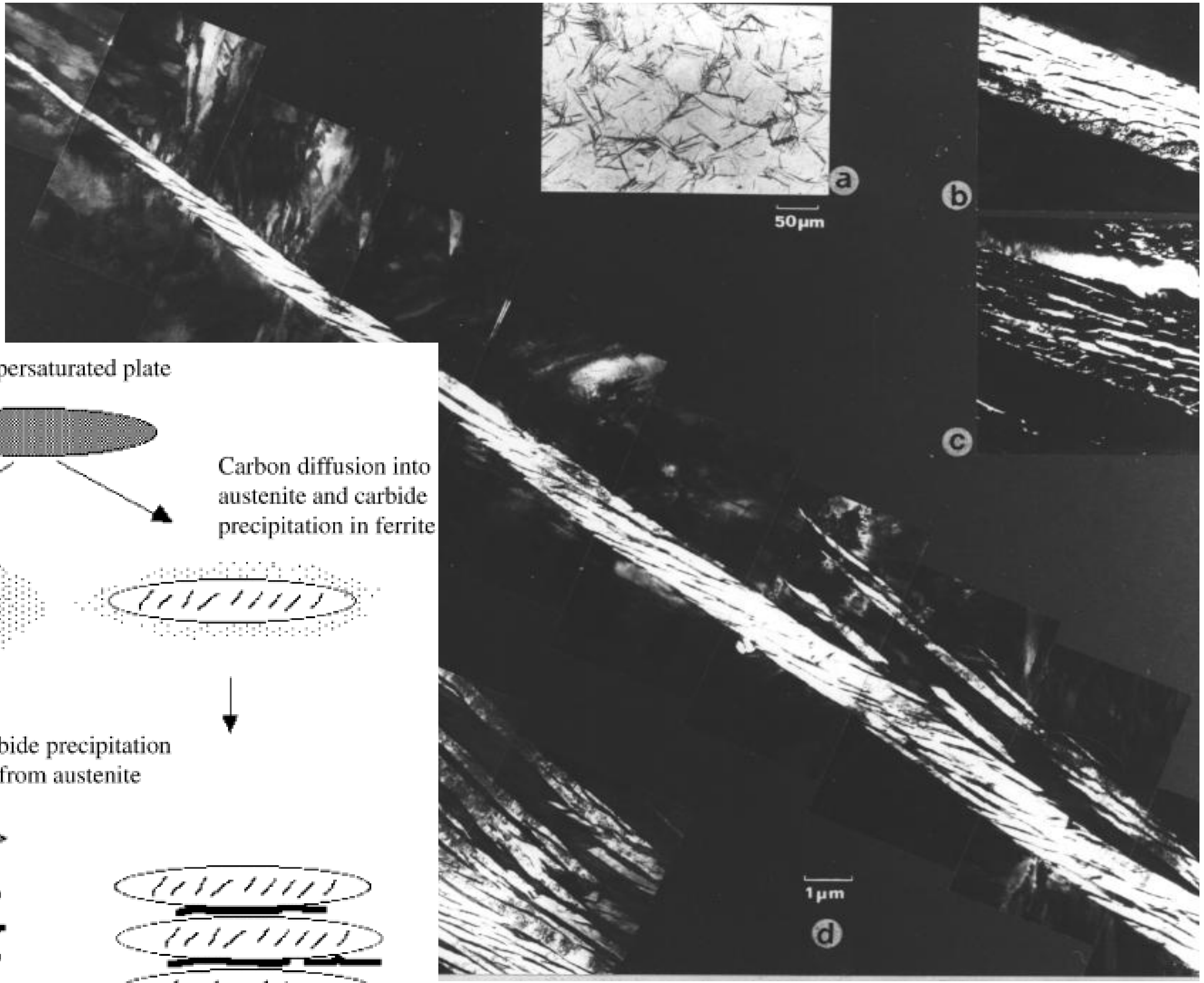

Bainite. Displacive transformation :

Pattern of atoms changes during transformation, a **disciplined motion** of atoms (**less than one inter-atomic spacing**) necessarily **leads** to a **change** in the **shape** of the **transformed region**, and like any deformation, such changes **cause strains** in the surrounding material.

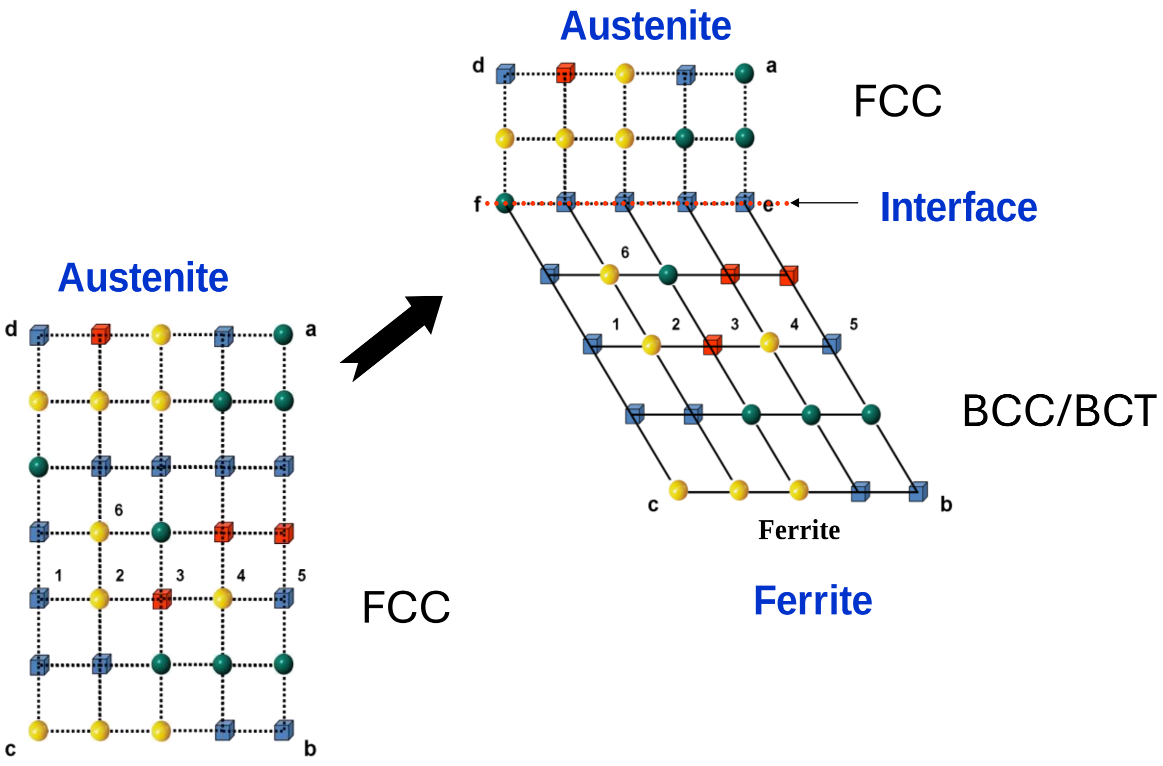

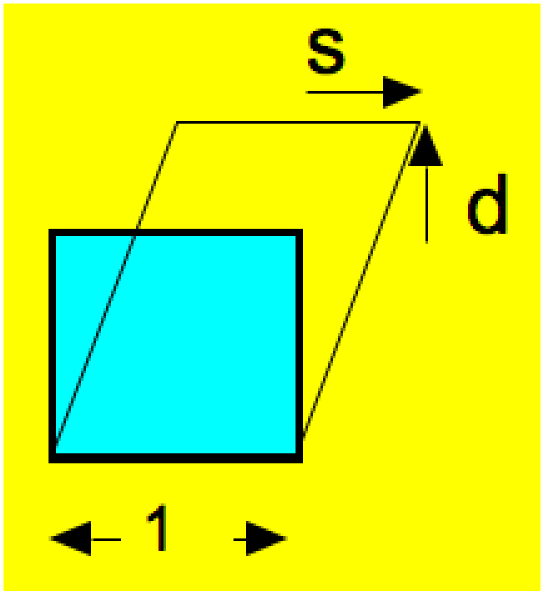

Invariant-plane strain shape deformation with **large shear** component (S) + **small dilatation** normal to the plane (d)

Bainite. Displacive transformation :

The **morphology** and **size of the bainitic ferrite** depend on the **minimization** of **strain energy** due to the shape deformation ➔ product phase **grows as thin plates/laths**

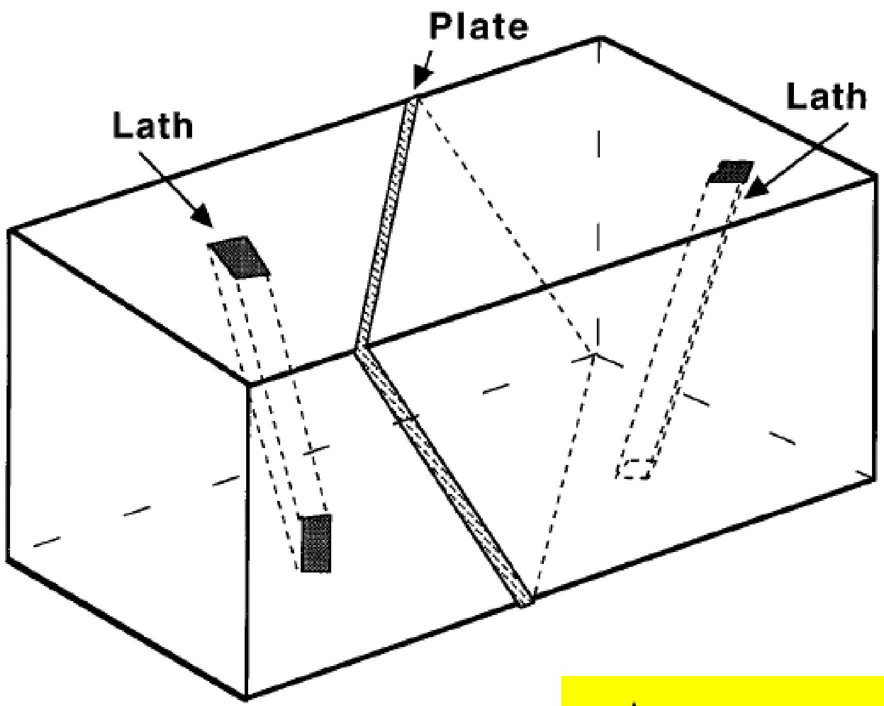

- Thin plate shape

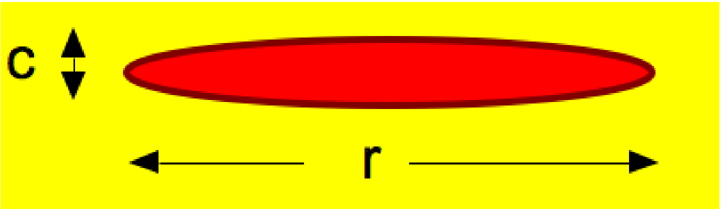

lath

plate

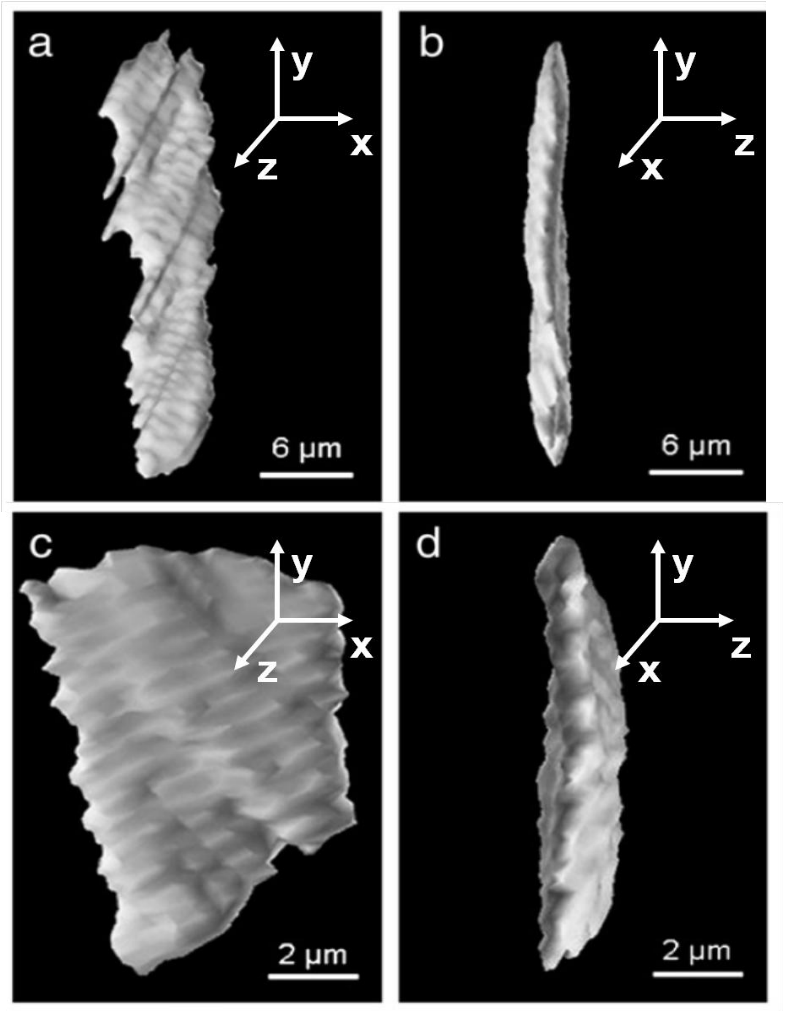

3D reconstruction of bainitic ferrite lath & plate .(FIB-Focused Ion Beam.) K. Liu, T.Q. et al Mater. Charact. 62 (2011)

Bainite. Displacive transformation :

•Bainite forms at a relatively high temperature when compared with martensite.

•The **parent austenite** is **weaker** at high temperatures and **cannot accommodate** the large **shape deformation elastically**.

• It therefore **relaxes by plastic deformation in the region adjacent to the bainite,** via **dislocations and accommodation twins**.

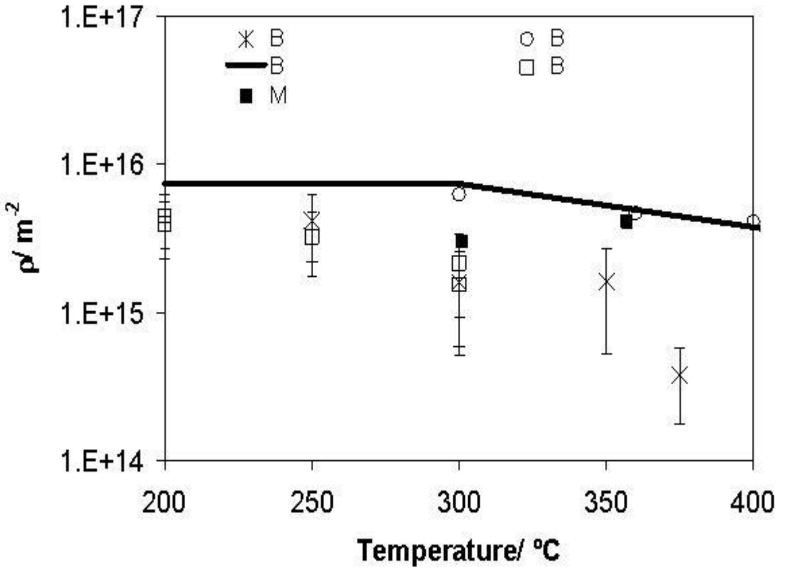

$$\log_{10}\{\rho_D\} = 9.2840 + \frac{6880.73}{T} - \frac{1780360}{T^2},$$

Structure	ρ x 10^{15} m^{-2}
Nanobain	2.2
Nanobain	4.5
Nanobain	6.4
Martensite	3.0-4.1
Conventional Bainite	0.2-0.4
Polygonal Ferrite	0.04-0.05

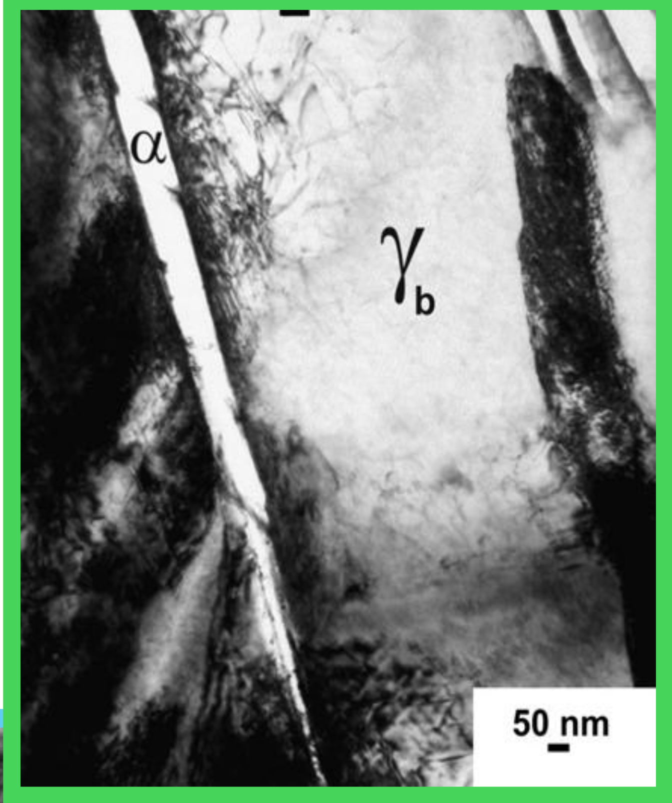

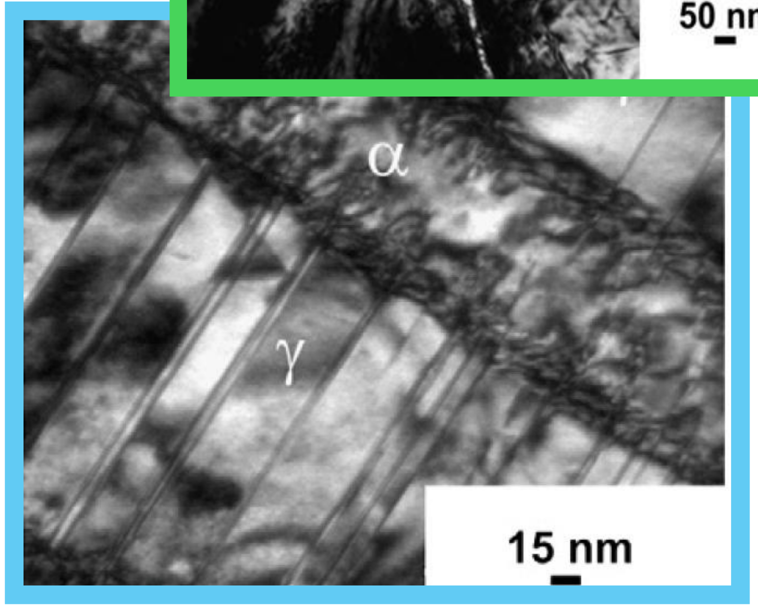

Taiwan Nat. Univ.

Garcia-Mateo et al. Scripta 61(2009)
F.G. Cabllero et al. Acta Mater. (2011)

Bainite. Diffusionless transformation :

No iron or substitutional solute diffusion.

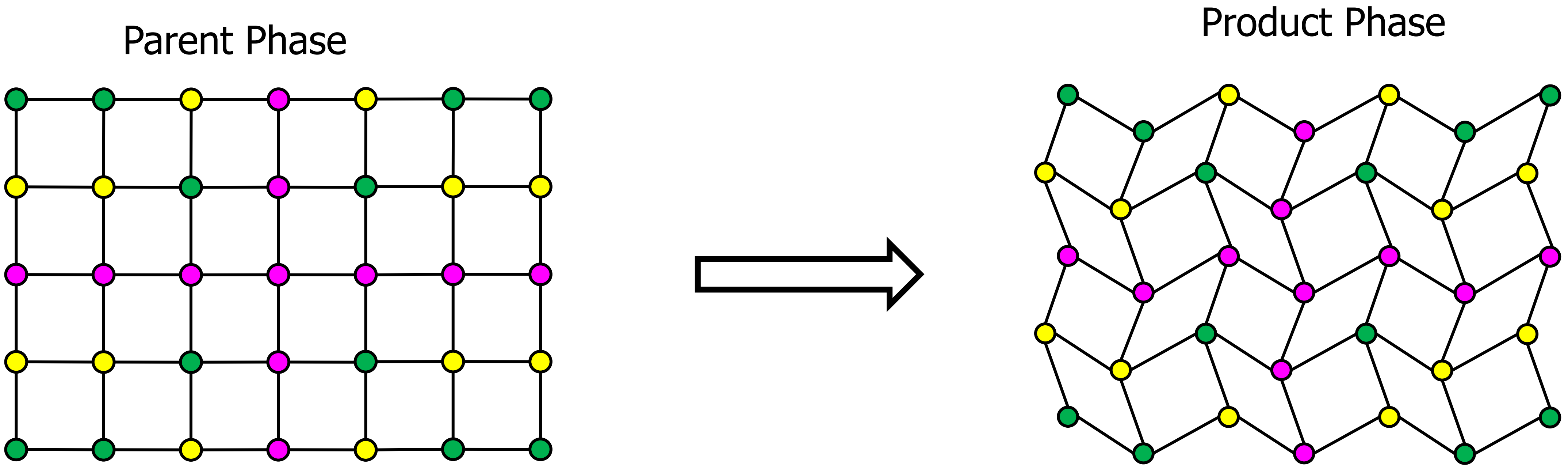

Bainite. Nucleation sites and growth evolution

At transformation temperature

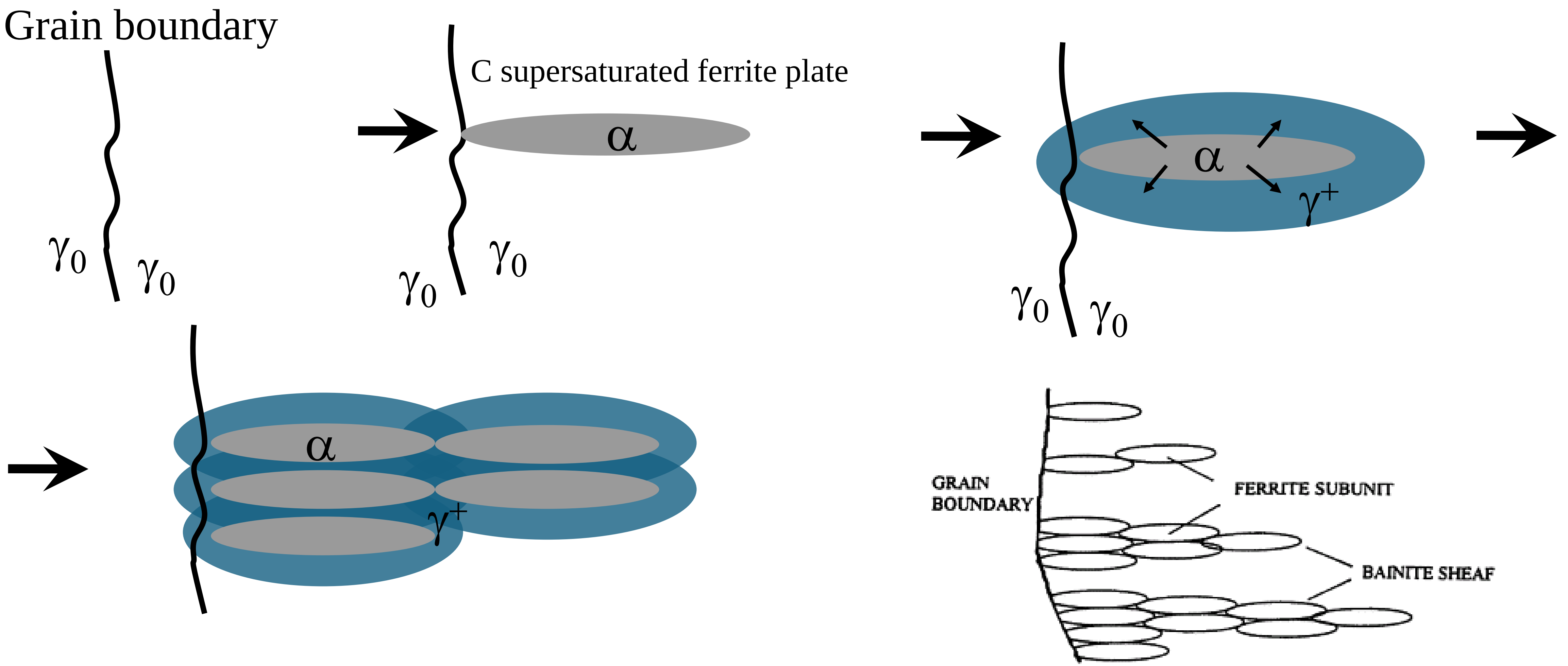

New formed bainitic plates provide new potential nucleation sites for **autocatalytic/sympathetic** nucleation

Bainite. Nucleation sites and growth evolution

At transformation temperature

Austenite grains boundaries from which they are forming, act as **physical barriers**.
It is a limiting barrier to end its growth

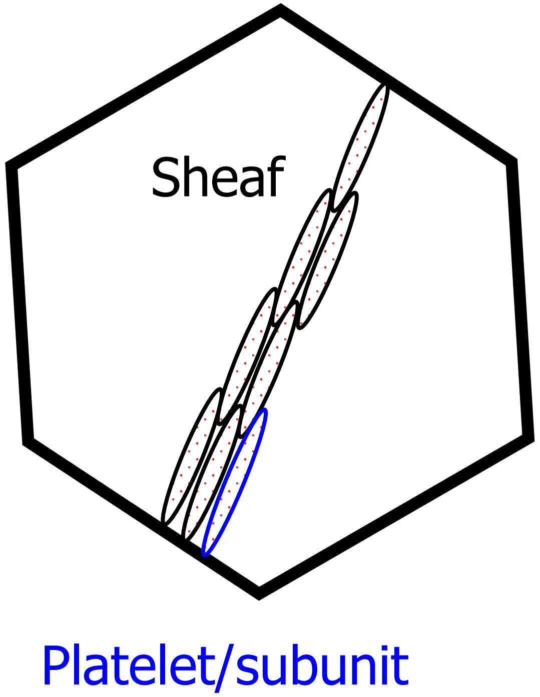

As multiple bainite plates/sheaves nucleate and grow, they will inevitably **collide with each other (hard impingement)**, **halts the growth/thickening**.

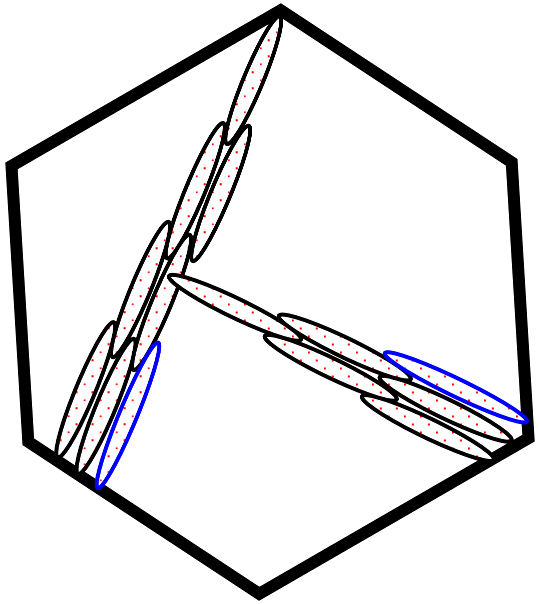

Oblak and Hehemann (1967) in Transformation and Hardenability in Steels, 15–30.
Kinsman and Aaronson (1967) in Transformation and Hardenability in Steels, 33–38.

Bainite. Nucleation sites and growth evolution

At transformation temperature

Cementite (θ) can then precipitate :

- from the γ^+ between the ferrite plates (both upper and lower bainite)
- within the bainitic ferrite plates

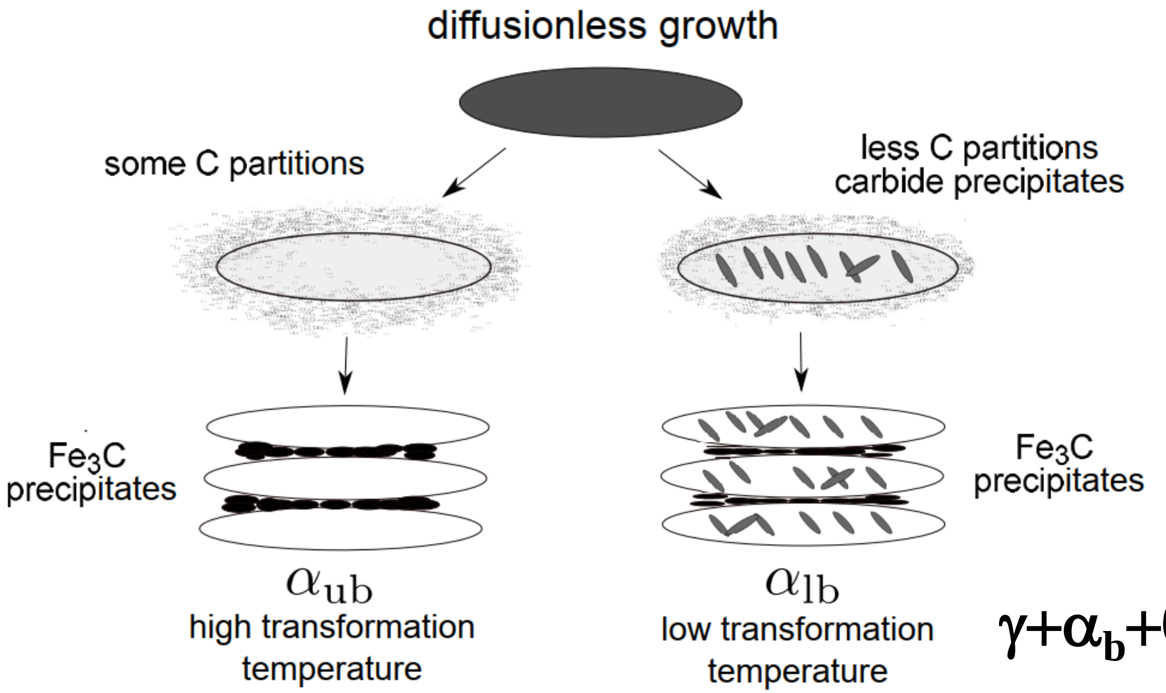

$\gamma+\alpha_b+\theta$

The difference comes from the **competition between the rate at which cementite can precipitate from ferrite and the speed with which C is partitioned from supersaturated ferrite into austenite.**

Bainite. Nucleation sites and growth evolution

At transformation temperature

Cementite (θ) **can be avoided** by the introduction of Si

Carbide free Bainite (CFB)

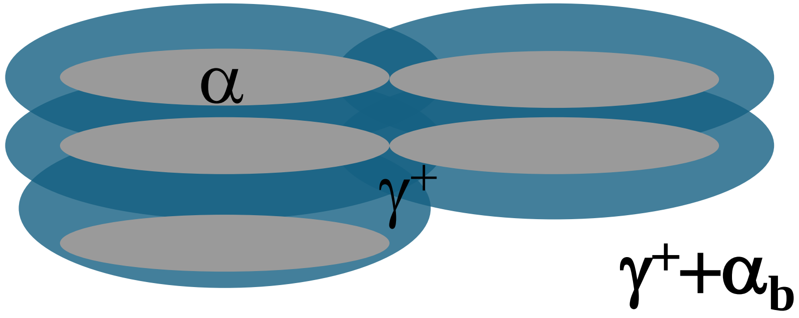

- Silicon has a **limited solubility in cementite** (Fe3C), retards the nucleation and growth of cementite.

Bainite. Nucleation sites and growth evolution

At transformation temperature

No Si

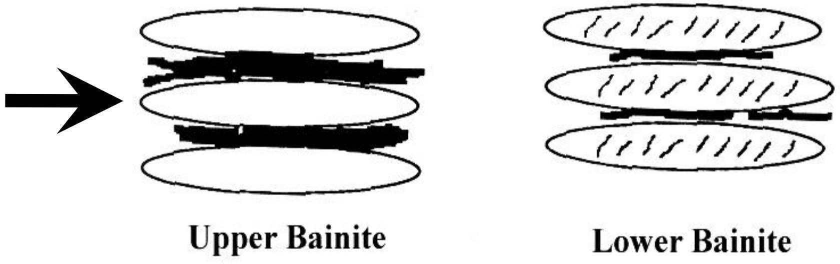

$\gamma+\alpha_b+\theta$

Si rich steels

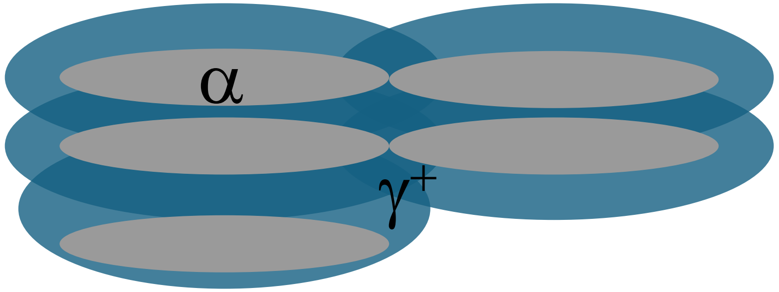

$\gamma^{+}+\alpha_b$

At room temperature

At room temperature Bainitic ferrite (α_b) +2nd phases → θ, γ^{+}, α'

Two main morphologies of austenite

- ❑ **Blocks** between the sheaves of bainite
- ❑ **Thin films**, in between the plates

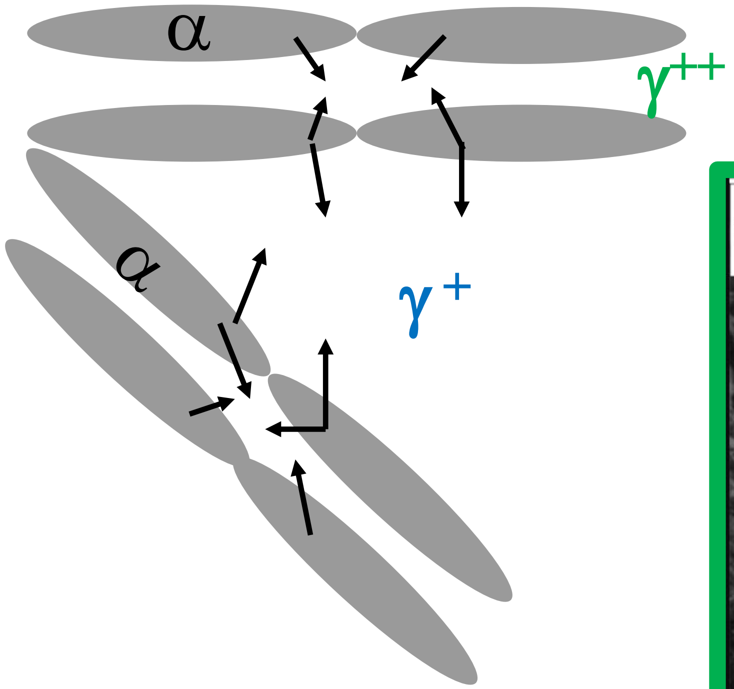

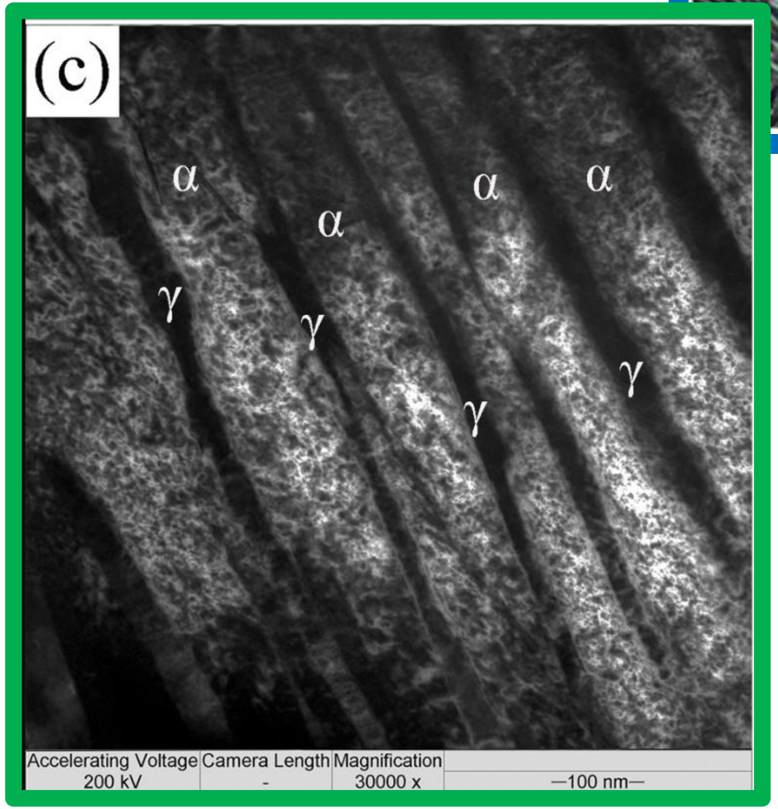

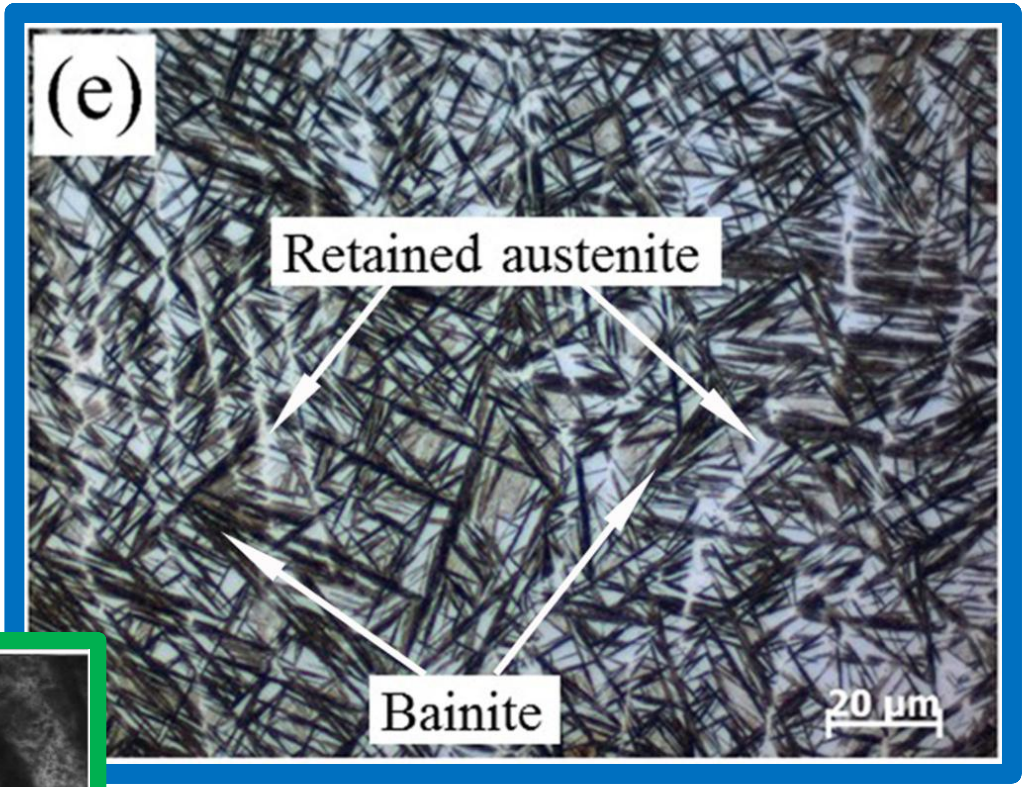

Guo, Y.; Feng, K.; Lu, F.; Zhang, K.; Li, Z.; Hosseini, S.R.E.; Wang, M, doi:10.1016/j.apsusc.2015.08.132.

Thermodynamics

Nucleation : Under paraequilibrium condition (only C diffuses)

$$\Delta G^{\gamma \rightarrow (\gamma+\alpha)_p} < G_N$$

G_N defines the **minimum free energy change** necessary in **any steel**, in order to **nucleate bainite.** It is a **universal nucleation function :**

$$G_N = 3.5463T(K) - 3499.4 \ J\,mol^{-1}$$

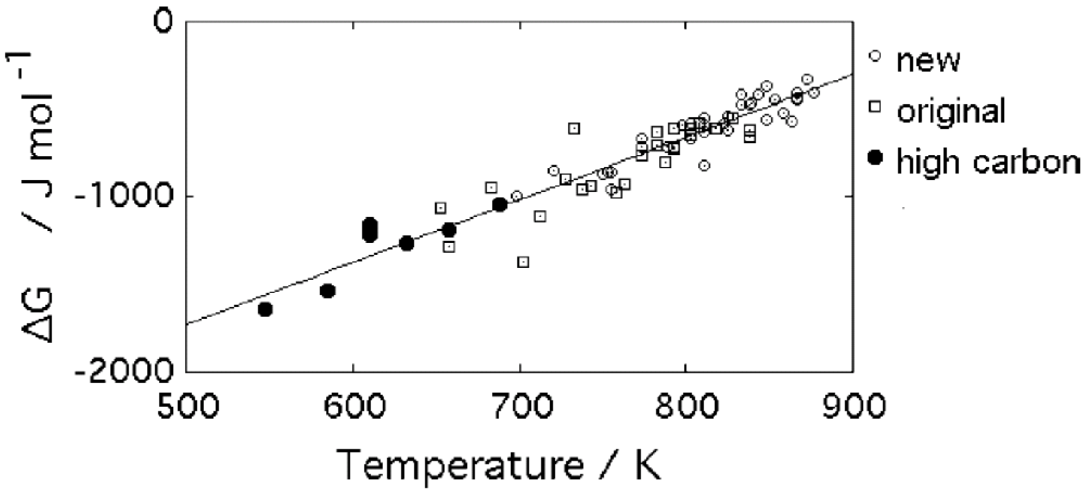

Bhadeshia, H. K. D. H. (2001). Bainite in Steels.
Garcia-Mateo, C. Mater. Sci. Eng. A

Thermodynamics

Growth : **Diffusionless growth**. No change of chemical composition from the parent phase to the product phase.

$$\Delta G^{\gamma \rightarrow \alpha}$$

Bhadeshia, H. K. D. H. (2001). Bainite in Steels.
Garcia-Mateo, C. Mater. Sci. Eng. A

Thermodynamics

Growth : **Diffusionless growth**. No change of chemical composition from the parent phase to the product phase.

$$\Delta G^{\gamma \rightarrow \alpha}$$

Displacive transformation :

Invariant-plane strain shape deformation with large shear component.

Stored energy of the ferrite due to the **displacive** mechanism of transformation **400 J/mol = G_{SB}**

Bhadeshia, H. K. D. H. (2001). Bainite in Steels.
Garcia-Mateo, C. Mater. Sci. Eng. A

Thermodynamics

Growth : Diffusionless & Displacive

$$\Delta G^{\gamma \rightarrow \alpha} < -G_{SB}$$

Stored energy of the ferrite due to the **displacive** mechanism of transformation **400 J/mol = G_{SB}**

Bhadeshia, H. K. D. H. (2001). Bainite in Steels.
Garcia-Mateo, C. Mater. Sci. Eng. A

Thermodynamics. Critical Transformation T

$$\Delta G^{\gamma\rightarrow(\gamma+\alpha)_p} < G_N$$

$$\Delta G^{\gamma\rightarrow\alpha} < -G_{SB}$$

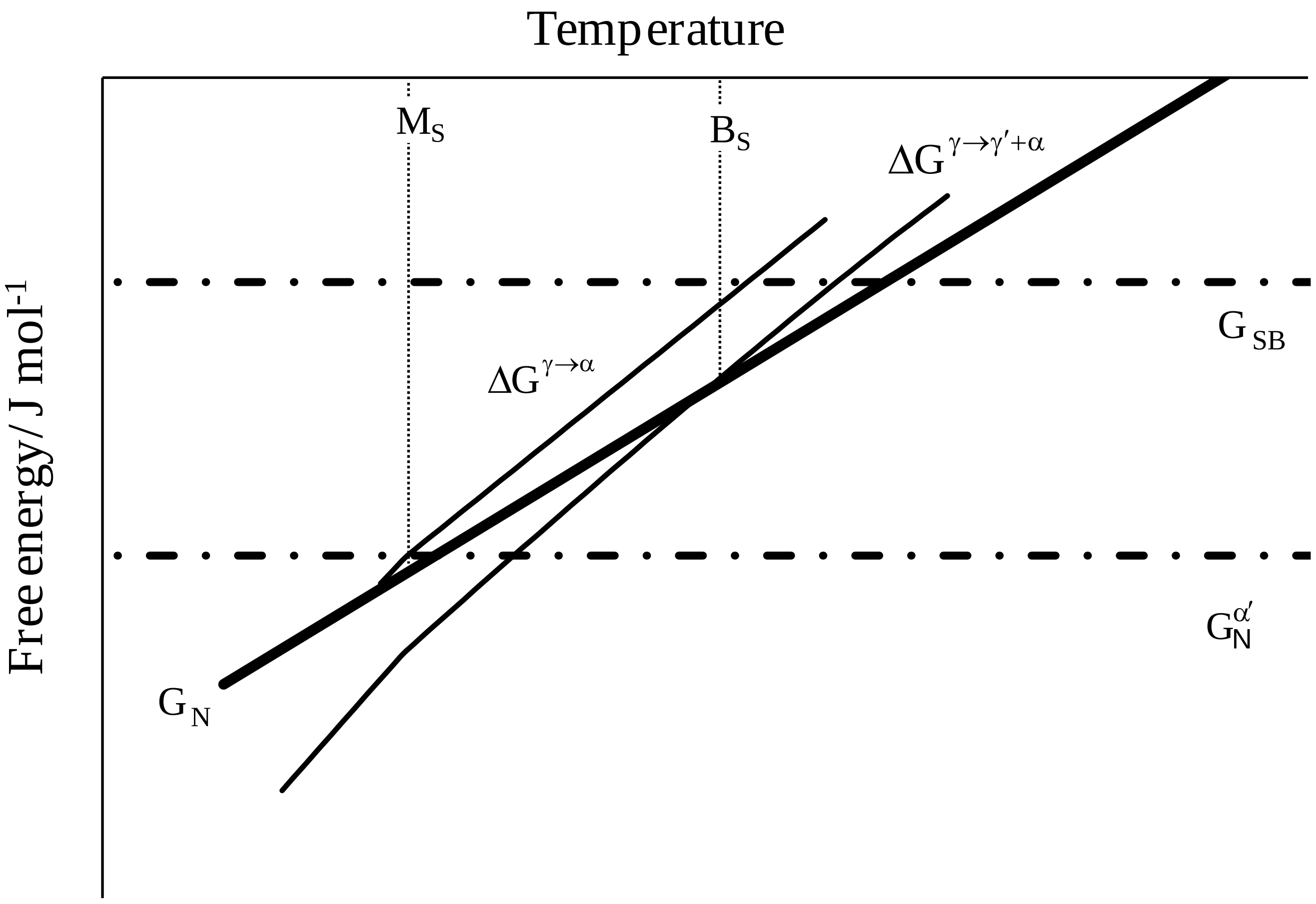

$G_N^{\alpha'}$ represents the critical value of the free energy change $\Delta G^{\gamma\rightarrow\alpha}\{M_s\}$

needed before the athermal, diffusionless nucleation and growth of martensite becomes possible

$$\Delta G^{\gamma\rightarrow\alpha}\{M_s\} < G_N^{\alpha'}$$

How far the transformation can proceed?

Does 100% of the austenite transform into bainite?

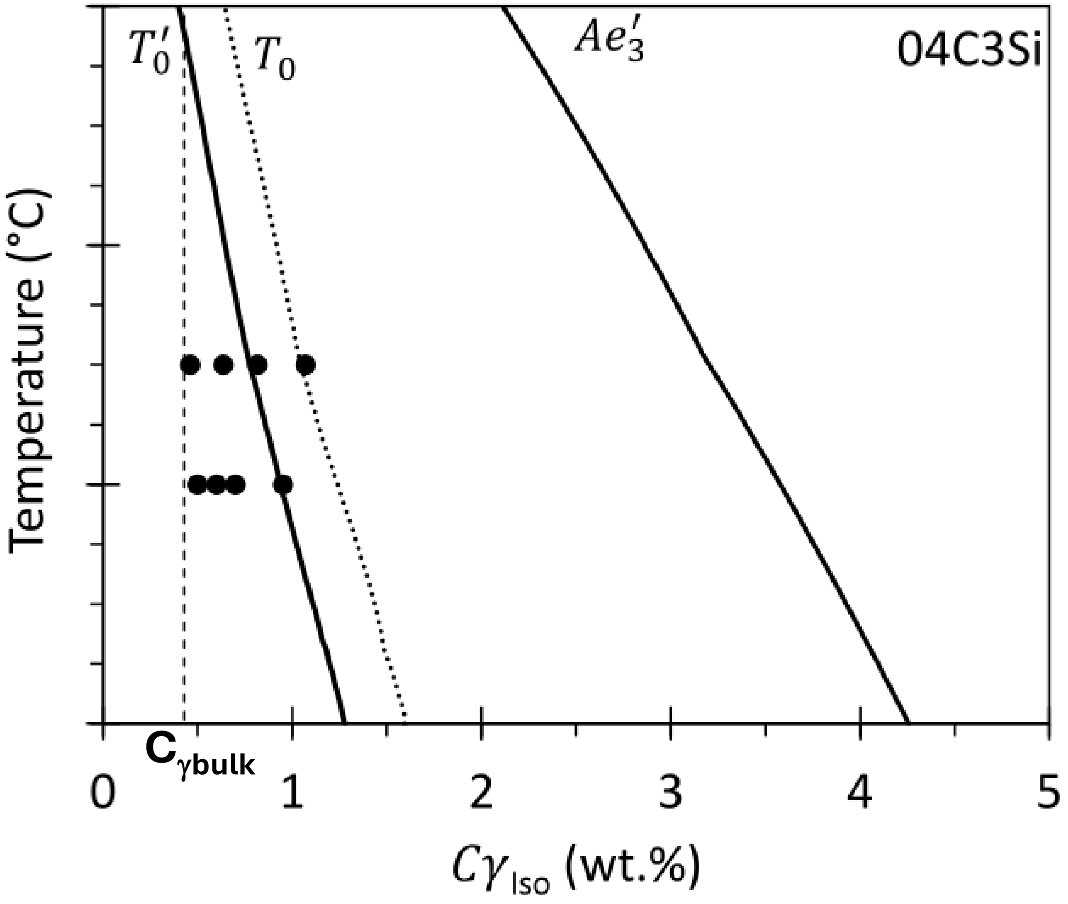

NO. As austenite gets richer and richer in C there is a limit where it is **thermodynamically impossible** for the transformation to proceed.

$$\Delta G^{\gamma \rightarrow (\gamma+\alpha)_p} < G_N$$

$$\Delta G^{\gamma \rightarrow \alpha} < -G_{SB}$$

Incomplete reaction phenomena, T_0 line

Incomplete reaction phenomena, T_0 line

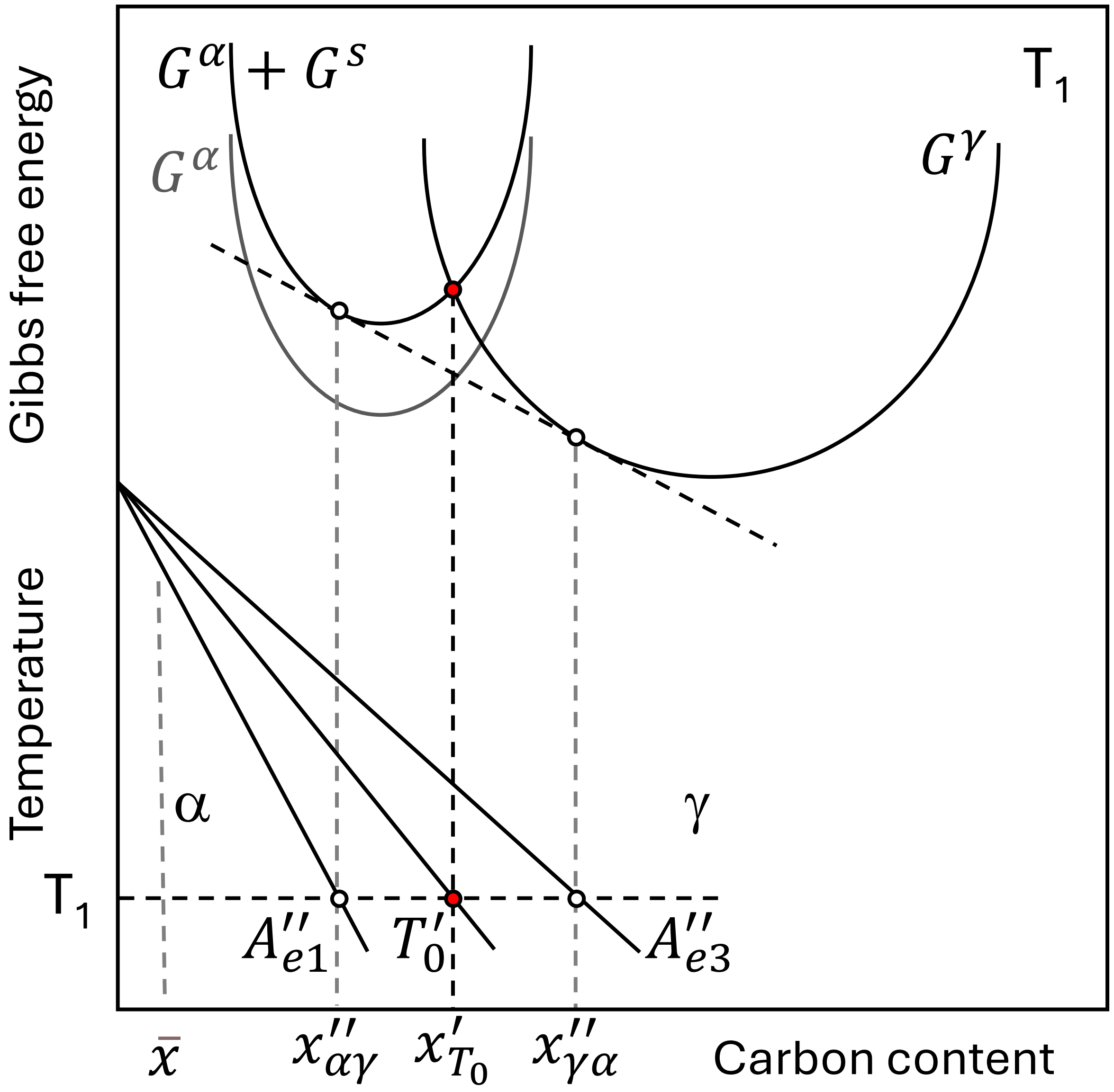

The **lower** the **transformation temperature**, the **further** the **transformation** can **proceed ➔ higher % C in austenite** is allowed **in austenite**; in other words ➔ **higher fractions of bainitic** ferrite are obtained.

↑V_b ↓T

$$v_{\alpha B-\max} = \frac{x_{T'_0} - \bar{x}}{x_{T'_0} - x^{\alpha\gamma}}$$

Bhadeshia and Christian (1990) Metall. Trans. A, 21 A(4):767–797.

Understanding the C journey in bainite. Tracking the C in its "journey" from $\alpha \rightarrow \gamma$

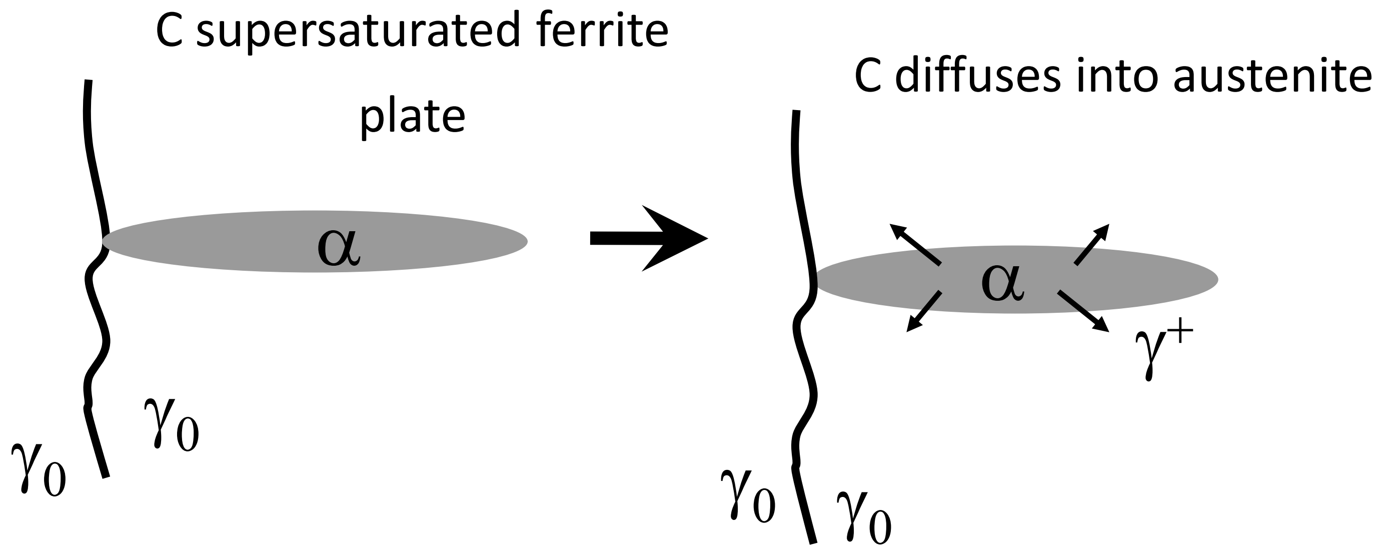

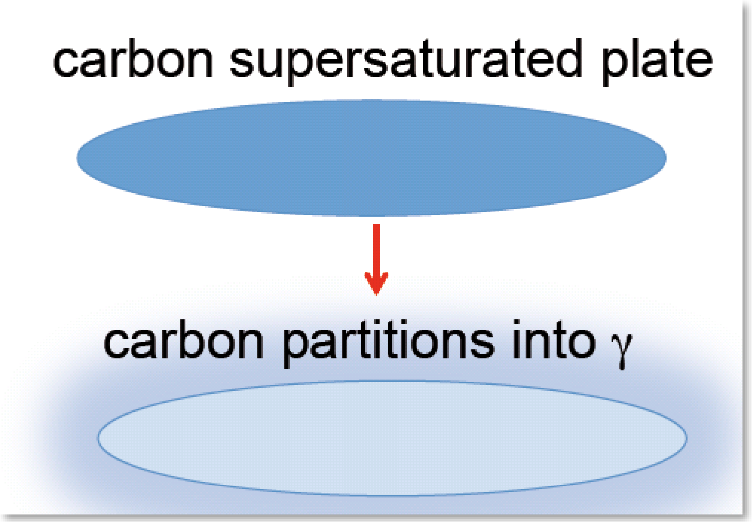

Q1-Does all the C reach the parent γ?

Q2- Does all the γ receive the same amount of C? (why/where & how to measure it?)

Q3-Does all the C escapes from α?

Tracking the C in its "journey" from

$\alpha \rightarrow \gamma$

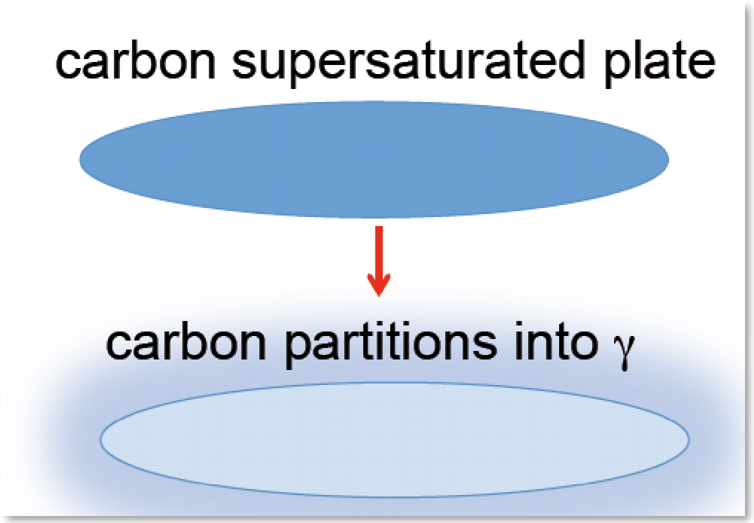

Q1-Does all the C reach the parent γ?

Q1. Does all the C reach the parent γ?

Relaxation of the strains via **dislocations** **and accommodation twins**

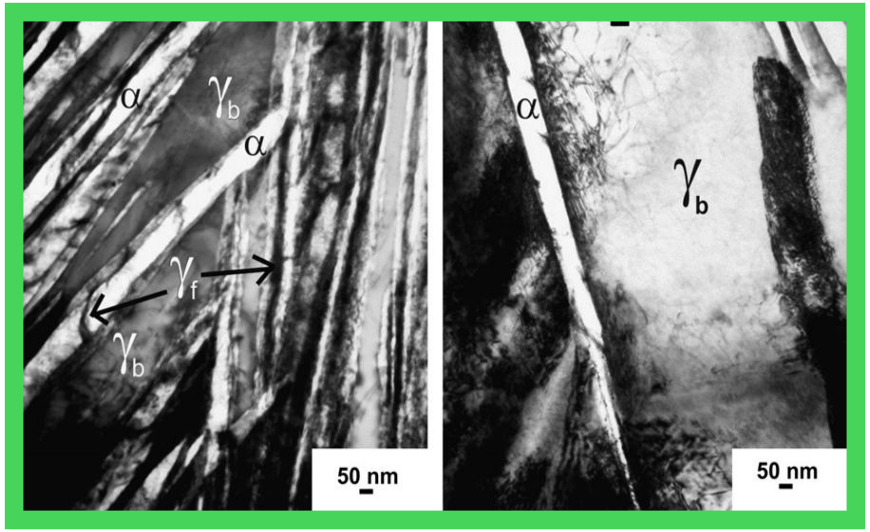

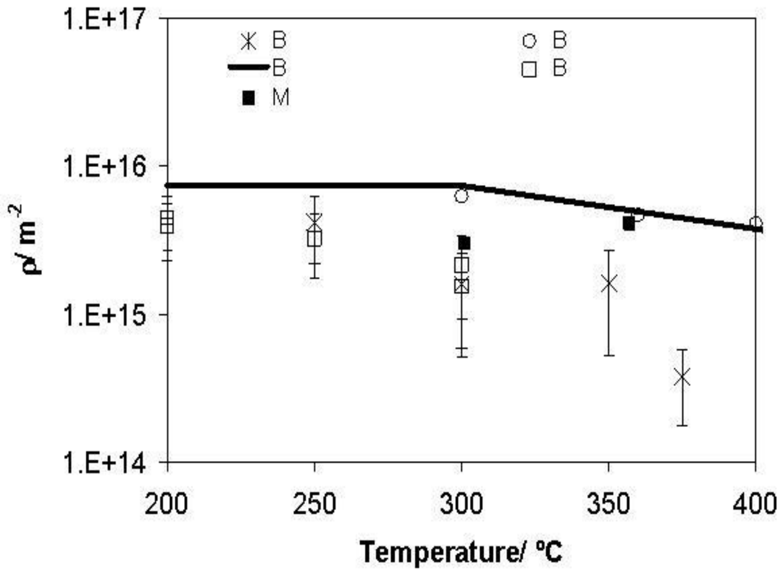

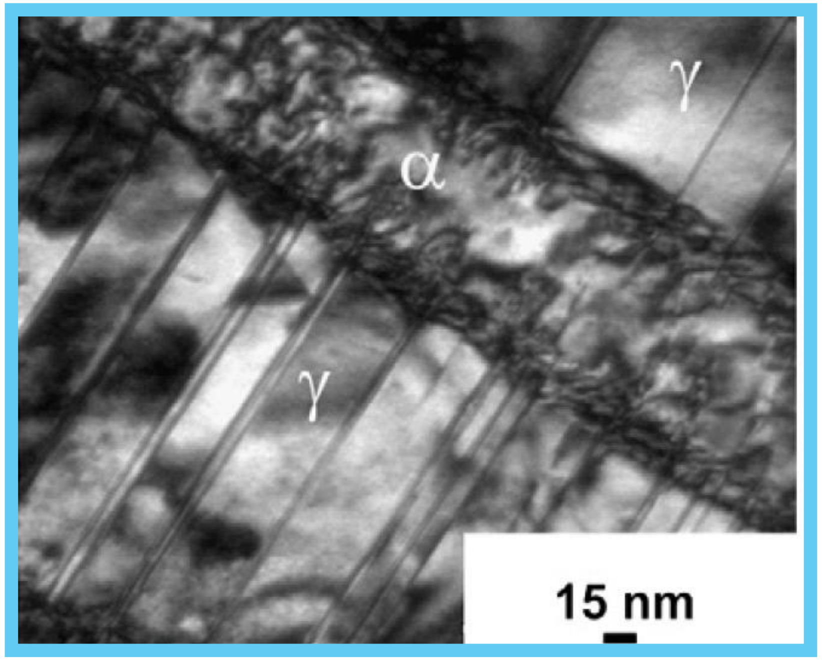

Q1. Does all the C reach the parent γ? A1- No

C is trapped at dislocations (**Cottrell atmosphere**) and twins, it also forms **clusters**

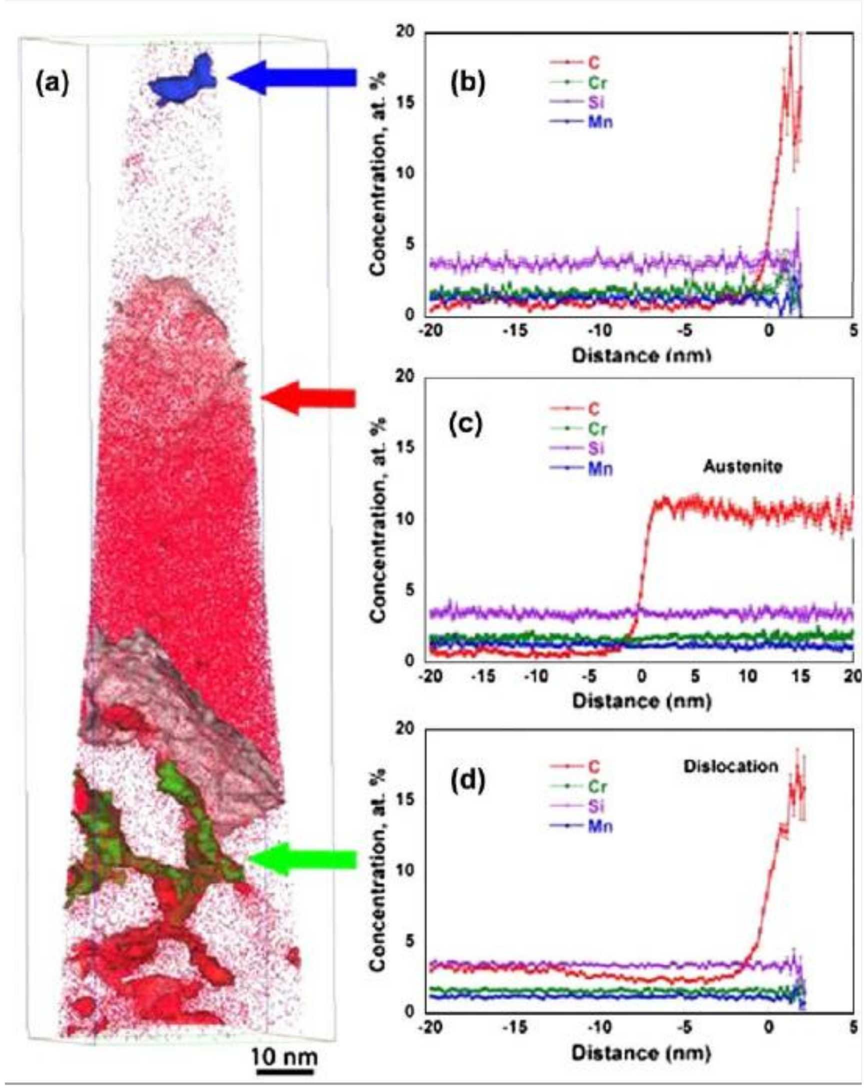

clusters

Cottrell atm.

twins

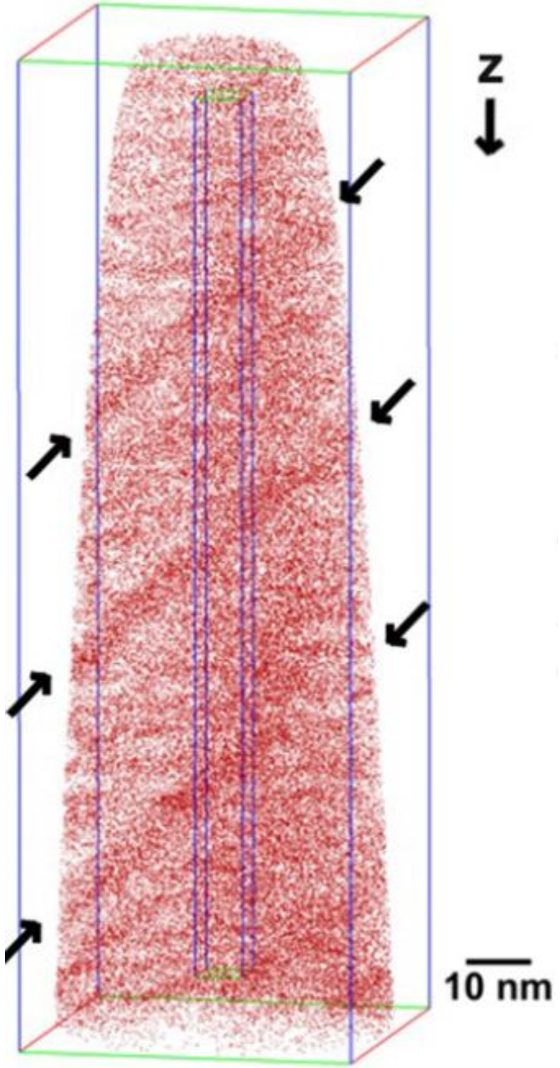

ORNL collab.

200 ºC for 2 days.

Caballero . Acta 2010 & 2011

Tracking the C in its "journey" from

$\alpha \rightarrow \gamma$

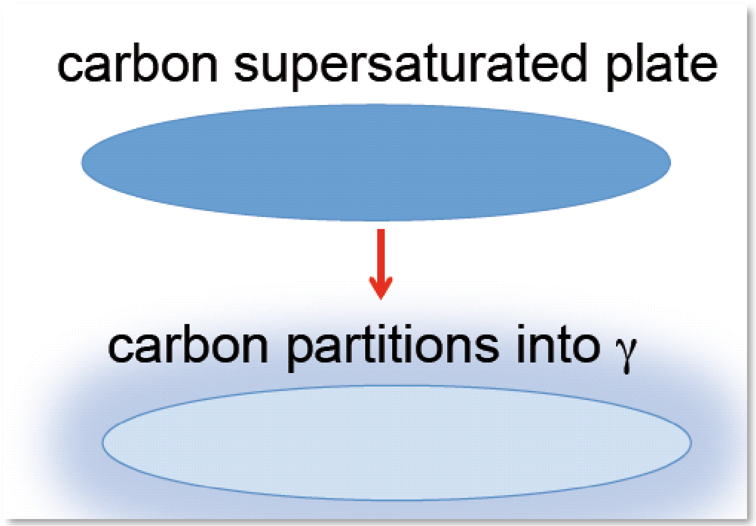

Q2- Does all the γ receive the same amount of C? (why/where & how to measure it?)

Q2- Does all the γ receive the same amount of C?

The amount of C that retained austenite receives from supersaturated plates of bainitic ferrite will depend on the neighbourhood…….

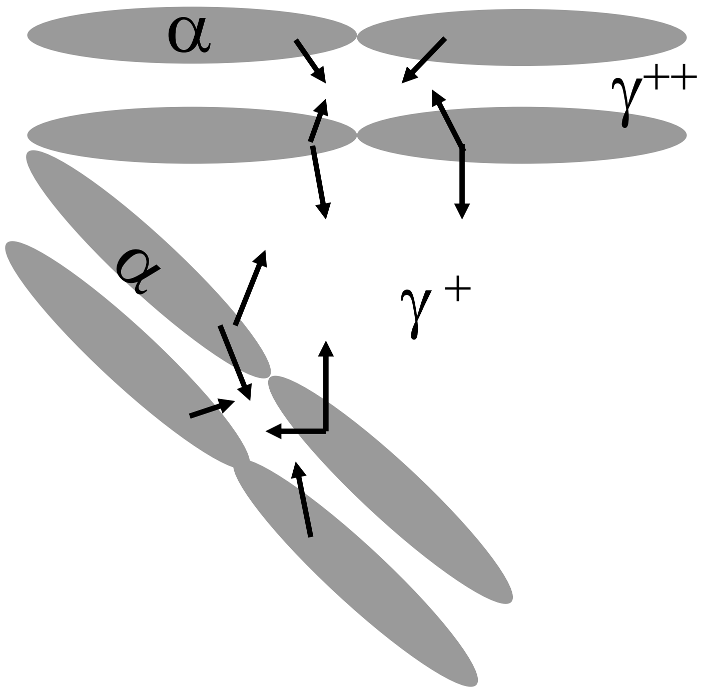

Thin films have many "close" neighbours willing to relieve some of its C content ➔ thin films will get "**a lot**" of C

Blocks have less neighbours, and some are far away ➔ block will get "**less**" C

Garcia-Mateo Mater. Sci. Eng. A (2012)

Q2- Does all the γ receive the same amount of C?

In-Situ Observations in a synchrotron beam line, **2^{nd} set of experiments , higher resolution**.

A-Initial pattern consisted of narrow peaks exclusively from austenite.

B-Their intensity decreased as transformation progressed.
In addition, **broad ferrite peaks** appeared along with **a second set of broad austenite peaks** at lower 2θ angles than the initial ones.

The **latter is caused by the partitioning of carbon from the bainite into the residual austenite, thereby leading to an increase in its lattice parameter.**

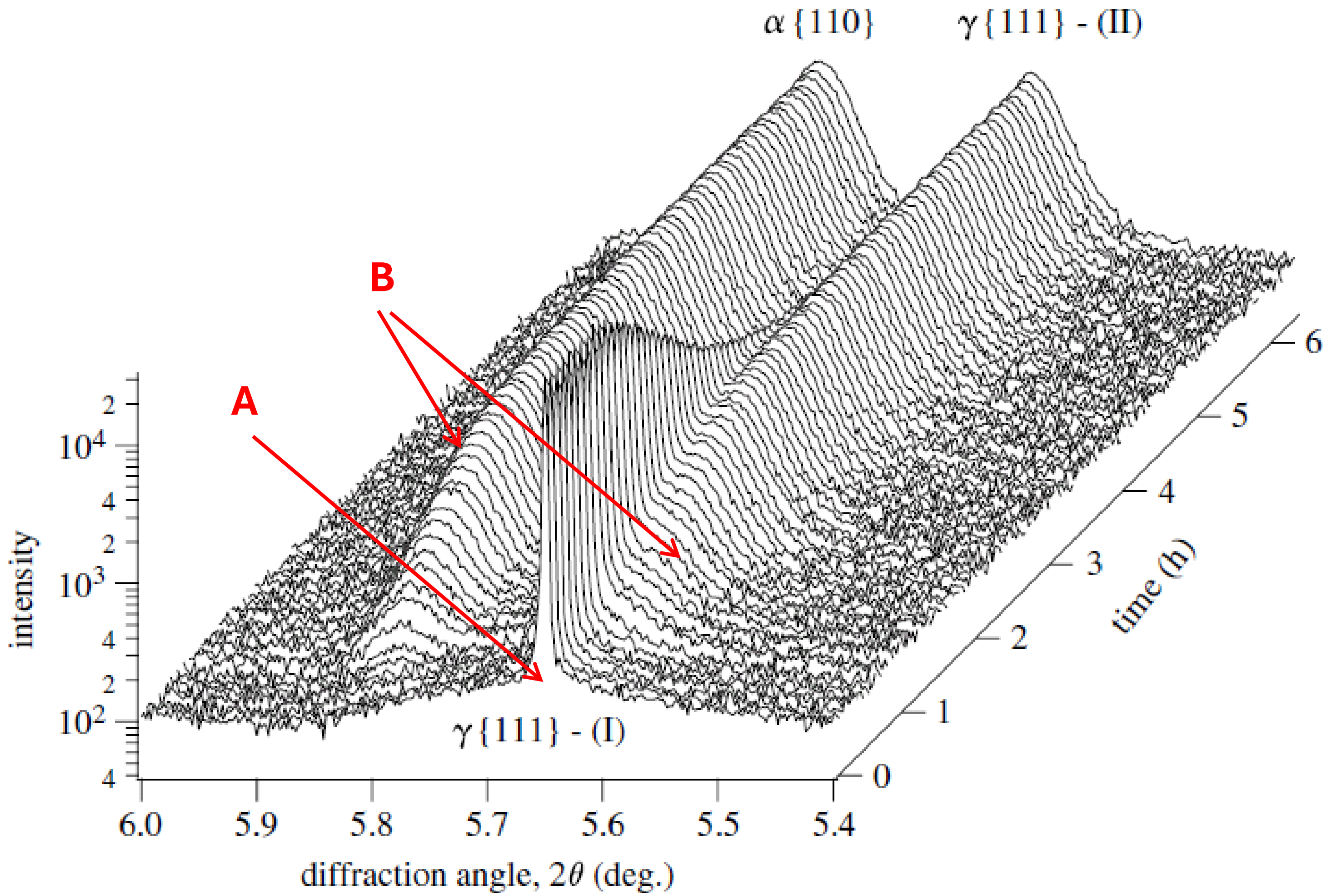

Stone, H. J., M. J. Peet, H. K. D. H. Bhadeshia, P. J. Withers, S. S. Babu and E. D. Specht (2008). Proc. R. Soc. A

Q2- Does all the γ receive the same amount of C?

In-Situ Observations in a synchrotron beam line, 2nd set of experiments , **higher resolution**.

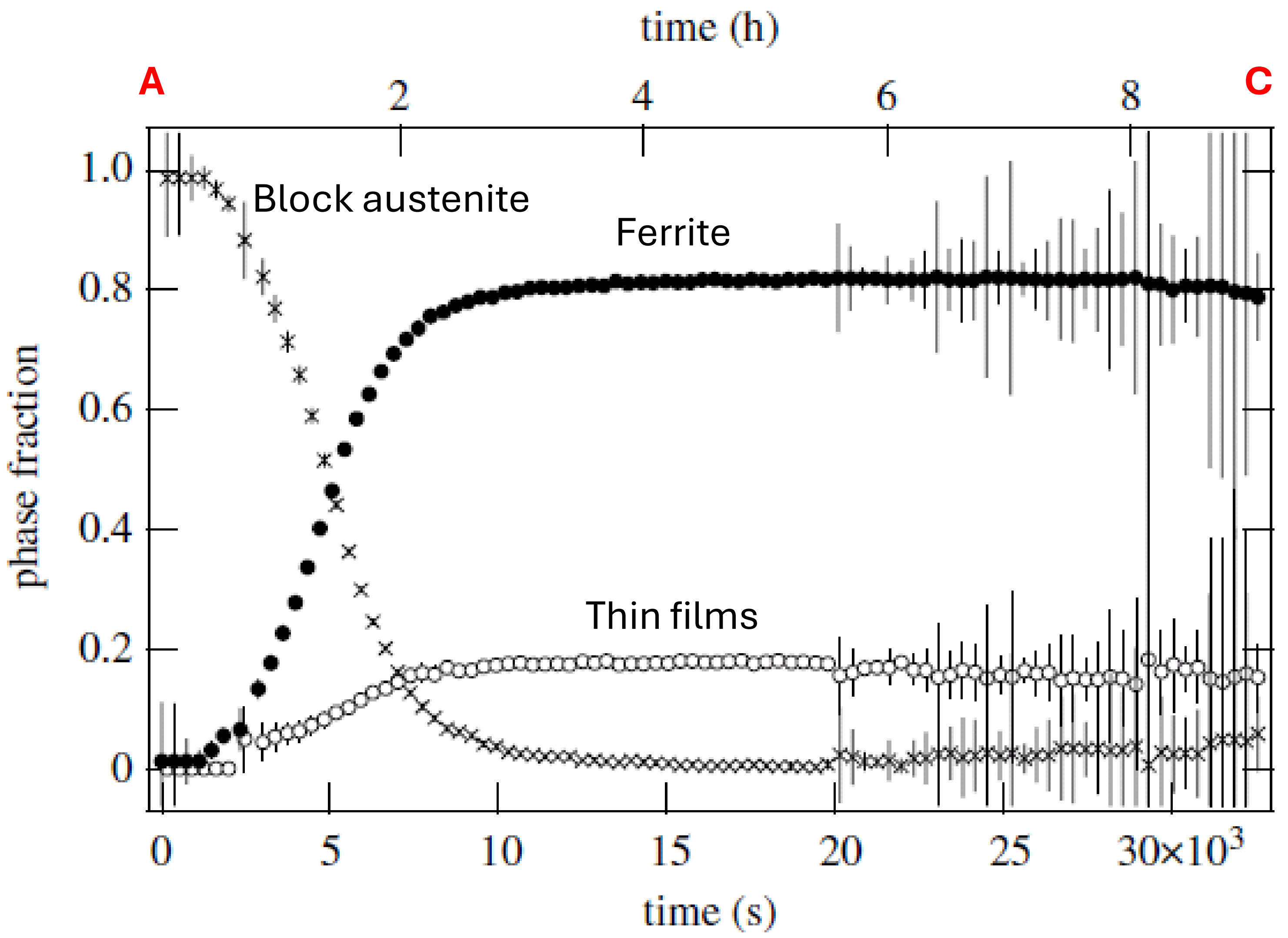

Q2- Does all the γ receive the same amount of C?

Ex-Situ Observations in a 3D Atom probe tomography

Fe-4.3C-2.8Si-1.2Mn-1.3Cr (at.%); 200 °C, 10 days

11 at.%C

12 at.%C

12 at.%C

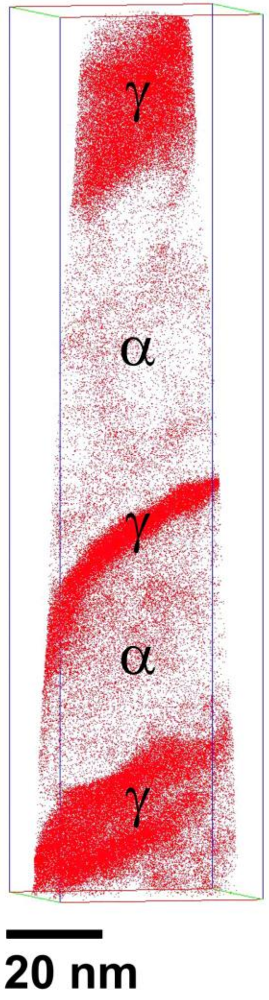

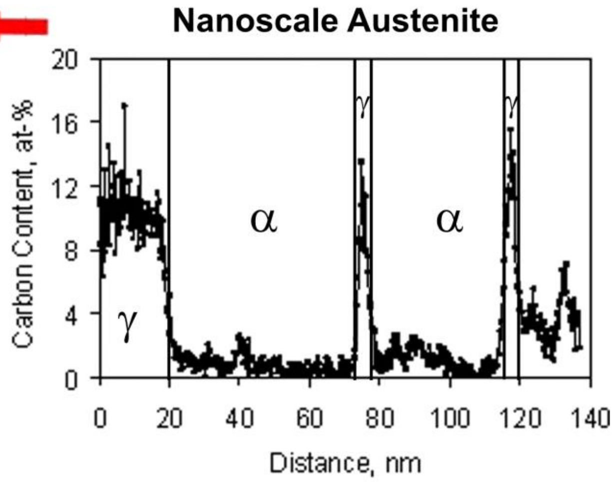

Nanoscale Austenite films

6 at.%C

Sub-micron Austenite block

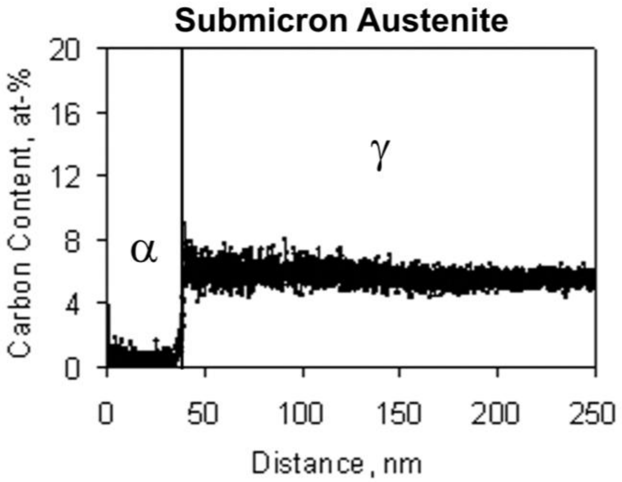

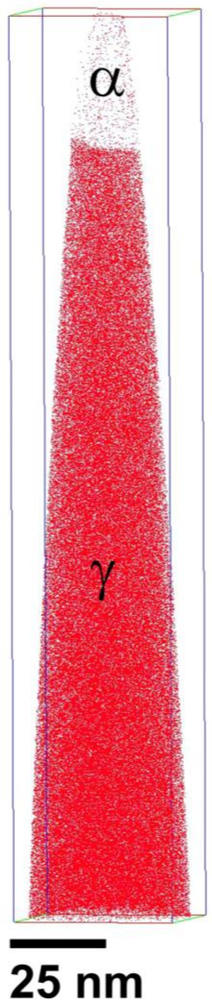

Austenite films entrapped between neighboring subunits of bainitic ferrite

Blocks of residual austenite located between the sheaves of bainite

Q2- Does all the γ receive the same amount of C?

A2- No

Size/location is paramount

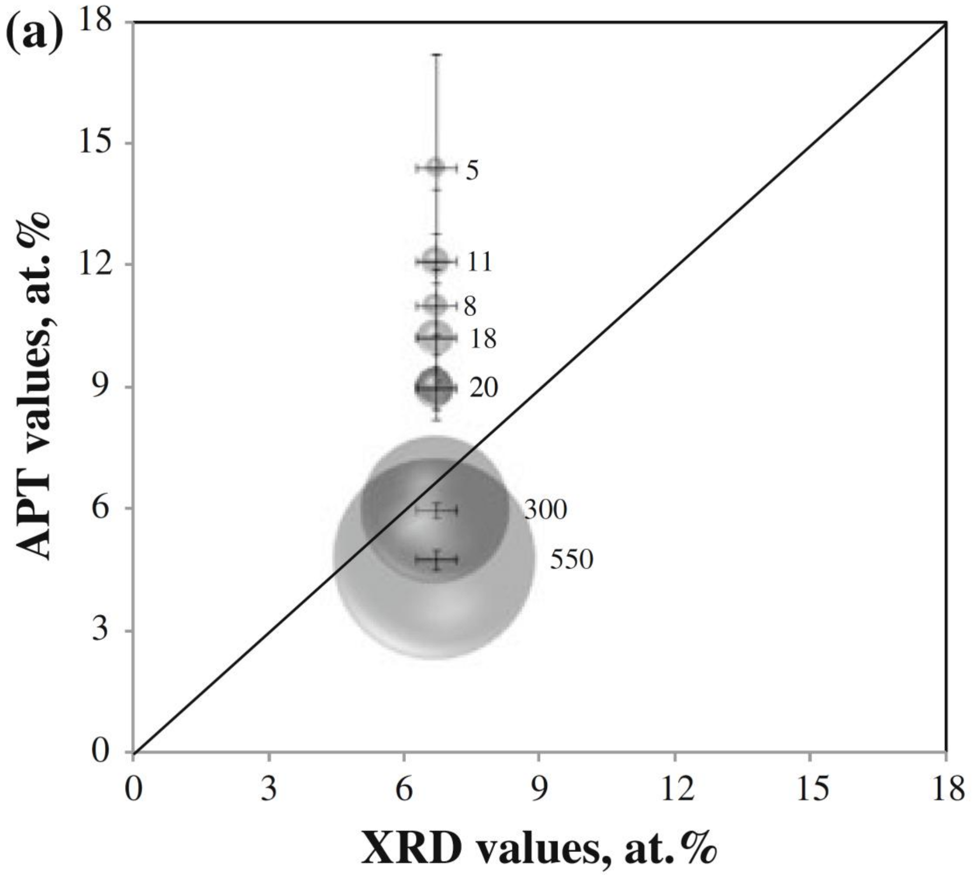

Tracking the C in its "journey" from

$\alpha \rightarrow \gamma$

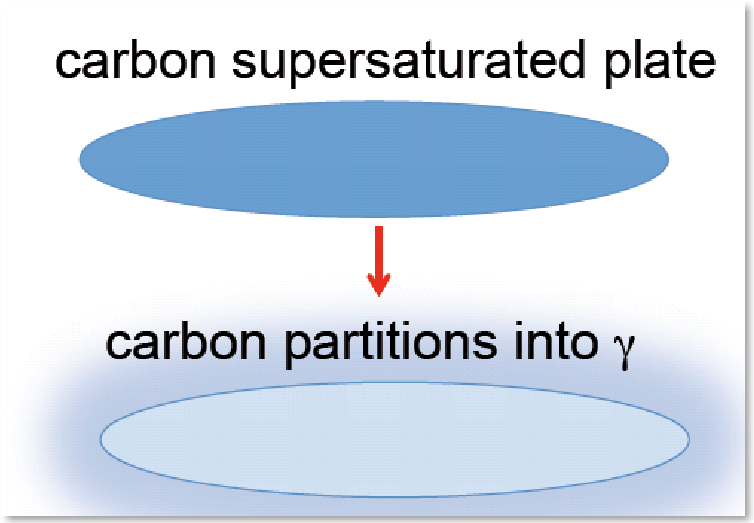

Q3-Does all the C escapes from α?

Q3-Does all the C escapes from α?

APT values away from defects or clusters

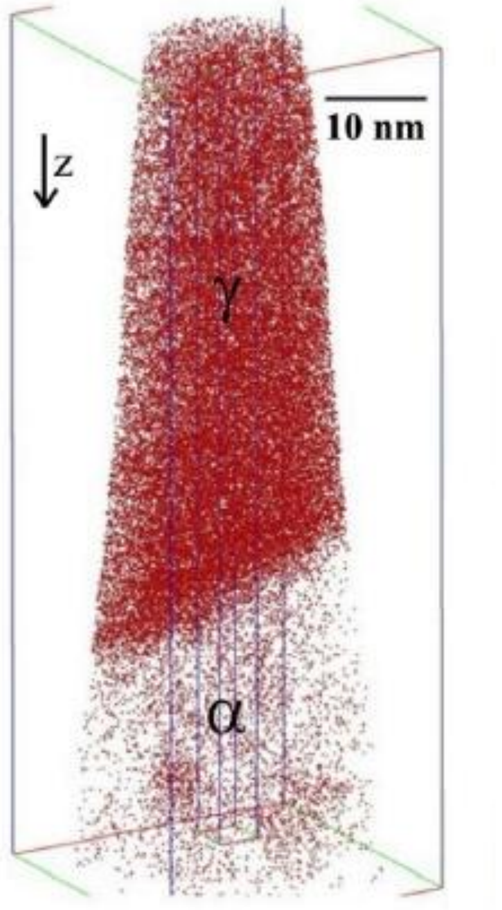

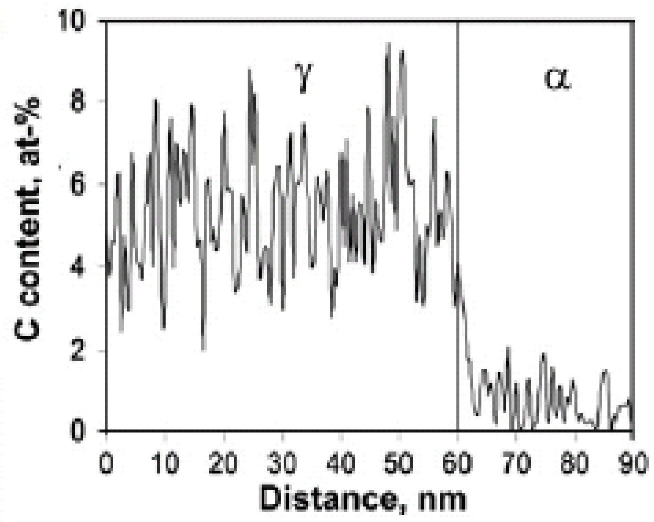

Carbon Supersaturation in Ferrite

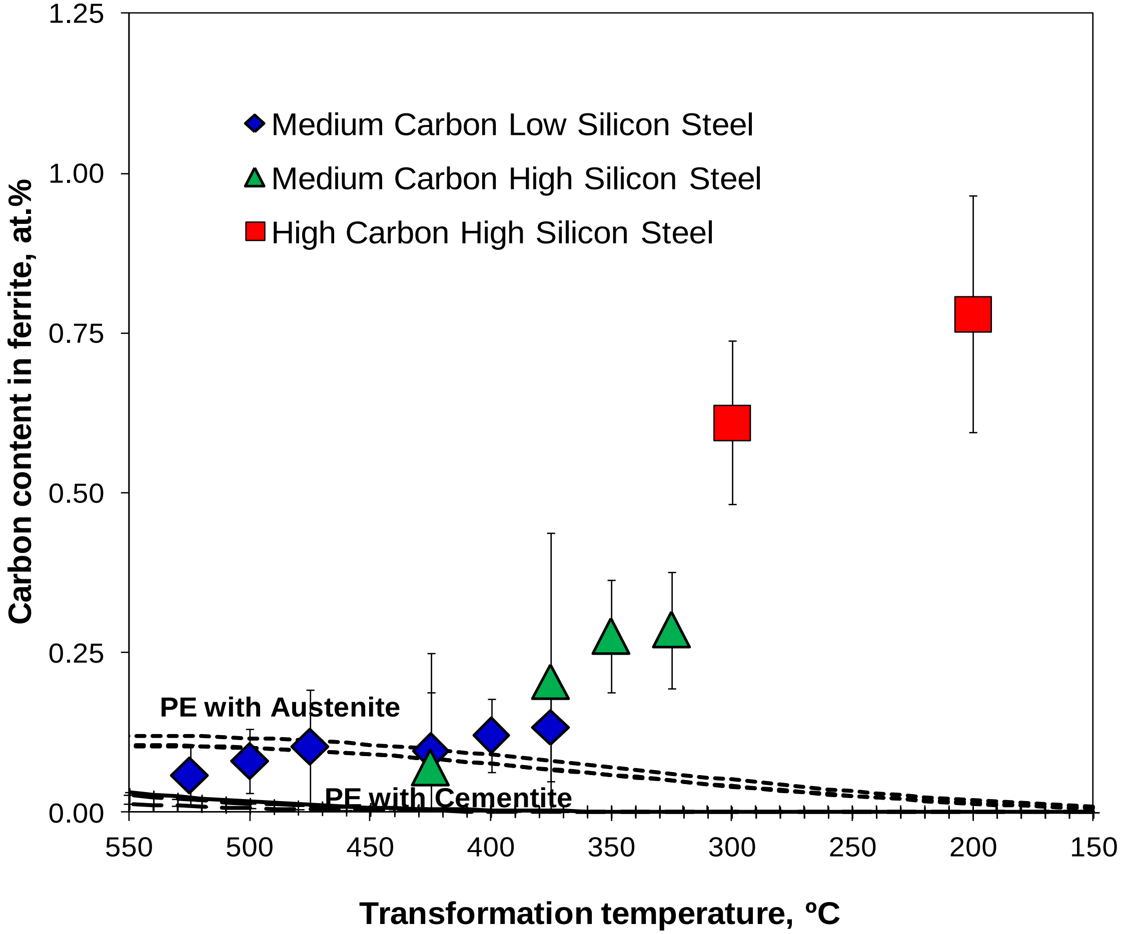

F.G. Caballero Acta (2008)
F.G. Caballero Scripta (2012)

Q3-Does all the C escapes from α?

APT values away from defects or clusters

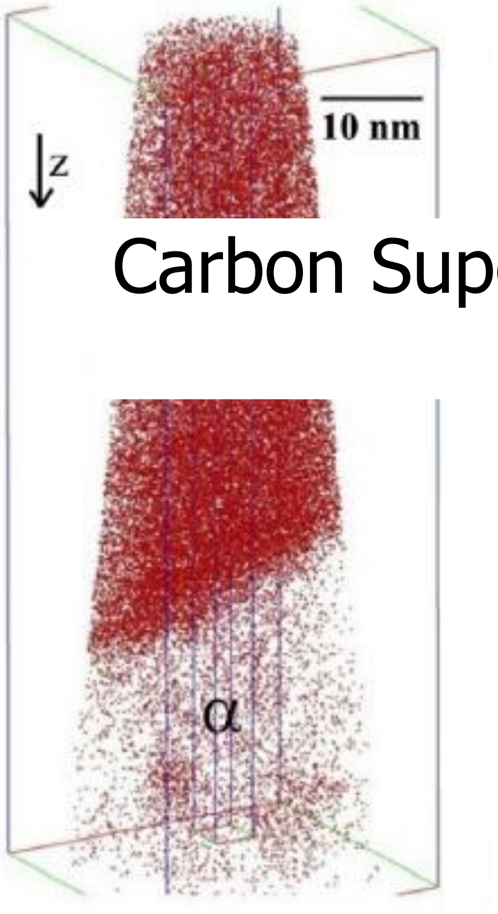

Carbon Supersaturation in Ferrite

Why?

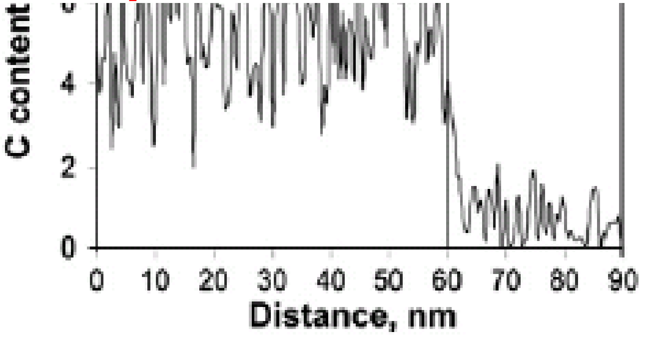

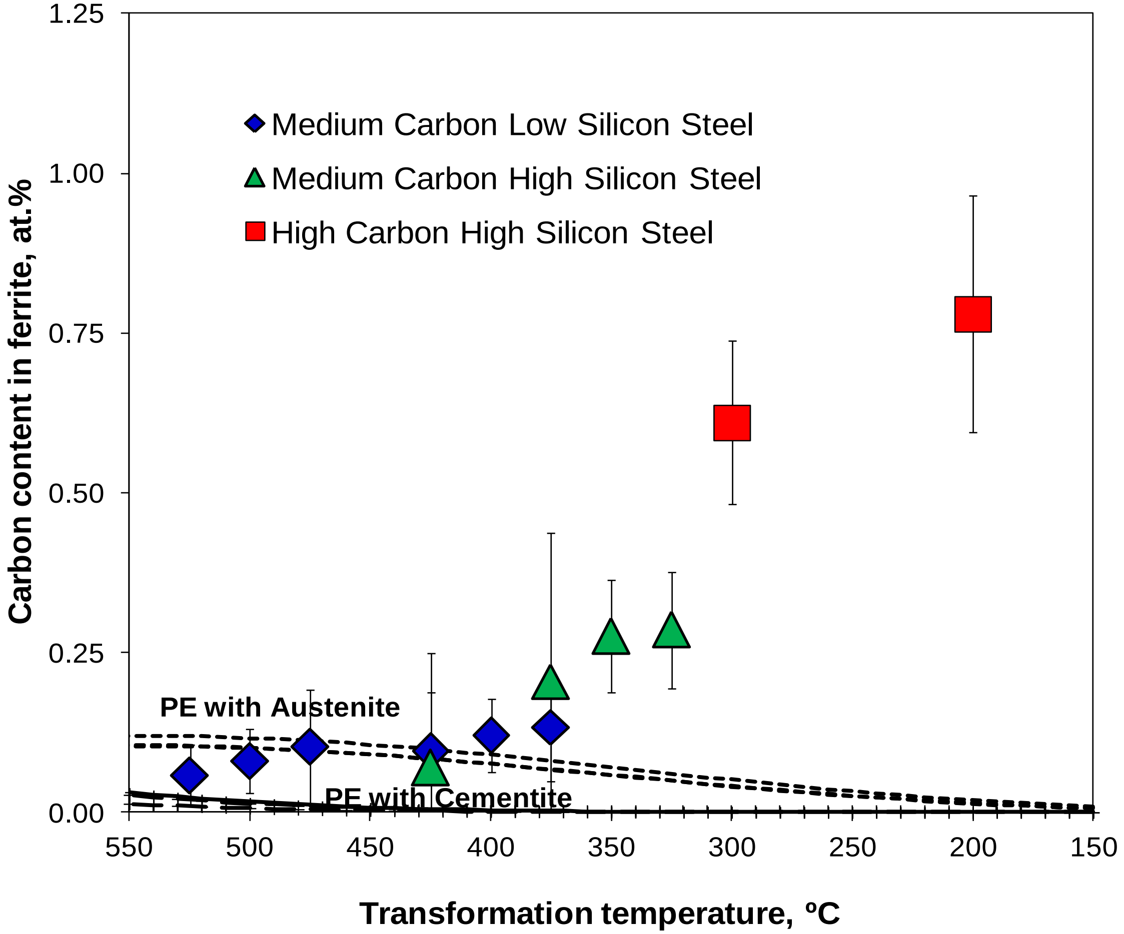

F.G. Caballero Acta (2008)
F.G. Caballero Scripta (2012)

Analysing XRD Spectra

A ***tetragonal phase*** with the space group I4/mmm was introduced as initial structural model in the Rietveld refinement.

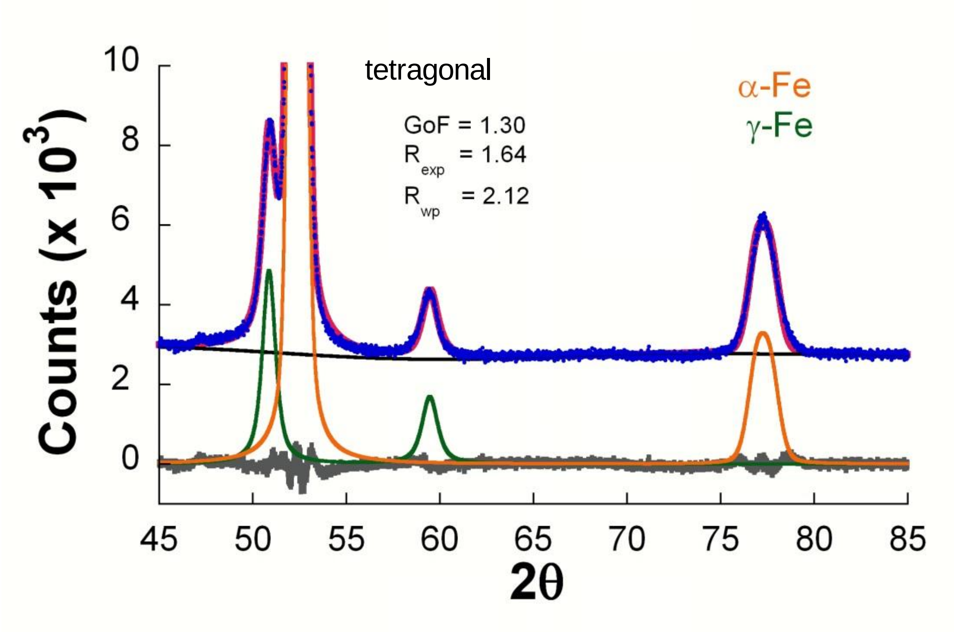

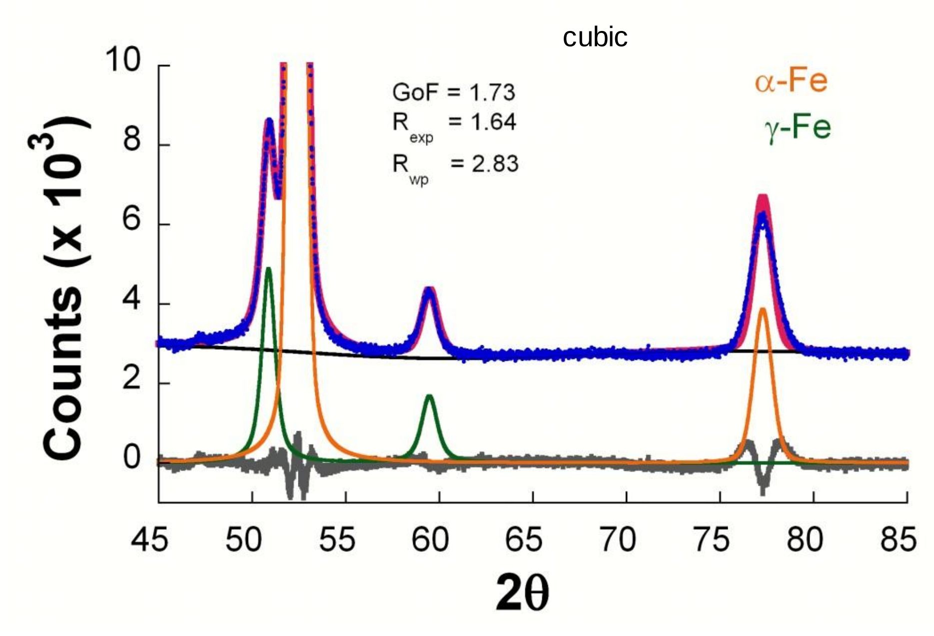

Since lower values of all residuals indicate a better fit, ***it is suggested that bainitic ferrite did not present a cubic structure, but a tetragonal structure***.

Garcia-Mateo, C et al. Low Temperature Bainitic Ferrite: Evidence of Carbon Super-Saturation and Tetragonality. *Acta Mater.* **2015**, *91*, 162–173, doi:10.1016/j.actamat.2015.03.018.

Tetragonality. XRD values

$c/a = 1 + 0.045\ C_{\alpha}$ (wt.%)

Transf. T/ ºC	Time/ h	a/ Ǻ	c/ Ǻ	c/a	C/ wt.%
220	24	2.857	2.880	1.0087	0.19
250	14	2.856	2.878	1.0078	0.17
300	5	2.857	2.877	1.0072	0.16
350	4.5	2.859	2.876	1.0059	0.13
Quench (α´+γ)	**----**	**2.856**	**2.932**	**1.0266**	**0.587**

Lose of tetragonality as transformation temperature increases

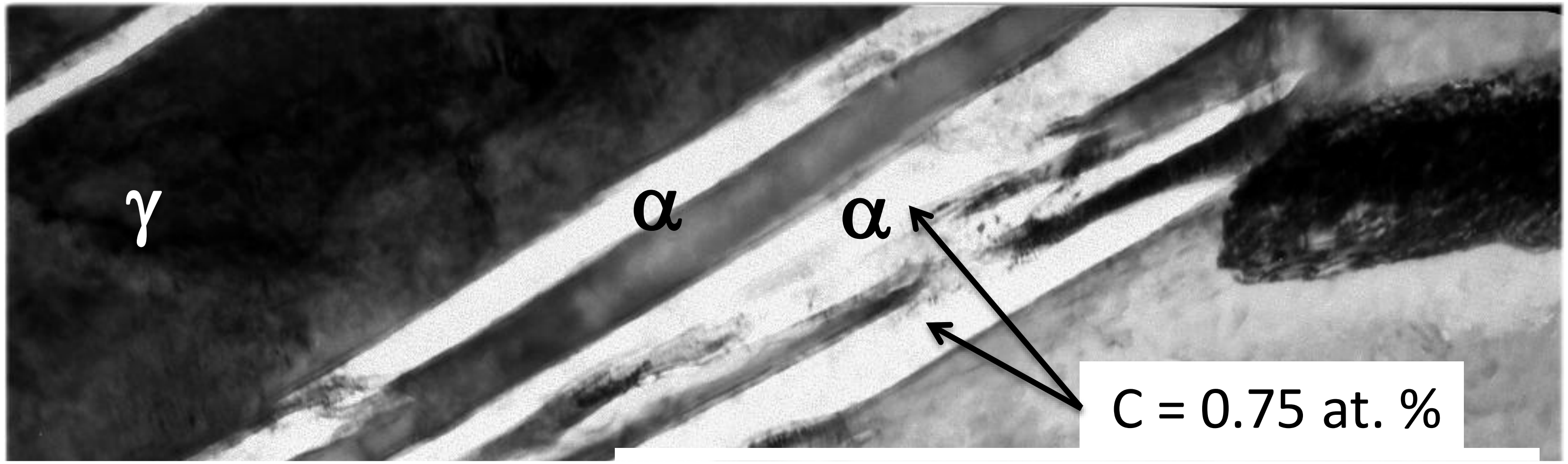

Tetragonality. TEM / HR-TEM

Measuring the lattice parameters of bainitic ferrite ***by the distance between the phase contrast peaks.***

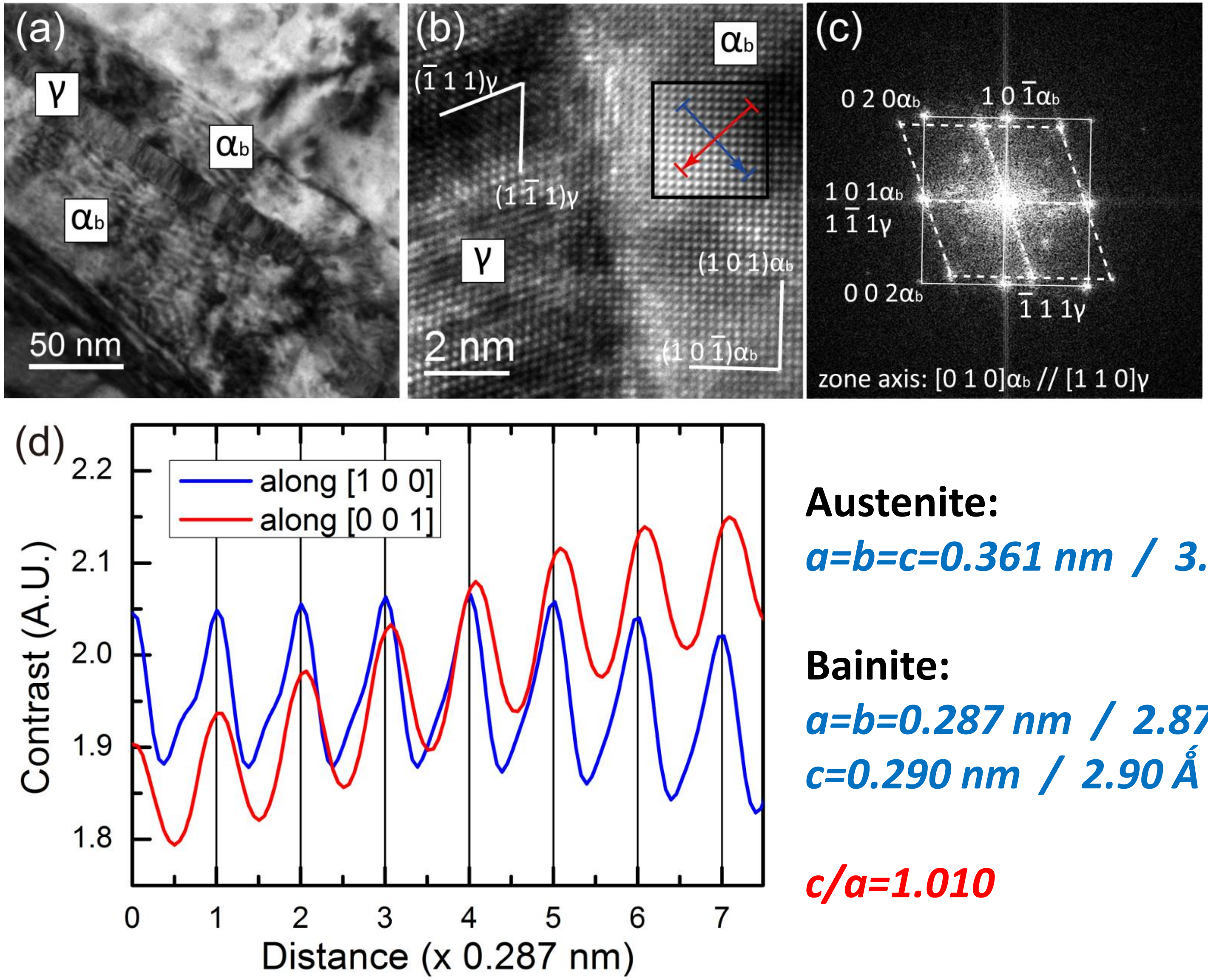

220 ºC for 7 days.

Austenite:

a=b=c=0.361 nm / 3.61 Å

Bainite:

a=b=0.287 nm / 2.87 Å

c=0.290 nm / 2.90 Å

c/a=1.010

Garcia-Mateo, C et al. *Acta Mater.* **2015**, *91*, 162–173

Tetragonality. Theoretical approach, first principle calculations

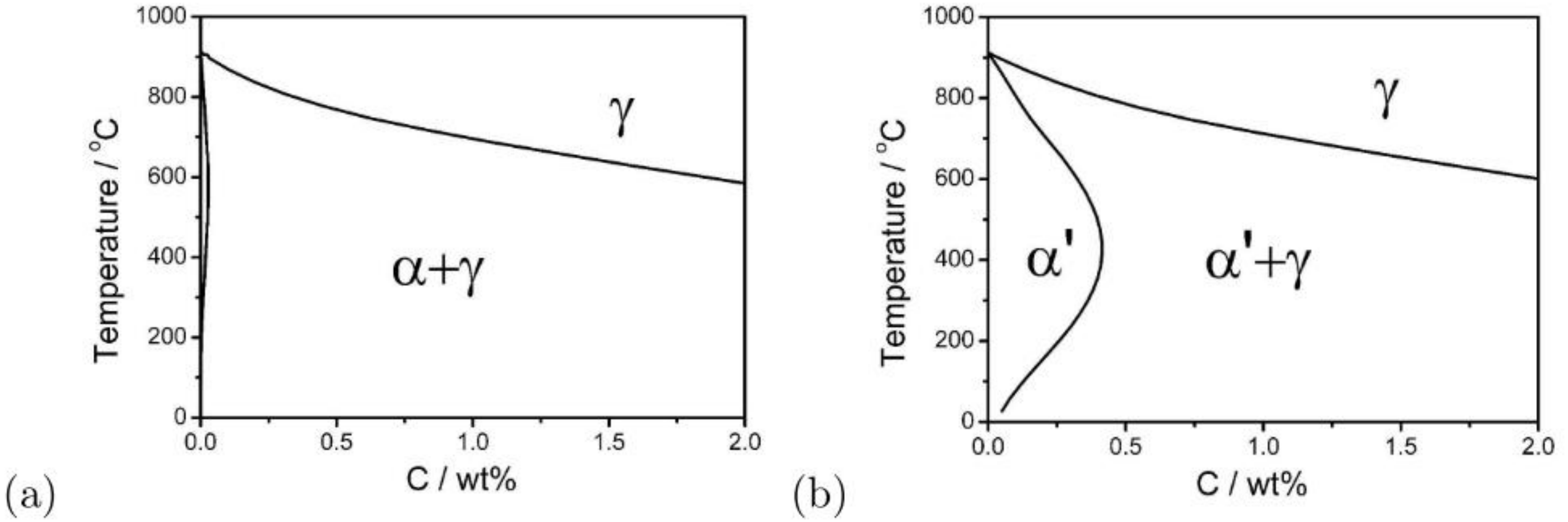

Figure 4. Binary phase diagrams of the Fe-C system allowing (a) equilibrium between body-centred cubic ferrite and austenite, (b) between body-centred tetragonal ferrite and austenite [33].

- **First-principles calculations** suggest that when tetragonal ferrite is in equilibrium with austenite, it has a much **greater solubility for carbon** than is the case for cubic ferrite in the same circumstances.
- It is possible that the present calculations may explain the observed **reluctance for the "excess" carbon present in bainitic ferrite to partition into the residual austenite despite prolonged heat treatment**, and a consideration of tetragonality might form a better basis for a variety of kinetic theories on industrially important processes.

Jang, J.H.; Bhadeshia, H.K.D.H.; Suh, D.W. Solubility of Carbon in Tetragonal Ferrite in Equilibrium with Austenite. *Scr. Mater.* **2013**, *68*, 195–198, doi:10.1016/j.scriptamat.2012.10.017.

Tetragonality. In-situ synchrotron high energy X-ray diffraction

Bainitic ferrite **remains tetragonal throughout the transformation**, suggesting that carbon-supersaturated ferrite **is an equilibrium constituent**.

The c/a ratio of bainitic ferrite is maintained upon cooling and increases with decreasing the transformation temperature.

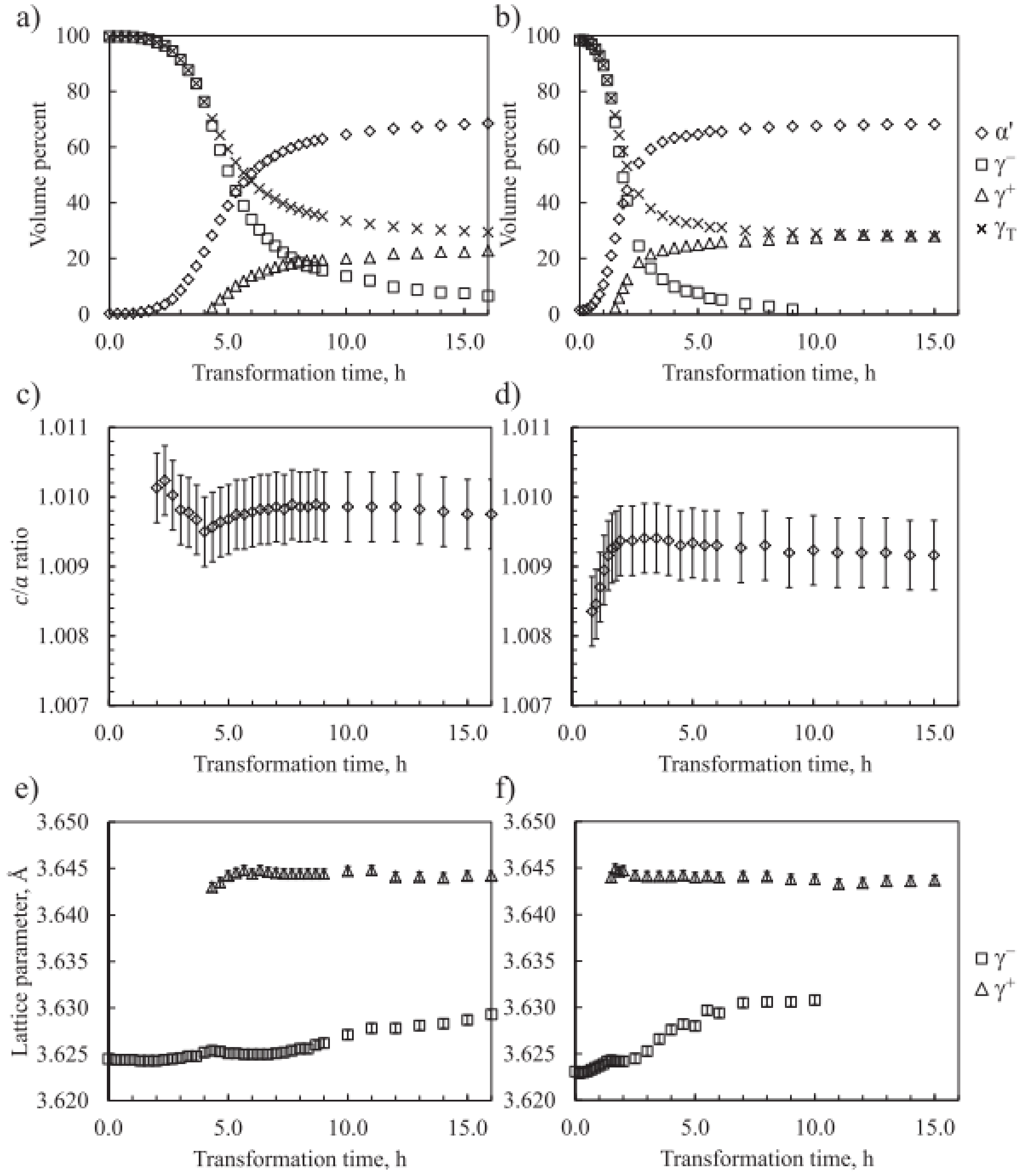

Rementeria, R et al. Quantitative Assessment of Carbon Allocation Anomalies in Low Temperature Bainite. *Acta Mater.* **2017**, *133*, 333–345

Q3-Does all the C escapes from α?

A3 – NO

Why ?

Bainitic ferrite is tetragonal and no cubic, much higher C solubility.

INDEX

❑**Assessment of the contributing factors to the scale of bainite**

- ➢ Ways and means to strengthen austenite
- ➢ Bainite growth to figure out some contributions.
- ➢ Models based on static inputs/contributing factors
- ➢ Beyond the models. Case Study
- ➢ Dynamic approach. Plate thickness evolution with transformation.

It is essential to understand WHAT controls the scale of the final microstructure → How Bainite Grows

Sub-micron → Nano

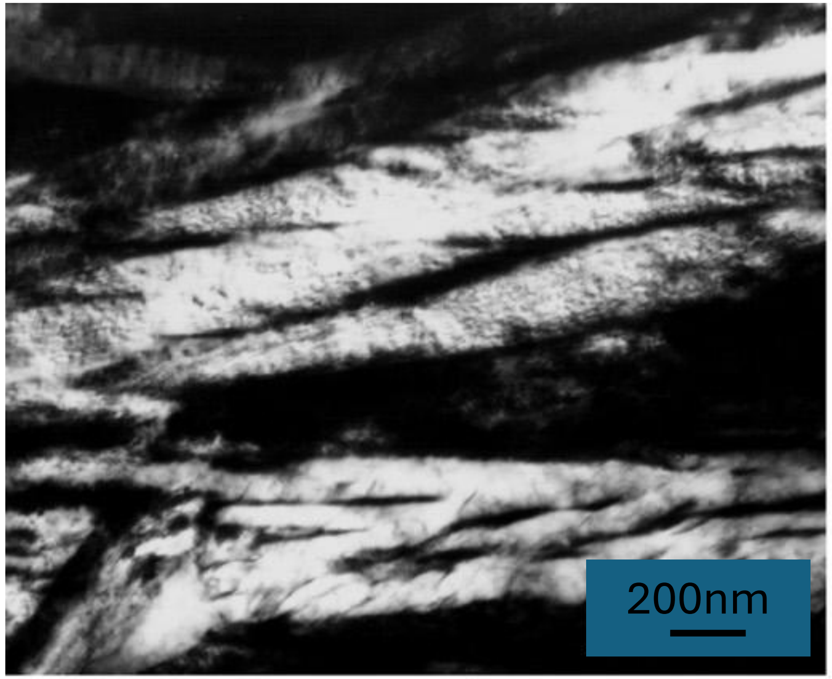

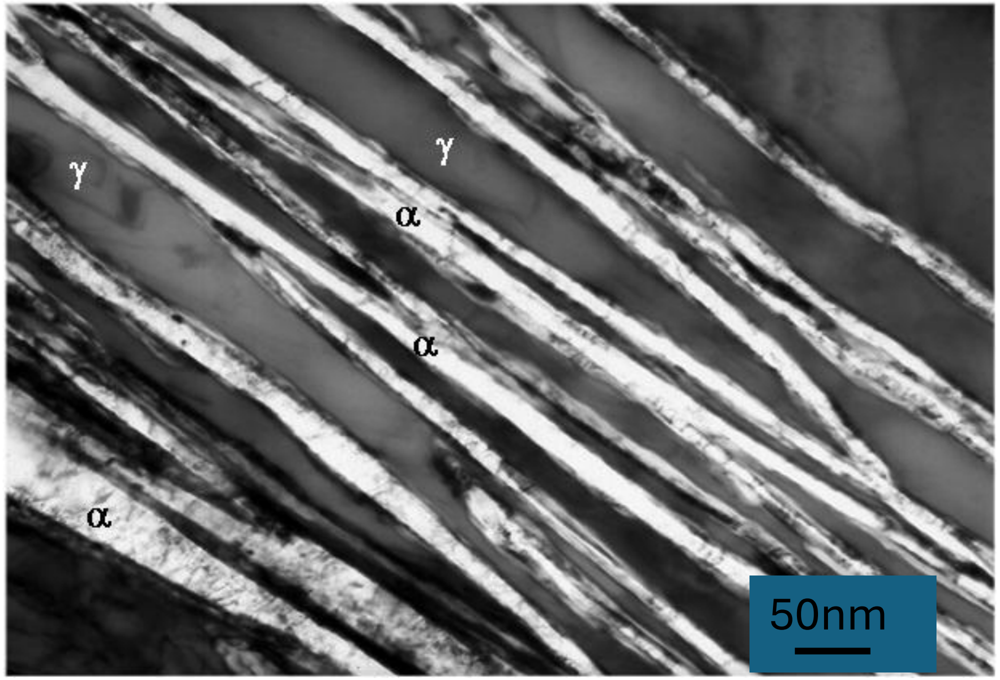

How Bainite Grows

Thus, the morphology and size of the bainite plates depend on the **minimization of strain energy** due to the shape deformation → product phase as thin plates/laths → thinner as the **strength of austenite increases** and there is an **increasing resistance to interface motion**.

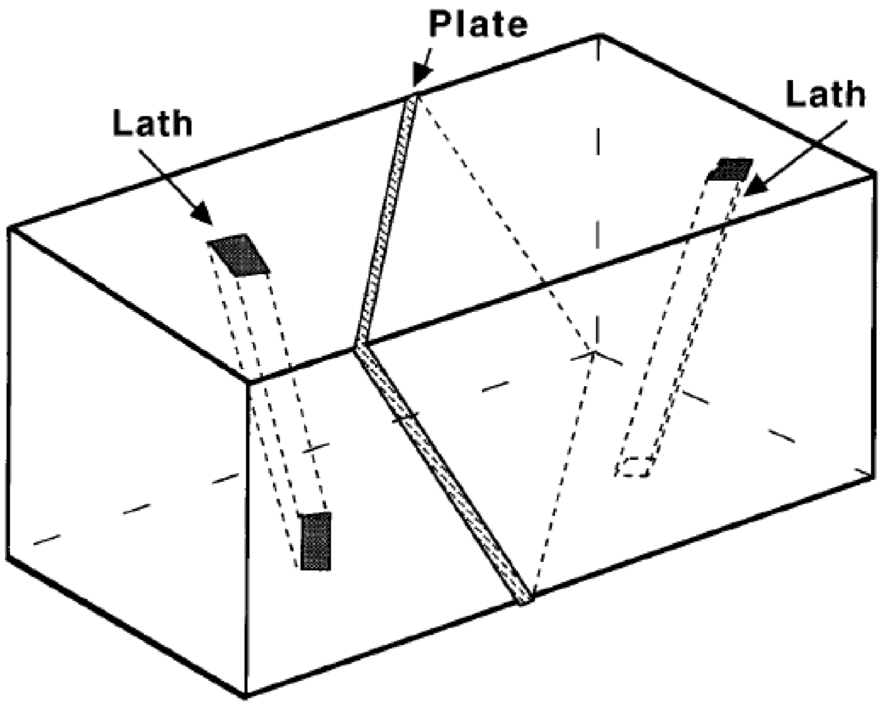

lath

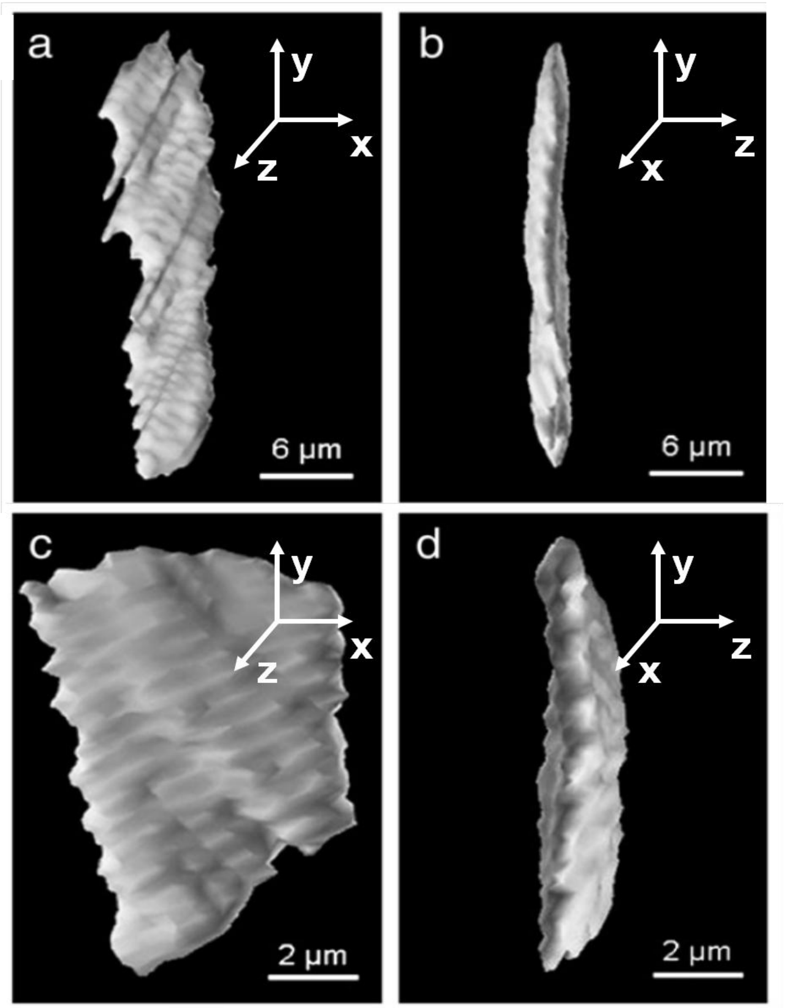

plate

3D reconstruction of bainitic ferrite lath & plate .(FIB-Focused Ion Beam.) K. Liu, T.Q. et al Mater. Charact. 62 (2011)

How Bainite Grows

Its growth is displacive & difussionless

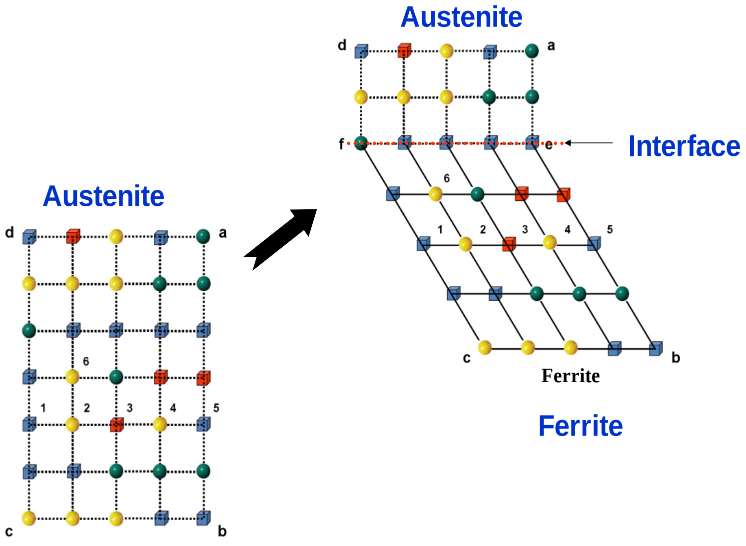

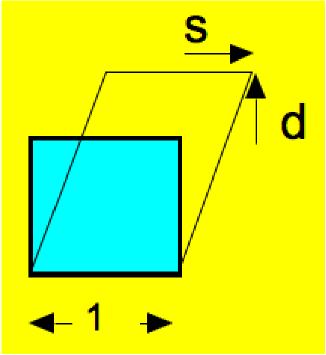

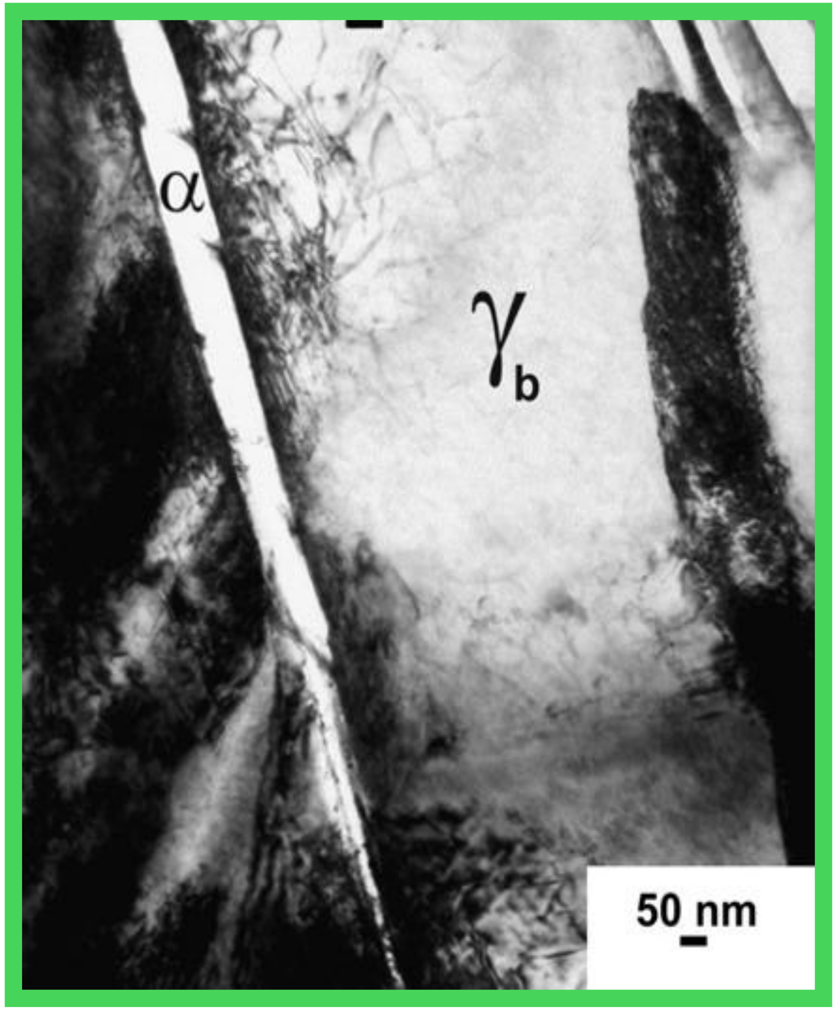

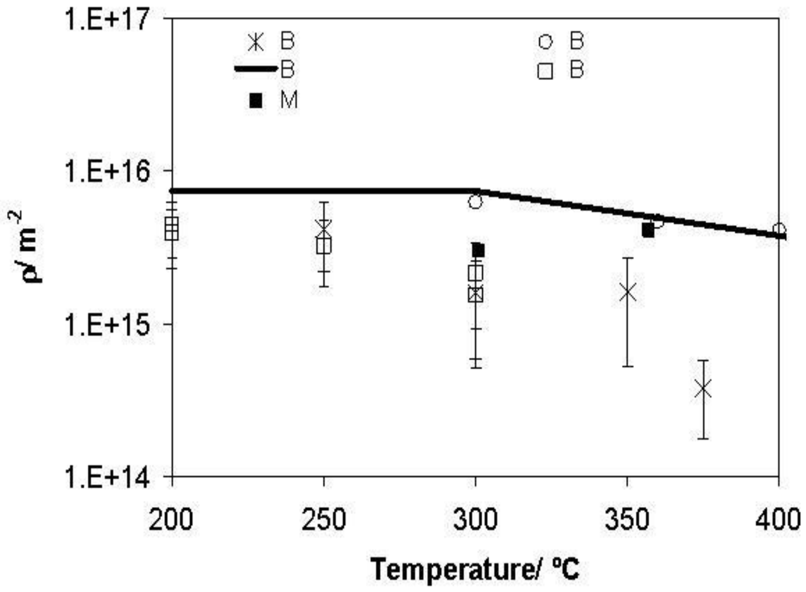

How Bainite Grows

Because there is plastic deformation there are **dislocations/twins** that help to relax the strain (mainly in austenite).

The local increase in **dislocation density** caused by the **yielding of the austenite**, **halts the movement of the glissile semi-coherent interface ➔ each plate only achieves a limited size (<PAGS) and impedes its thickening…..**

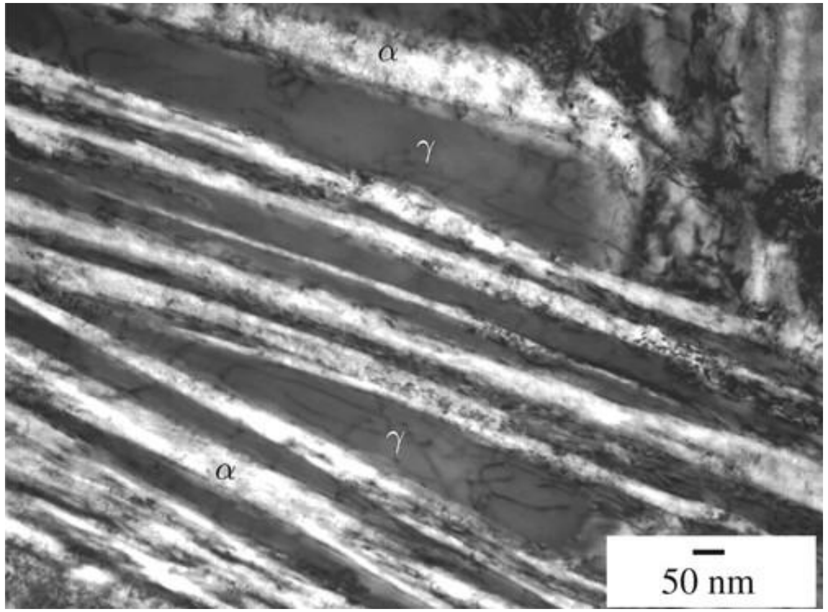

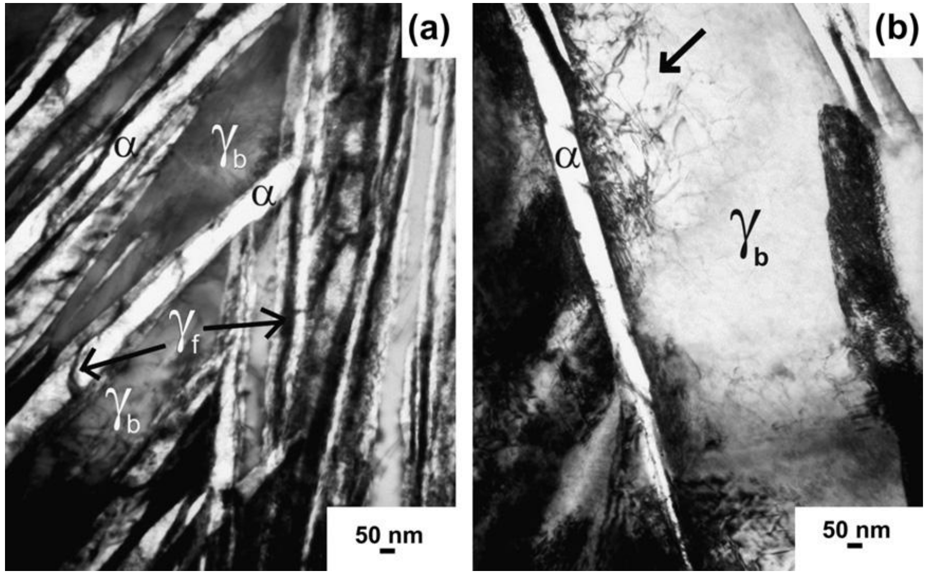

F.G. Caballero et al. / Acta Materialia 59 (2011) 6117

Ways and means to strengthen austenite

Strengthening ➔ impede dislocation movement

$$\sigma_{(YS)} = \sigma_{Fe} + \sigma_{Interstitials\ (C,N)} + \sum_i k_i\, \sigma_{ss}^{i} + K(\bar{L})^{-1/2} + k_P L^{-1} + C\, p^{0.5}$$

- ❑ Interstitials (C,N) have strong effect
- ❑ Dislocations (e.g. deformed austenite)
- ❑ Small austenite is stronger than bigger austenite

How Bainite Grows

On the course of the transformation, plates collide and impede further lengthening or thickening → **hard impingement**

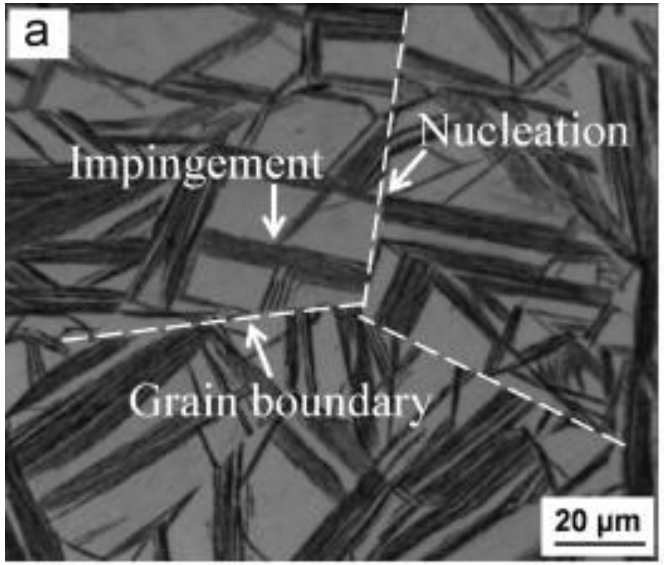

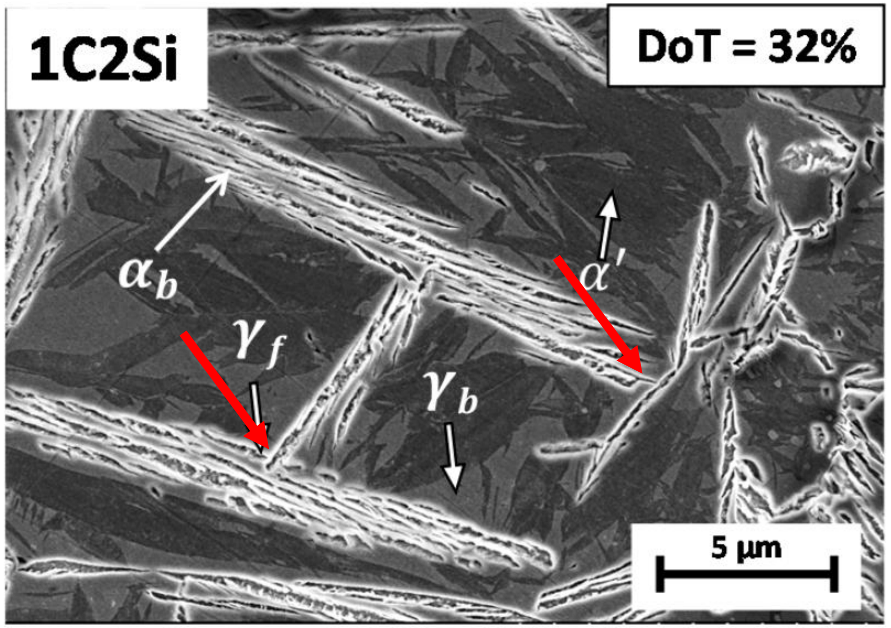

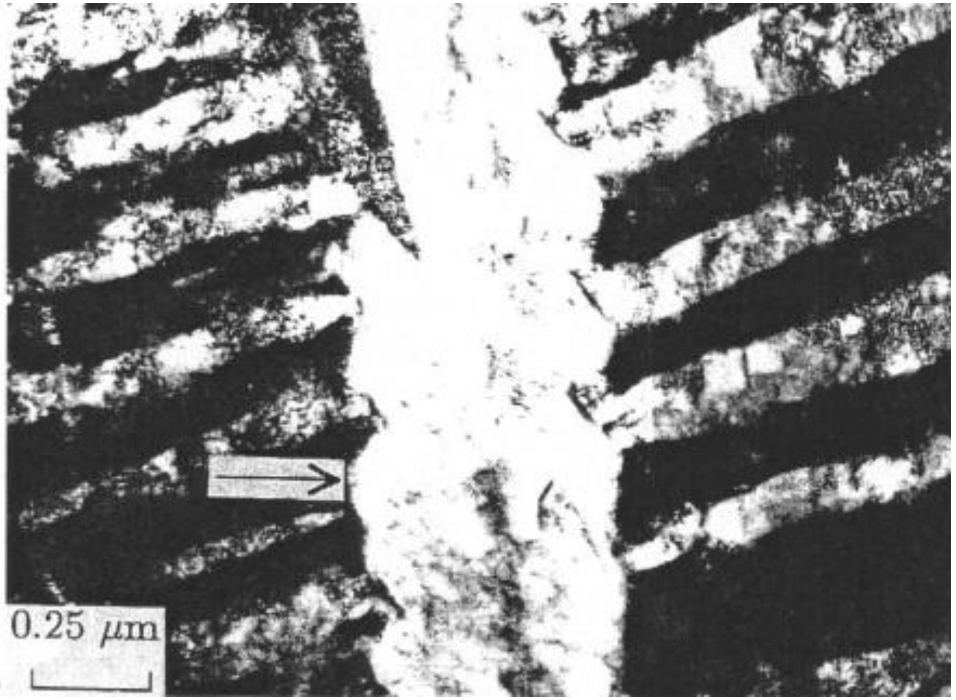

Bowing of transformation interface at **strong pinning points**, particularly prominent in regions identified by arrows

V. Ruiz-Jimenez Materials 2021
Hu et. Al. Mater. Letters 2014
Chang, L. C. and H. K. D. H. Bhadeshia (1995). Mater. Sci. Technol.

Identified important factors (so far) affecting the scale

Strength of austenite f **(wt.%, L,** $\rho,$ **T)**

$$\sigma_{(YS)} = \sigma_{Chemical\ Comp} + K(\bar{L})^{-1/2} + C\ p^{0.5} + Temperature$$

Hard impingement f **(**$\Delta G^{\gamma \to \alpha}$**)**

$$\Delta G^{\gamma \to \alpha} = f(Chemical\ composition, Temperature)$$

Dislocation density f **(**T**)**

$$p = f(T)$$

Bainitic ferrite plate thickness

Description of bainite scale by ANN model

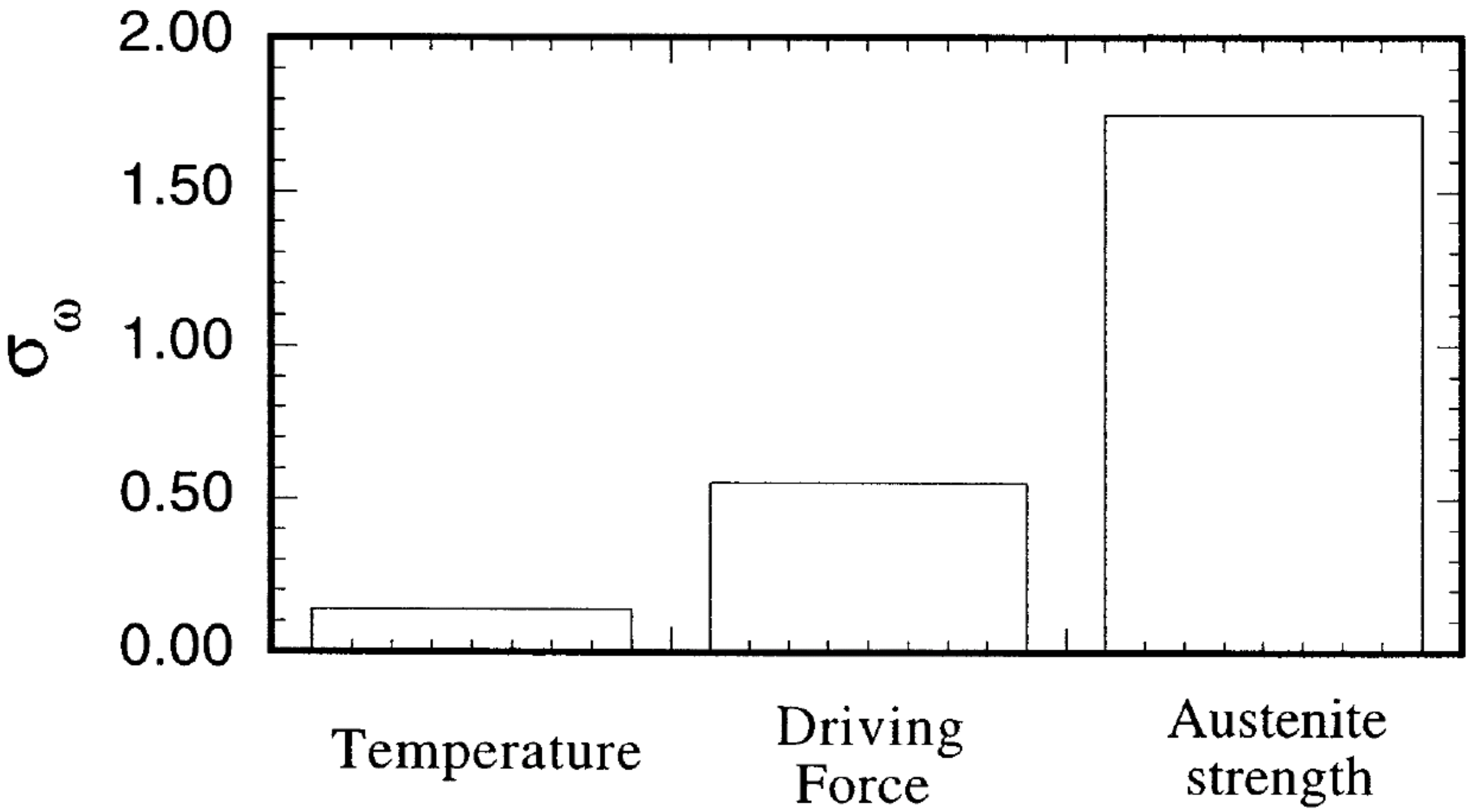

S.B. Singh, Mater. Sci. Eng. A 245 (1998) 72–79

Dislocation density ρ (T) not included

Bainitic ferrite plate thickness

Yang et. al. Mater. Sci. Eng. A 748 (2019) 16-20

$$t = \mathrm{f}(\mathrm{T},\sigma_y^{\gamma},\Delta G^{\gamma\rightarrow\alpha}) = 222 + 0.01242 \times\ T + 0.01785 \times \Delta G^{\gamma\rightarrow\alpha} - 0.5323 \times\ \sigma_y^{\gamma}$$

Dislocation density $\rho\ (T)$ not included

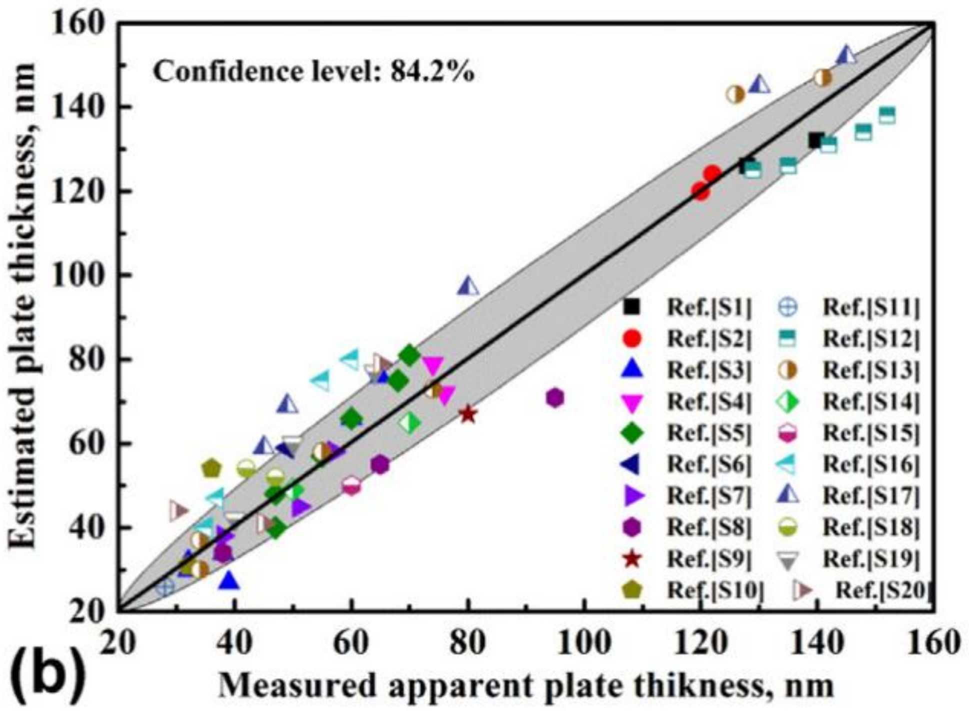

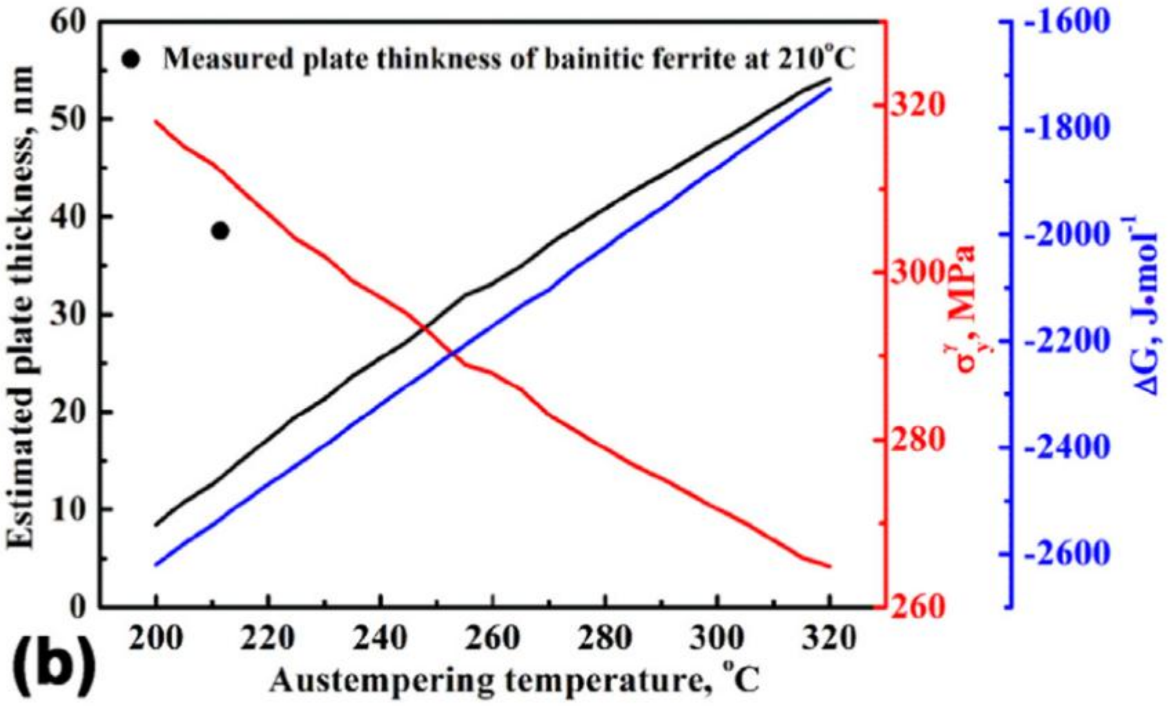

Dislocation density ρ (T) effect exists

Strong correlation ⬆ ρ and ⬇ t

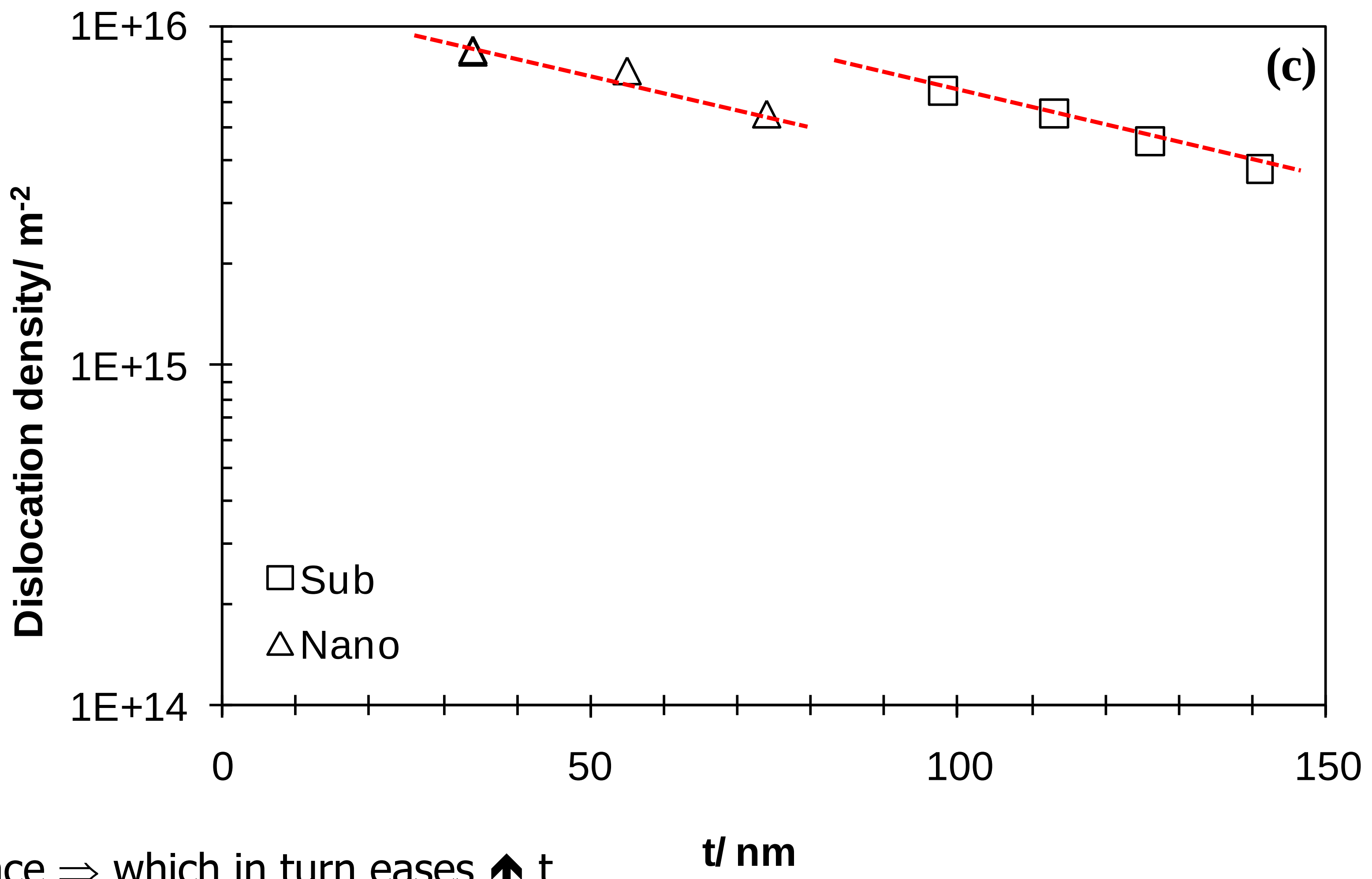

⬆T ⇒ dynamic recovery may take place ⇒ which in turn eases ⬆ t

Trapping of C in dislocations as Cotrell in the vicinity of the interface might exert an extra contribution ⬆ as T ⬇

Dislocation density ρ (T) effect exists

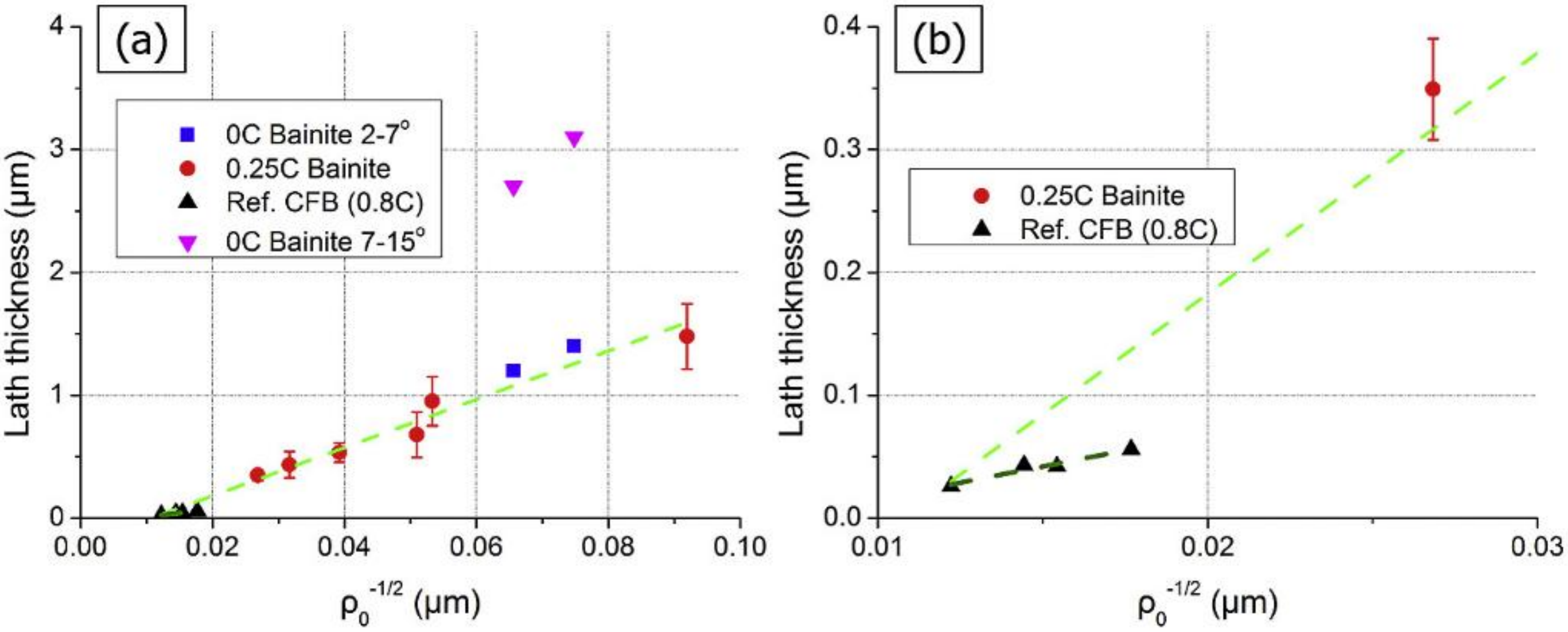

S.H. He et al. / Acta Materialia 135 (2017)

As transformation progresses, is the plate size smaller?

As transformation progresses, is the plate size smaller?

Alloy	Composition (wt.%)						T (°C)				
	C	Si	Mn	Cr	Mo	Cu	Ac1	Ac3/Acm	Ms	Ms [15]	Bs [16]
1C2Si	0.99	2.4	0.75	0.98	0.02	0.19	815	844	112	106	425
04C3Si	0.43	3.05	0.71	0.97	0.21	0.14	845	915	287	276	566

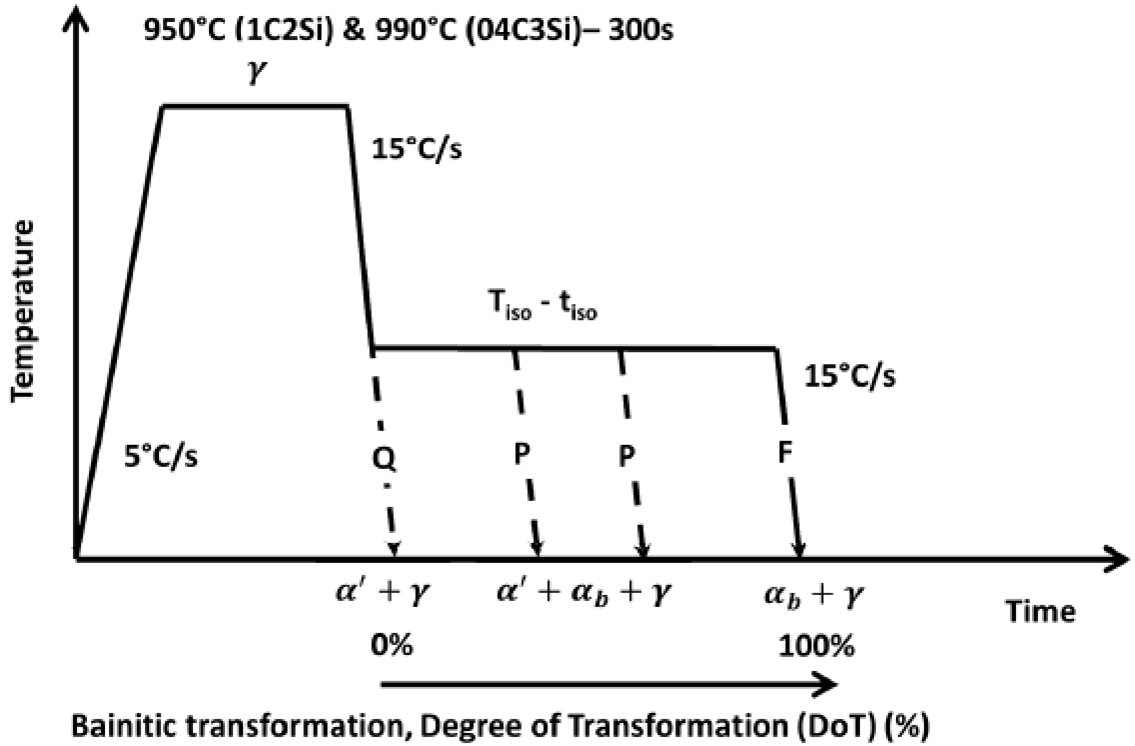

Ruiz-Jimenez, V *Materials (Basel).* **2021**,

As transformation progresses, is the plate size smaller?

Two bainitic steels, very different C contents but common range of Bs-Ms & similar theoretical t (plate thickness)

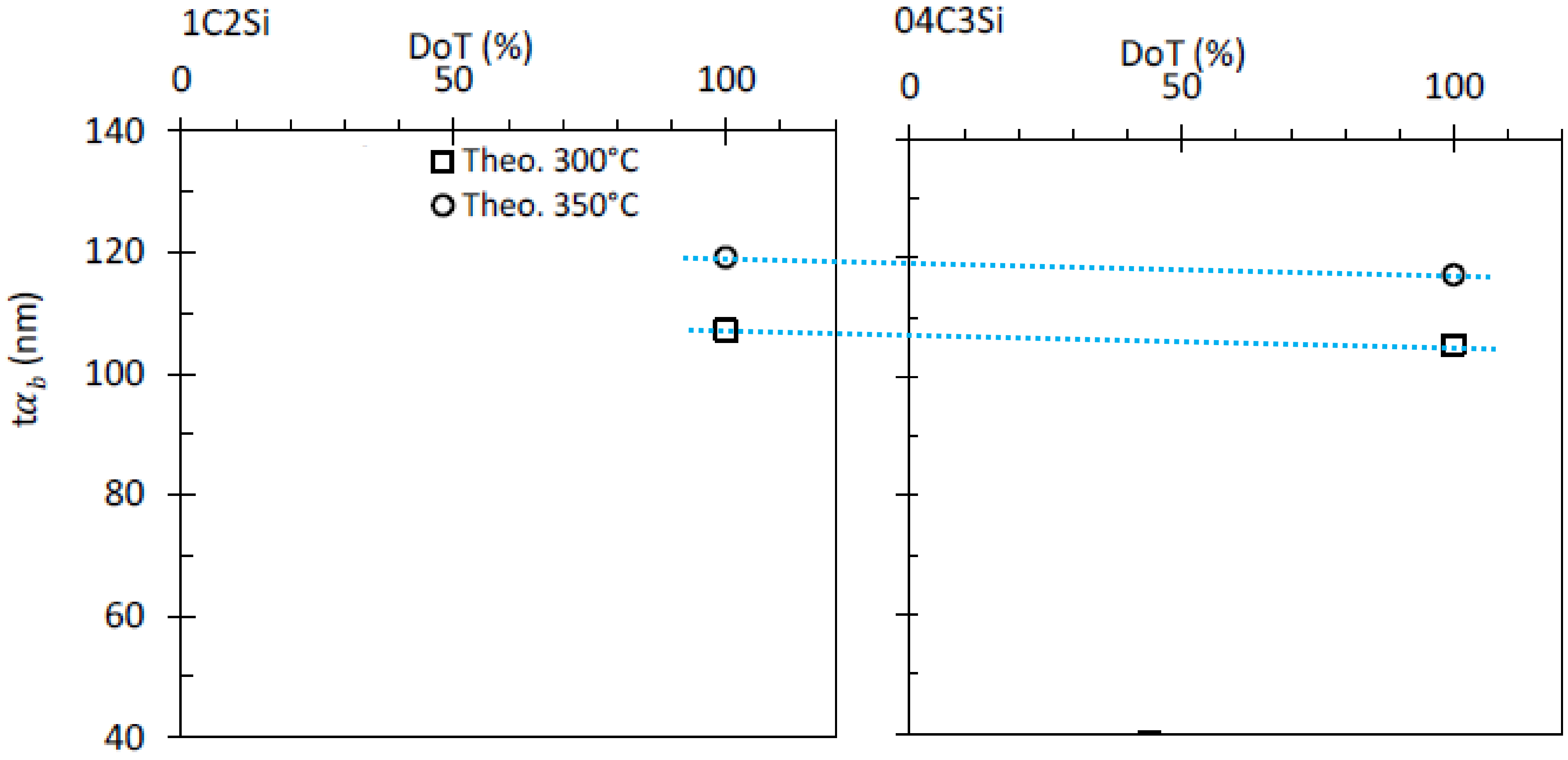

$$t = f(T,\sigma_y^{\gamma},\Delta G^{\gamma\rightarrow\alpha}) = 222 + 0.01242 \times T + 0.01785 \times \Delta G^{\gamma\rightarrow\alpha} - 0.5323 \times \sigma_y^{\gamma}$$

As transformation progresses, is the plate size smaller?

- Theory **can predict**, for the same steel, the trend as a function of the T.
- Theory **cannot predict the differences between both steels.**

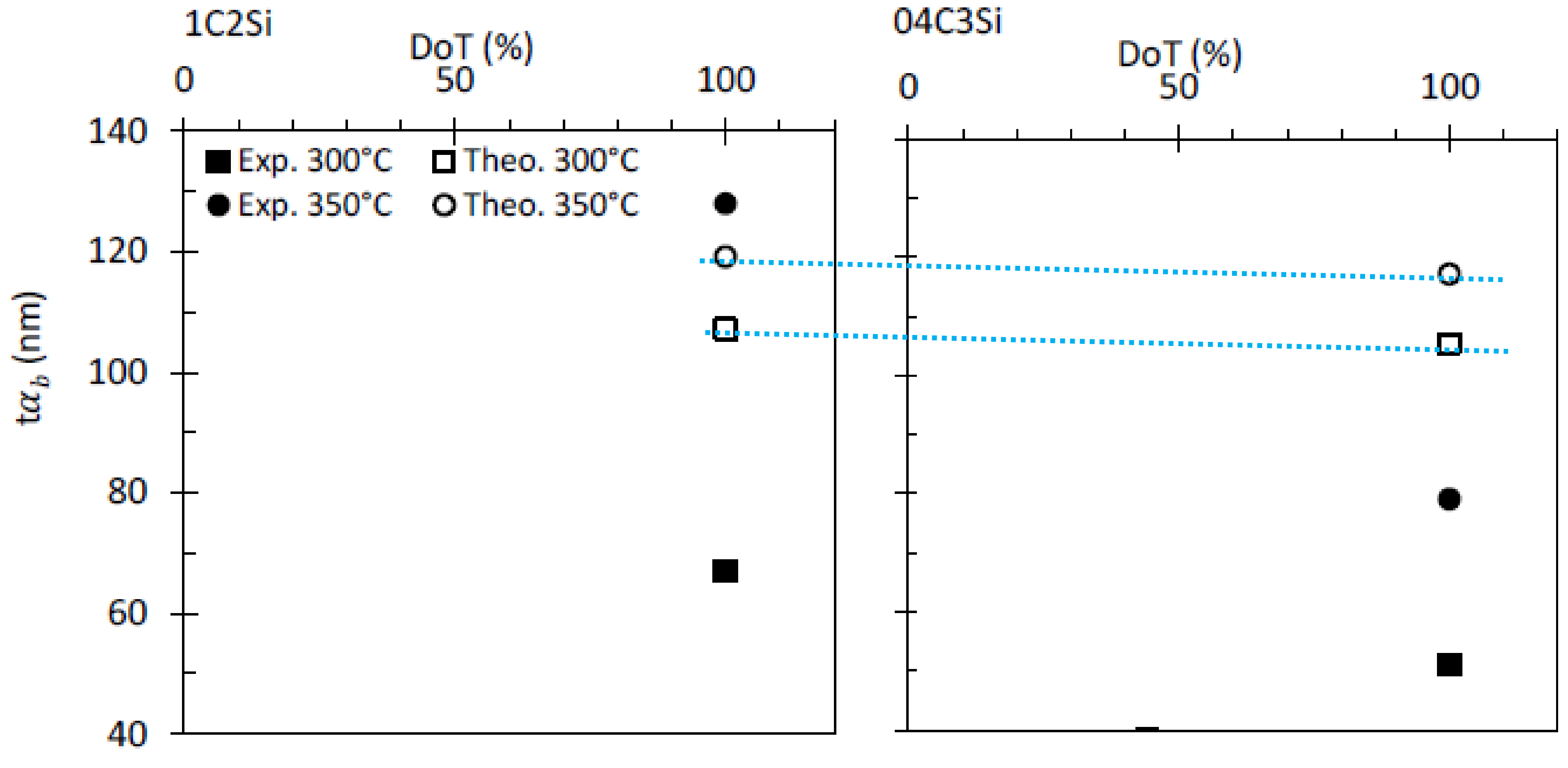

$$t = f(T, \sigma_y^\gamma, \Delta G^{\gamma\rightarrow\alpha}) = 222 + 0.01242 \times T + 0.01785 \times \Delta G^{\gamma\rightarrow\alpha} - 0.5323 \times \sigma_y^\gamma$$

Why weren't we successful?

Considerations are made as if the whole **system were static**.

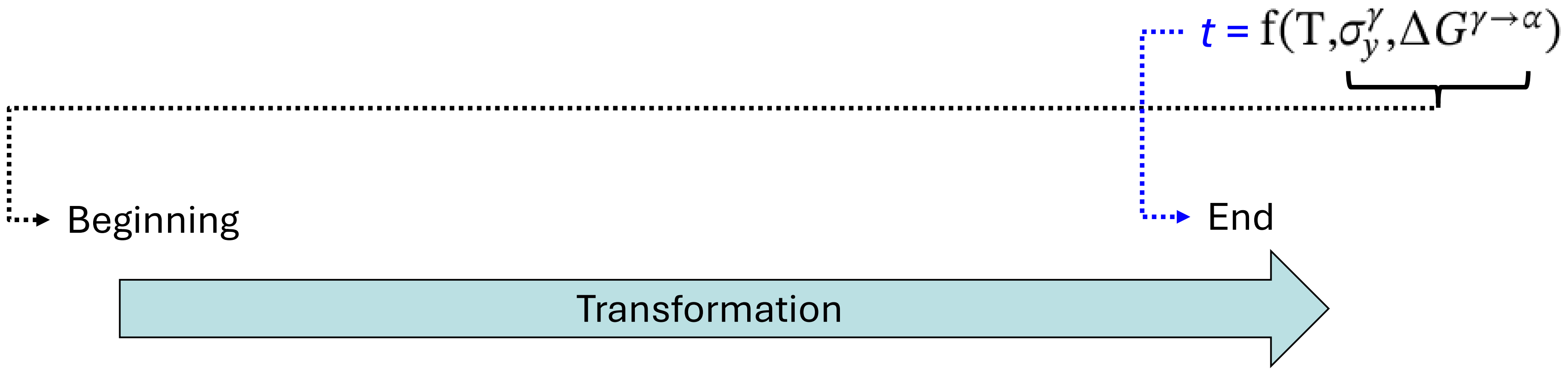

Why weren't we successful?

$$t = \mathrm{f}(\mathrm{T}, \sigma_y^{\gamma}, \Delta G^{\gamma \rightarrow \alpha}):$$

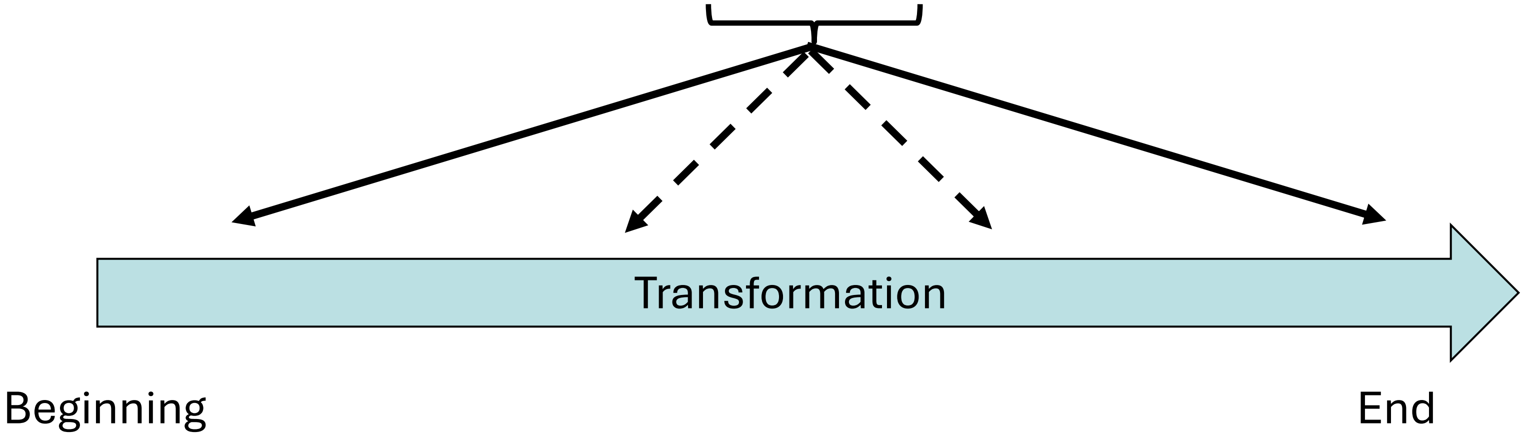

We can't ignore the fact that the **whole system is dynamic** ➔

evolves during the transformation ➔

all relevant parameters affecting the plate thickness ➔

C content in austenite (YS, ΔG), ρ and hard impingement events ➔

change on the course of the transformation.

Whole system is dynamic

C content in austenite changes

Transformation

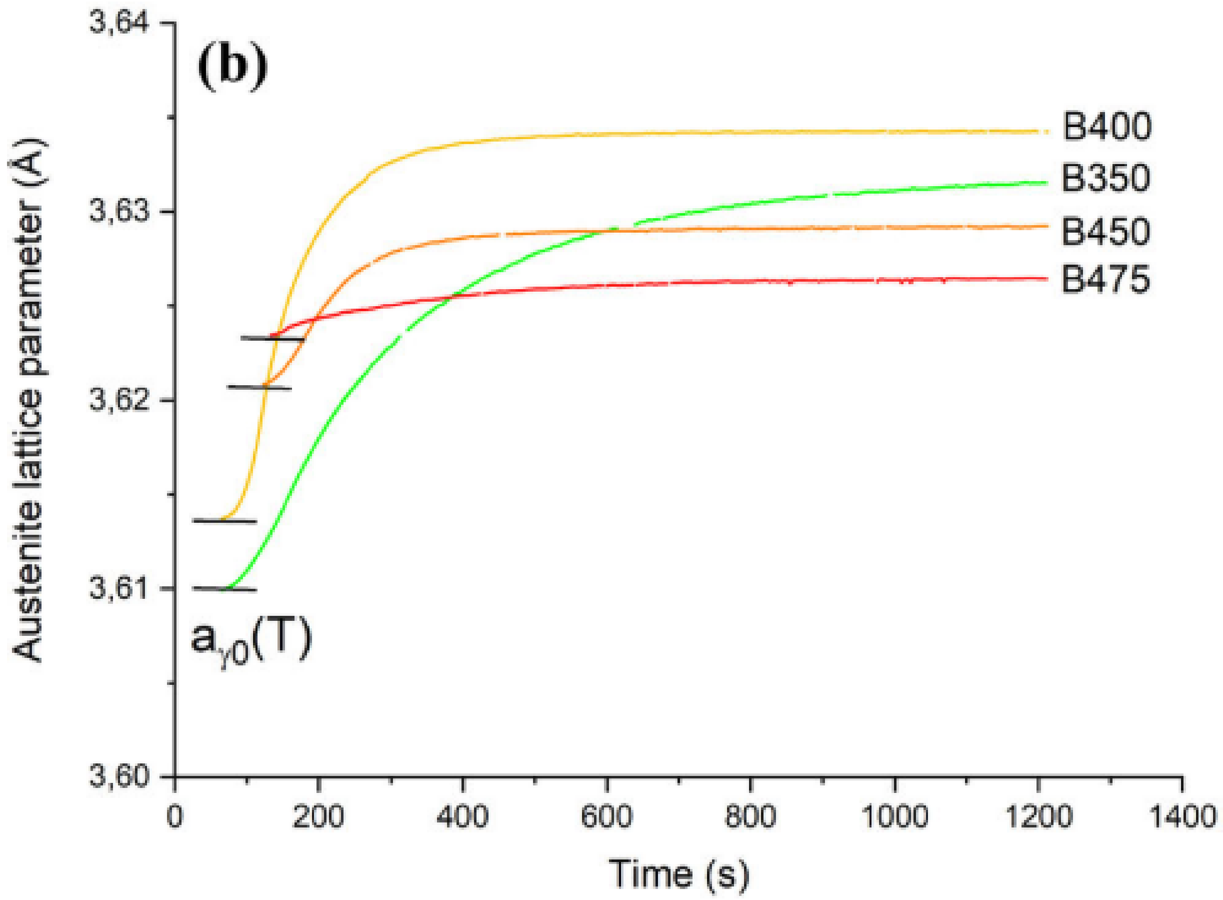

Rampelberg, C.; et al. *JOM* **2021**

Whole system is dynamic

Dislocation density

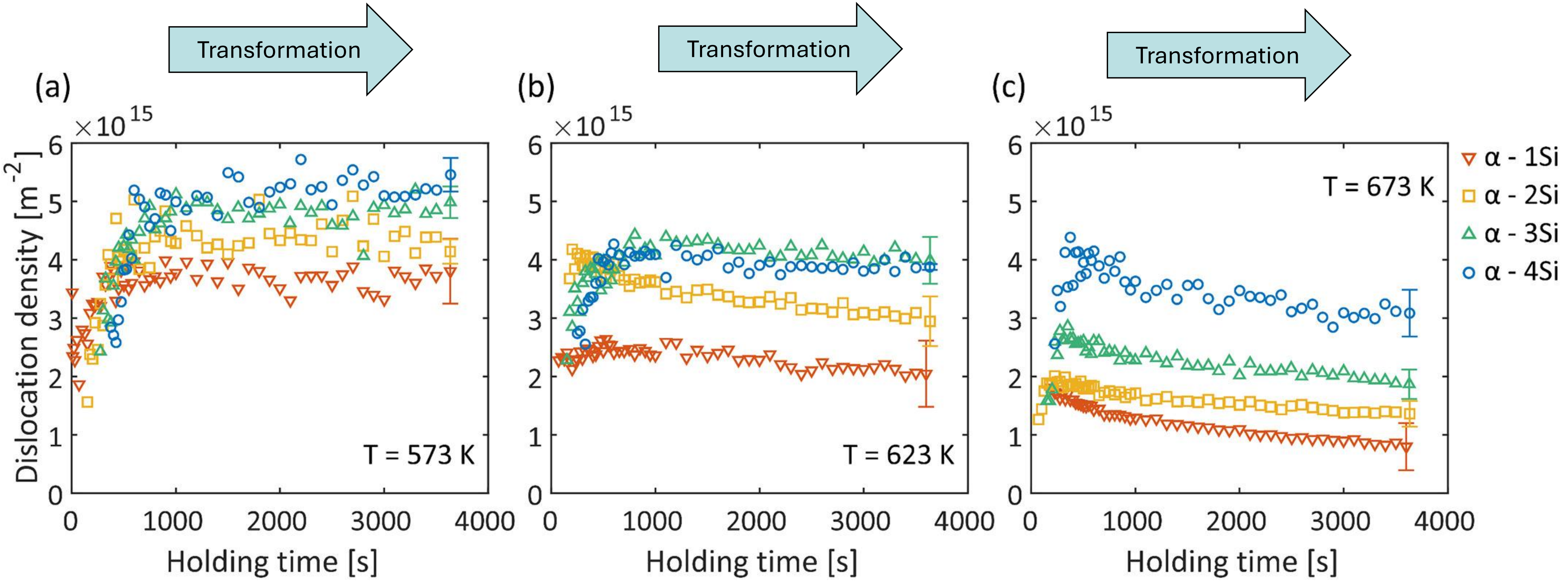

Lin, S. et al.. *Mater. Charact.* **2022**,

Whole system is dynamic

Transformation rate

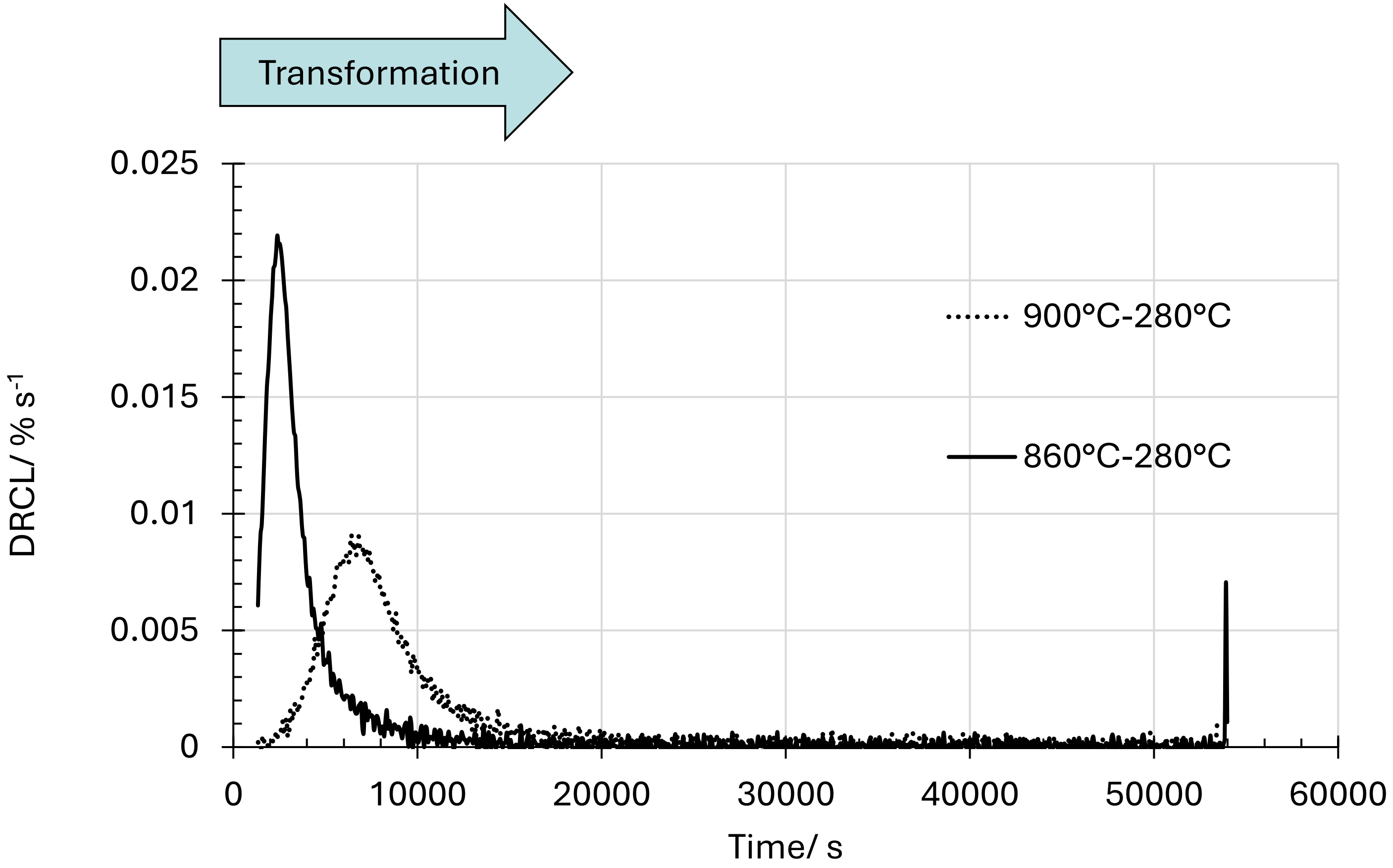

THE SYSTEM IS DYNAMIC

Transformation kinetics considerations

Typical stages during bainitic transformation

Incubation period

Fast transformation up to the Max.

Deceleration of the transformation, very sluggish

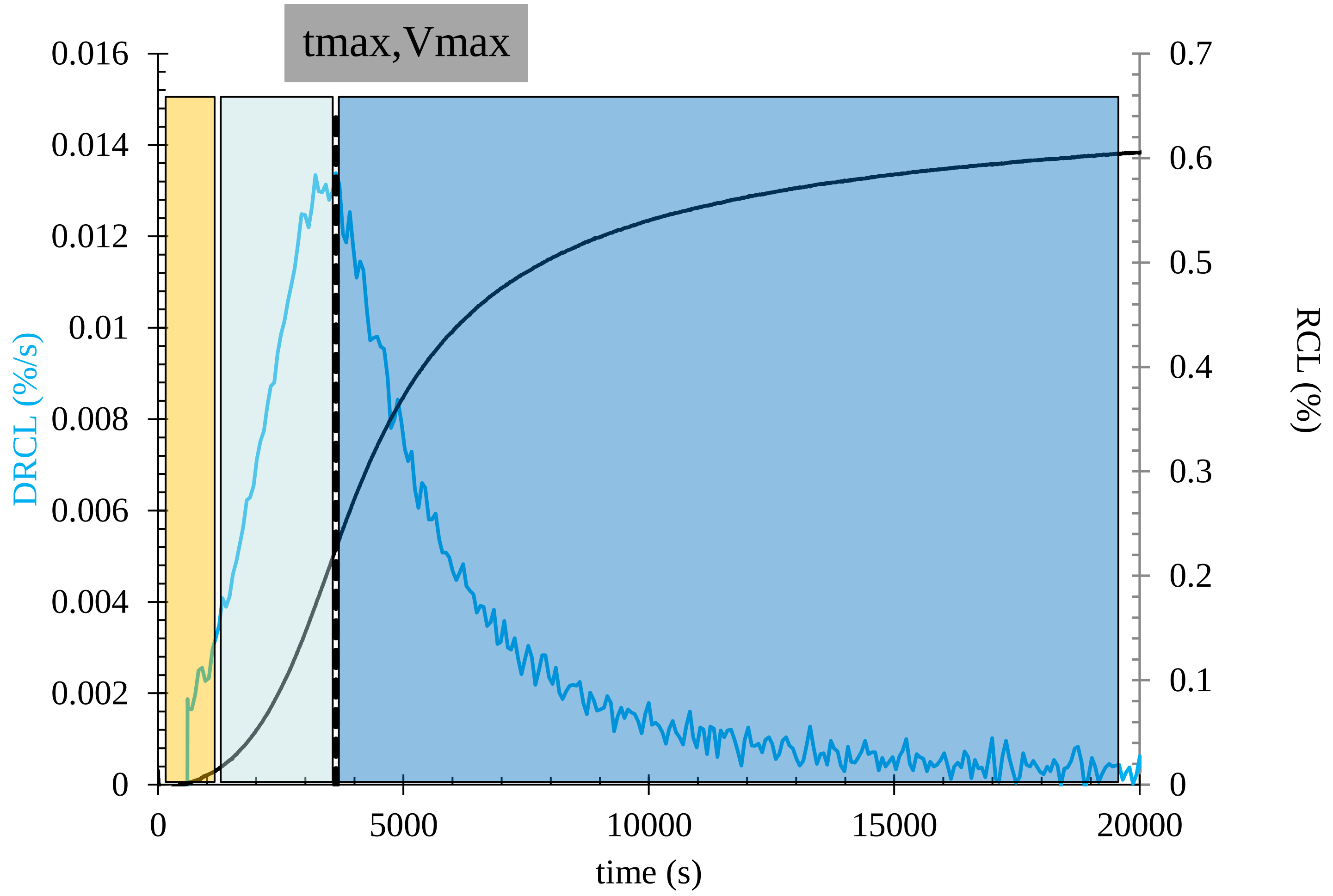

Why weren't we successful?

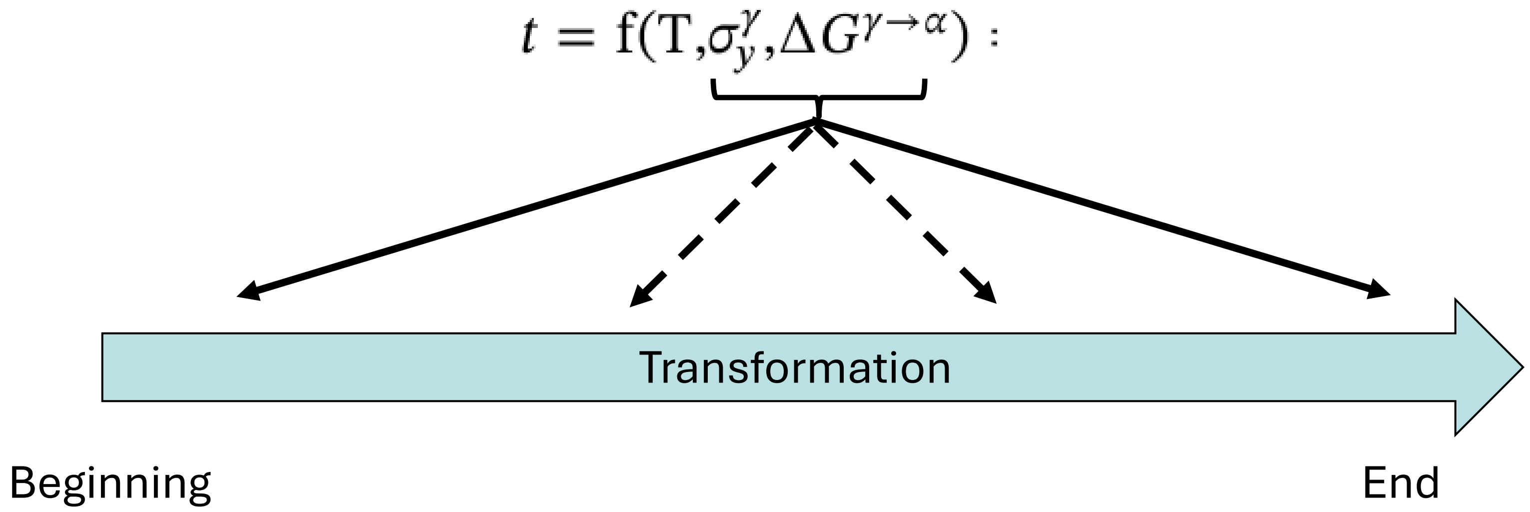

Logic and metallurgical data seem to indicate that **as transformation progresses, <u>plate size should be smaller</u>**

As transformation progresses, is the plate size smaller? ➔ NO

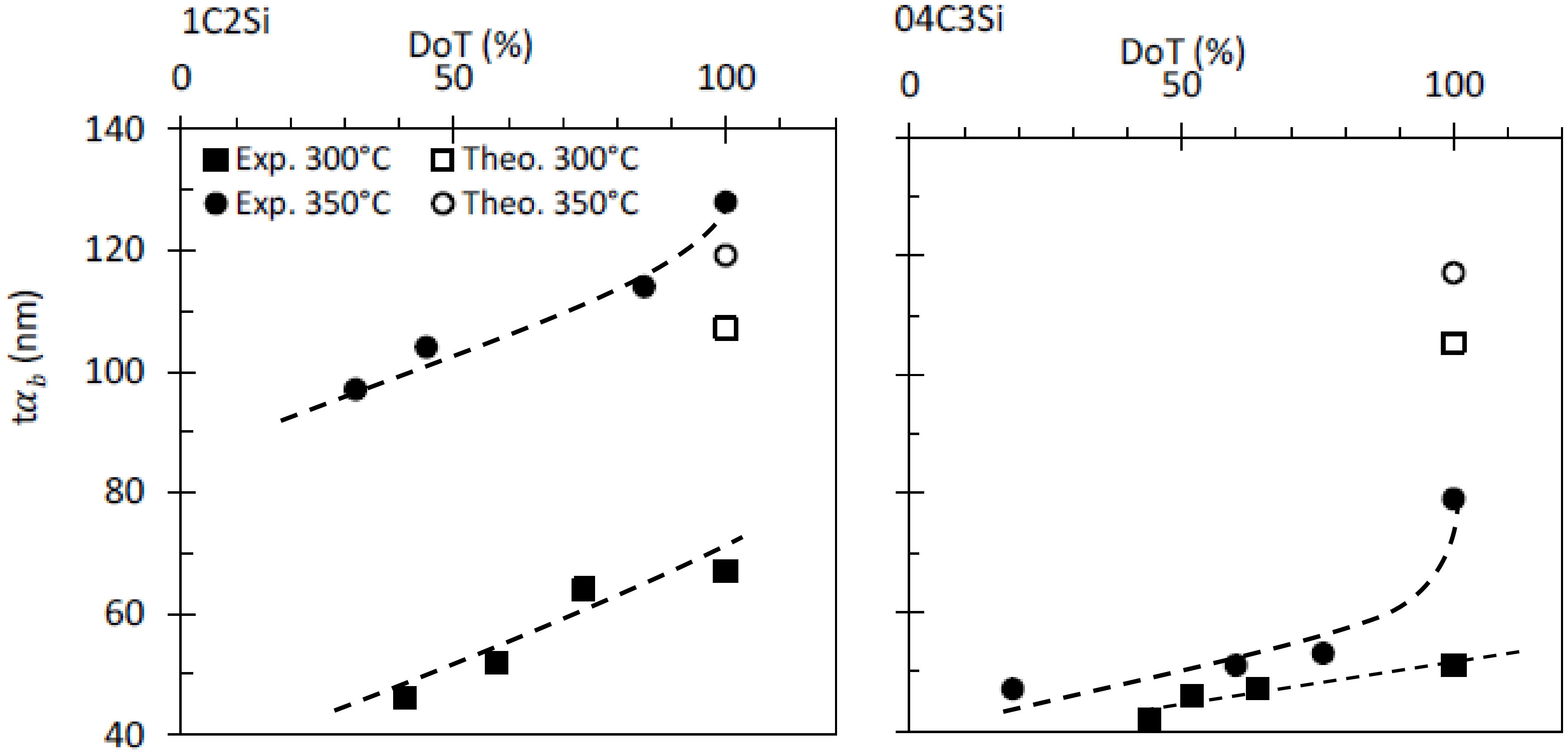

*Chang, L.; Bhadeshia, H.K.D.H. *Mater. Sci. Technol.* 1995, *11*,

THE SYSTEM IS DYNAMIC

Calculations were made considering the parameters at each stage (DoT) → Cγ (ΔG,YS)

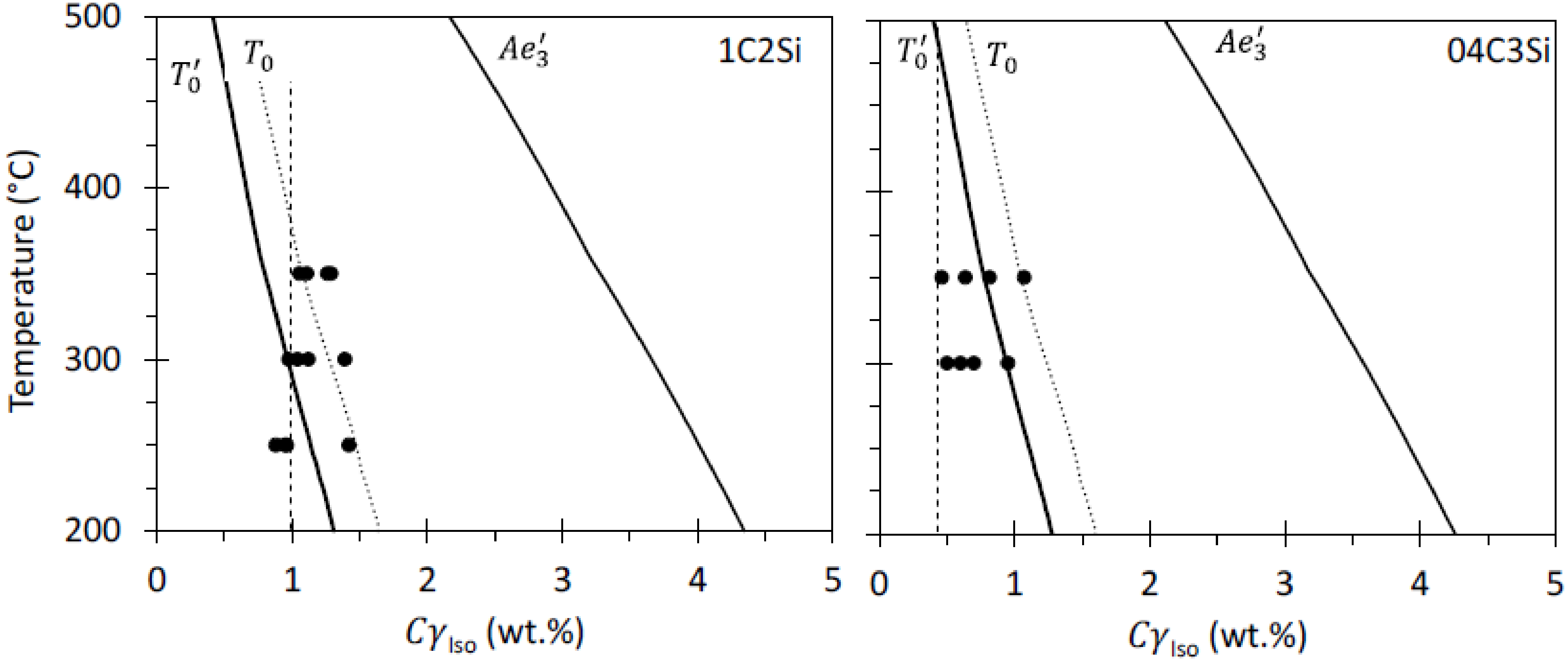

THE SYSTEM IS DYNAMIC

Calculations were made considering the parameters at each stage (DoT) → Cγ (ΔG,YS)

Max. rate of transformation (grey band)

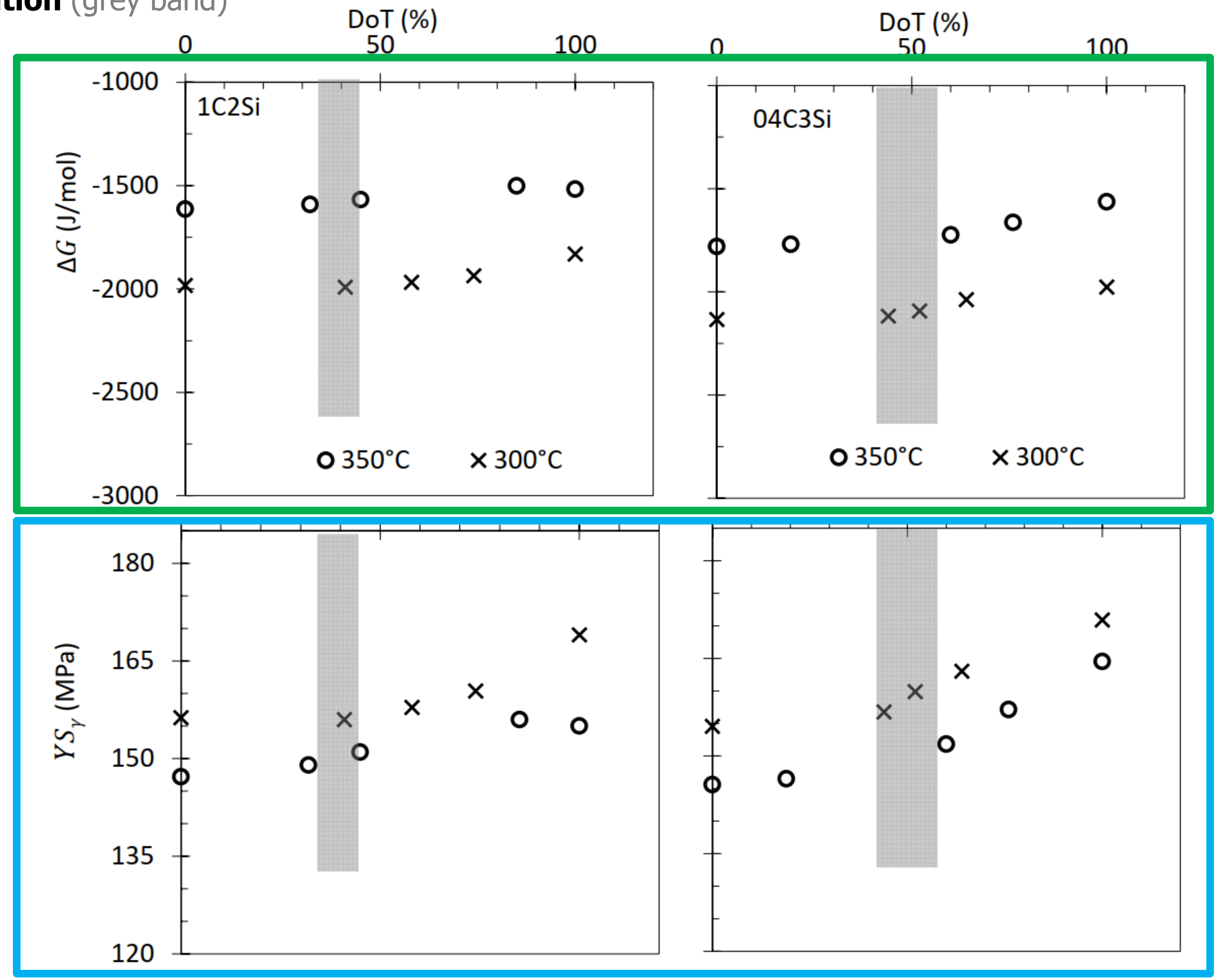

THE SYSTEM IS DYNAMIC

Calculations were made considering the parameters at each stage (DoT) → Cγ (**YS,ΔG**)

- **Theory** still **predicts** that **plate** thickness becomes **thinner** as **transformation progresses**.
- The **thickening** of the plates is **greater** after the **Max. rate of transformation** (grey band)

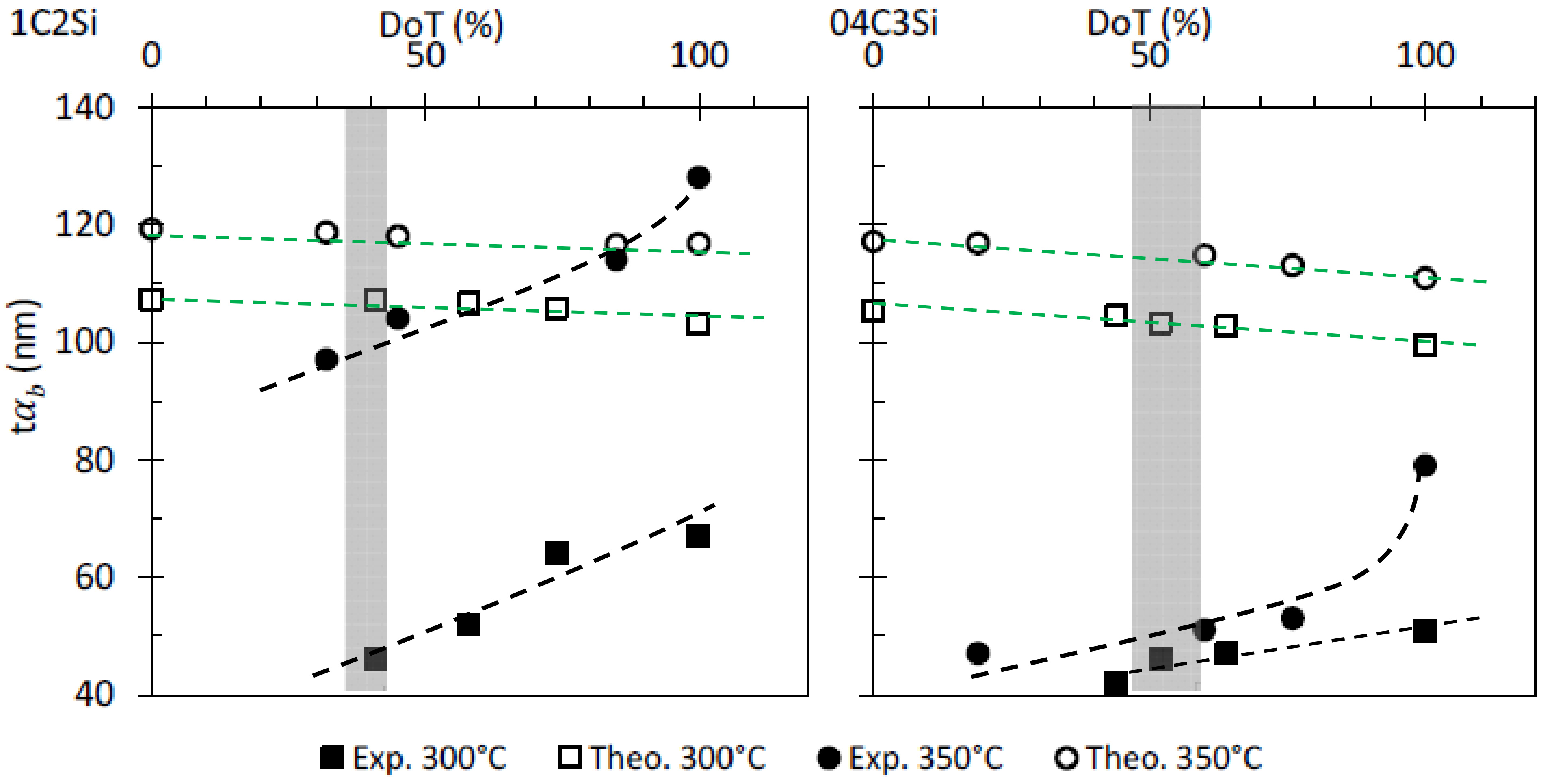

$$t = \mathrm{f}(\mathrm{T},\sigma_y^{\gamma},\Delta G^{\gamma\to\alpha}) = 222 + 0.01242 \times T + 0.01785 \times \Delta G^{\gamma\to\alpha} - 0.5323 \times \sigma_y^{\gamma}$$

THE SYSTEM IS DYNAMIC

Experimental measurements at each DoT are considering all the plates ➔ those formed at previous stages and the actual stage ➔ is an **accumulative measurement**.

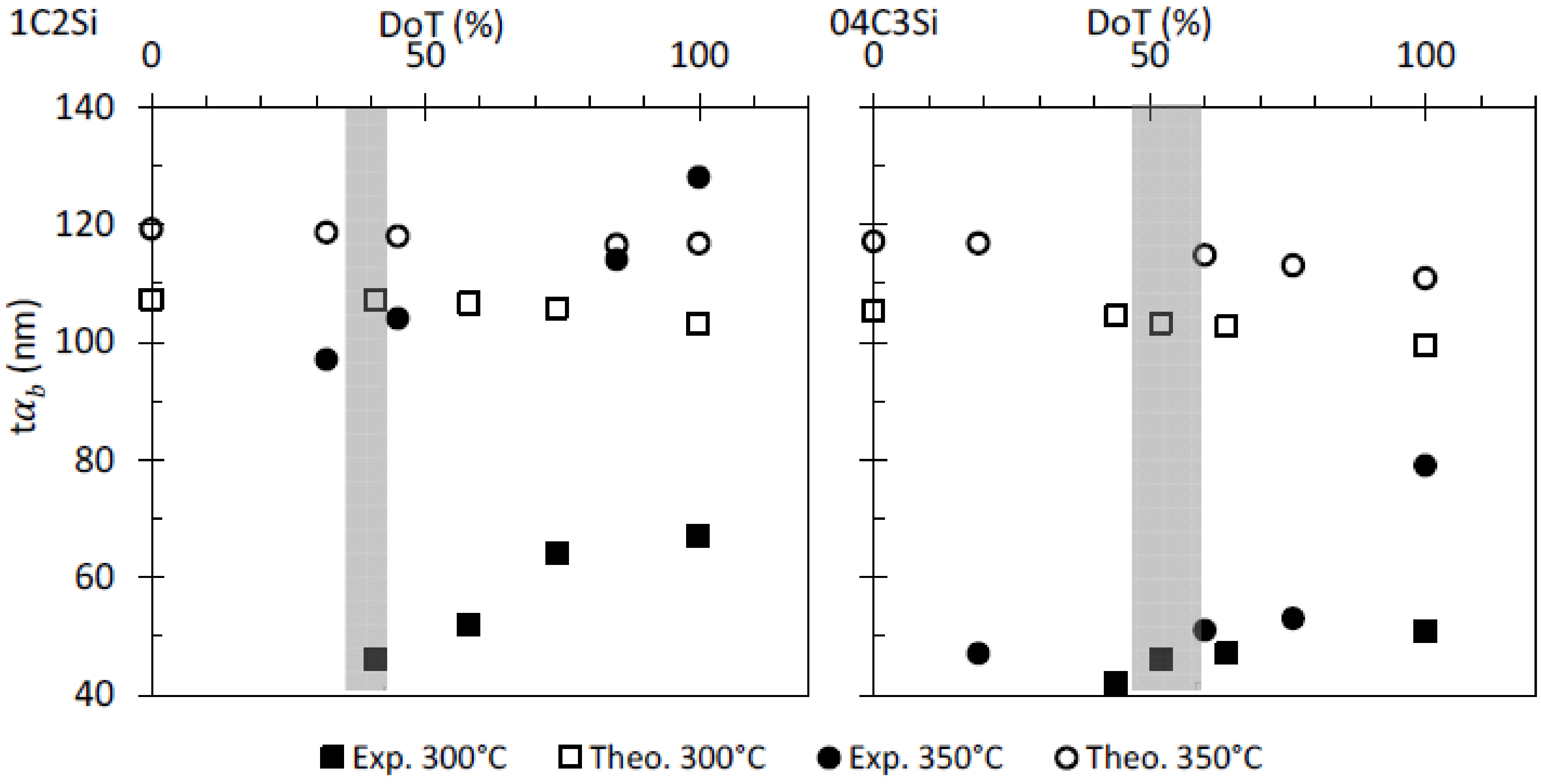

$$t = f(T, \sigma_y^{\gamma}, \Delta G^{\gamma\rightarrow\alpha}) = 222 + 0.01242 \times T + 0.01785 \times \Delta G^{\gamma\rightarrow\alpha} - 0.5323 \times \sigma_y^{\gamma}$$

THE SYSTEM IS DYNAMIC

Experimental measurements at each DoT are considering all the plates ➔ those formed at previous stages and the actual stage ➔ is an **accumulative measurement**.

Calculate the thickness of the plates formed at a certain stage (DoT), $t^{*}\alpha_b$ i.e. not considering what it was formed at previous stages

$$t\alpha_b = \sum_{DoT=initial}^{DoT=...,100\%} (f\alpha_b)_{DoT}\, \underline{(t^{*}\alpha_b)_{DoT}} \Big/ \sum_{DoT=initial}^{DoT=...,100\%} (f\alpha_b)_{DoT}$$

THE SYSTEM IS DYNAMIC

The thickening of the plates ($t^*\alpha_b$) <u>is greater after the Max. rate</u> of transformation (grey band)

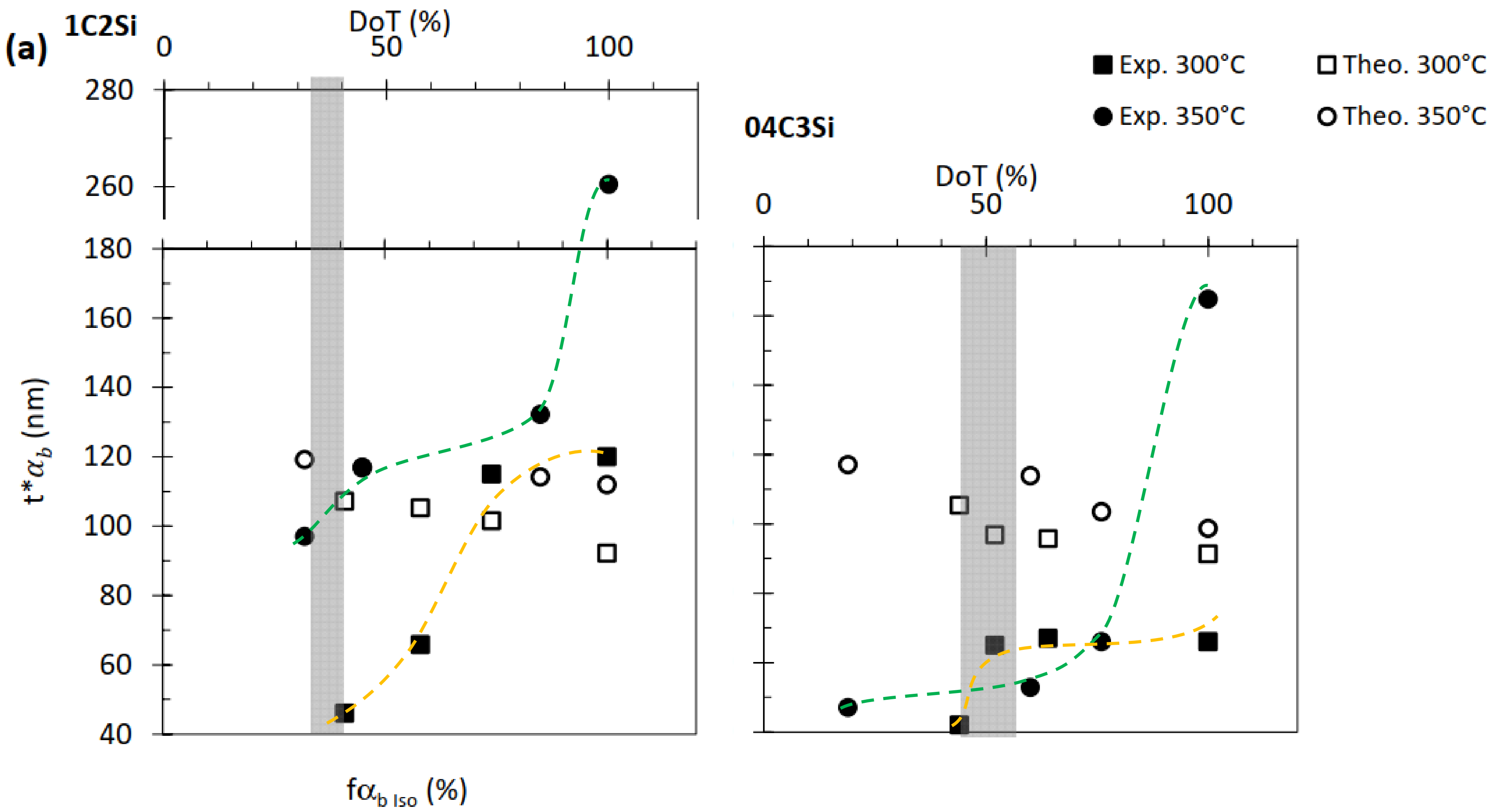

Two bainitic steels, very different C contents & very different transformation kinetics and $f_{bainite}$ (%)

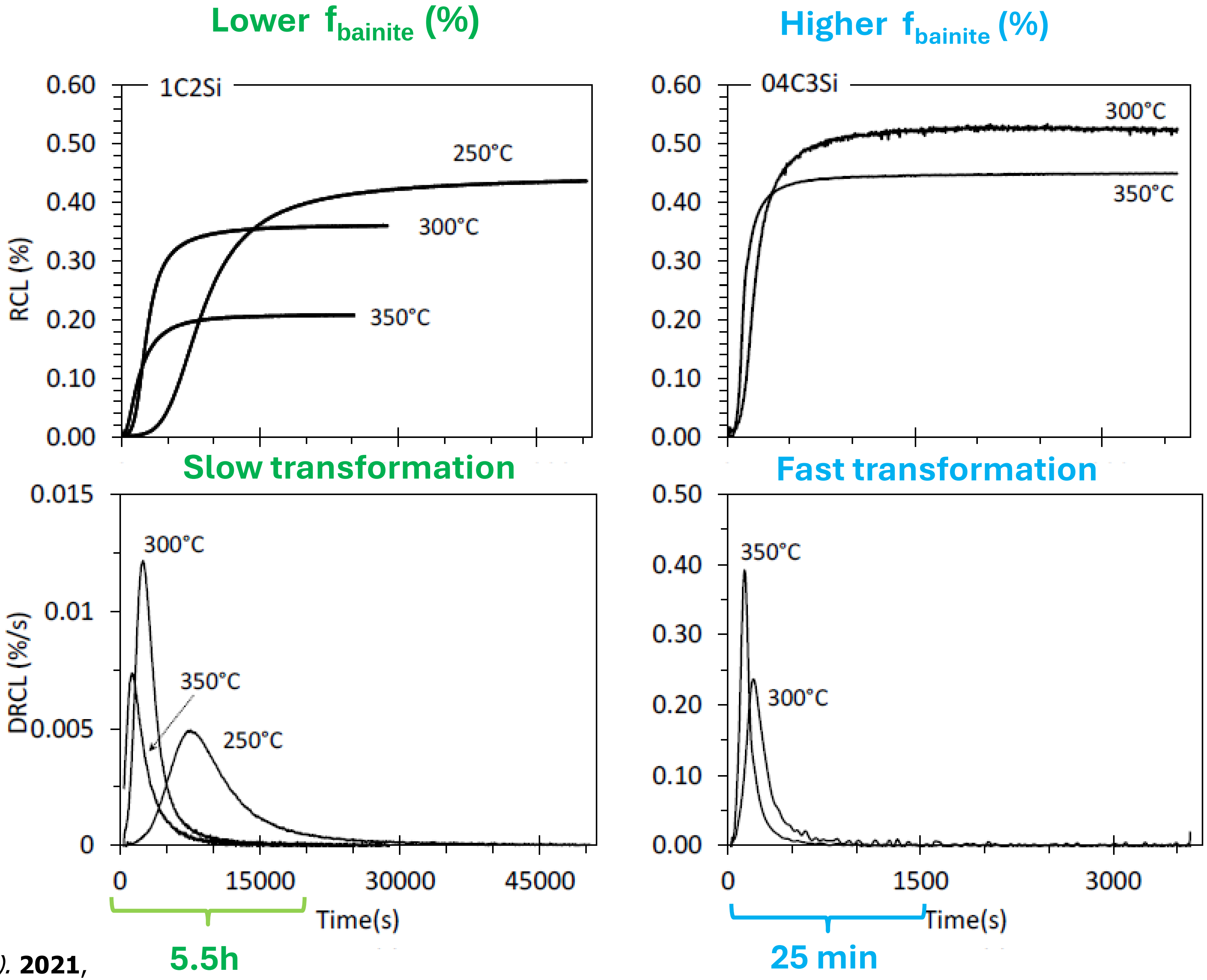

Ruiz-Jimenez, V *Materials (Basel).* **2021**,

THE SYSTEM IS DYNAMIC

- X indicates $f_{bainite}$ (%)/ minute, at both sides of the Max. Transformation rate region (grey band)
- **High** X values (a bigger fraction of bainitic ferrite is achieved in shorter times) leads to **thinner plates (t^*a_b)** ➔ **increase of the hard impingement events**

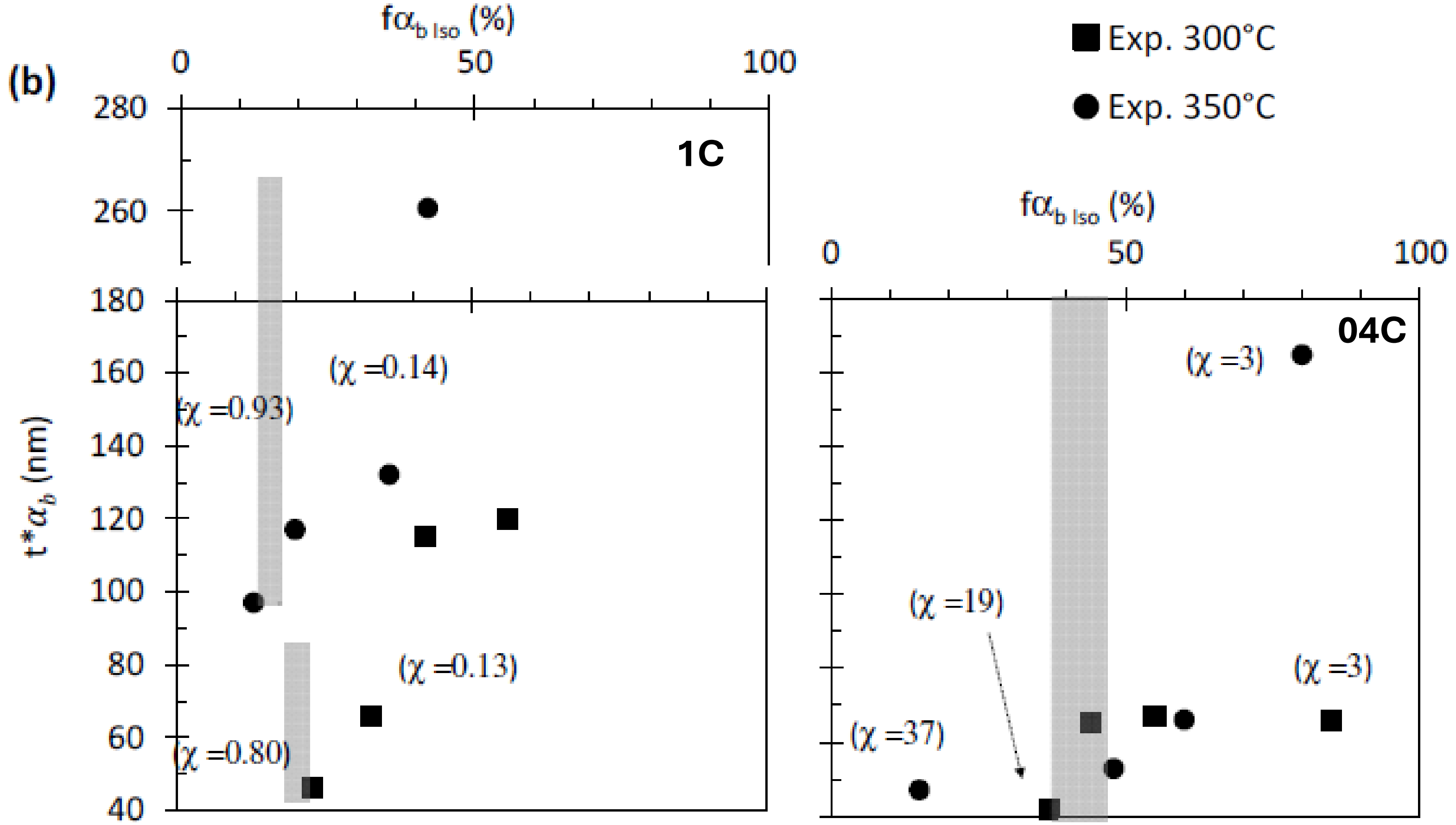

Section Summary

- ❑ Plate/Lath morphology is a natural consequence of the strain accommodation due to the transformation
- ❑ Austenite strength (YS), $\Delta G^{\gamma \rightarrow \alpha}$ and T are considered by existing models
- ❑ Dislocation density contribution exists but is not included in any model
- ❑ System must be consider as dynamic (evolving during transformation)
  - kinetics of the transformation ➔ stronger influence on $t\alpha_b$ than anticipated by existing theories.
  - Opposite to what is anticipated by the existing theory and models ➔ experiments show that $t\alpha_b$ increases as the transformation proceeds ➔ effect is more pronounced after the Max. rate of transformation.
  - A larger transformation rate corresponds to a finer microstructure ➔ There is an associated increase of the hard impingement events.

CENIM

Centro Nacional de Investigaciones Metalúrgicas

CSIC

CONSEJO SUPERIOR DE INVESTIGACIONES CIENTÍFICAS

Thank you!

Dziękuję!

WebPage: https://www.cenim.csic.es/dr-carlos-garcia-mateo/
Phase Transformation lab. : https://www.cenim.csic.es/laboratorio-de-transformaciones-de-fase/

Email: cgm@cenim.csic.es & c.g.mateo@csic.es

European Commission

This research is funded by the European Union under the RFCS project WarP – Grant Nº 101112425.

Silesian University of Technology